2010

FUNCTIONALIZATION OF MULTI-WALLED CARBON NANOTUBES IN EPOXY COMPOSITES

Chris Fitzwater
University of Kentucky, chris.fitz@uky.edu

ABSTRACT OF THESIS

FUNCTIONALIZATION OF MULTI-WALLED CARBON NANOTUBES AND THE INTERACTIONS OF MULTI-WALLED CARBON NANOTUBES IN EPOXY COMPOSITES

Multi-walled carbon nanotubes (MWNTs) are a relatively new allotrope of carbon that have potentially useful properties that may improve polymer composites. The work of this thesis explores the interactions between MWNTs and functionalized MWNTs within epoxy matrix and the properties of the MWNT/epoxy composite. These interactions were characterized with an emphasis on finding how well the MWNT/epoxy composite flows and how conductive it is after curing.

KEYWORDS: Carbon nanotubes, Composites, EMI shielding, Rheology, Nanotechnology

_____

_____

FUNCTIONALIZATION OF MULTI-WALLED CARBON NANOTUBES AND THE INTERACTIONS OF MULTI-WALLED CARBON NANOTUBES IN EPOXY COMPOSITES

By

Chris Fitzwater

Dr. Mark Meier
Director of Thesis

Dr. Mark Meier
Director of Graduate Studies

Date

RULES FOR THE USE OF THESIS

Unpublished theses submitted for the Master's degree and deposited in the University of Kentucky Library are as rule open for inspection, but are to be used only with due regard to the rights of the authors. Bibliographical references may be noted, but quotations or summaries of parts may be published only with the permission of the author, and with the usual scholarly acknowledgments.

Extensive copying or publication of the thesis in whole or in part also requires the consent of the Dean of the Graduate School of the University of Kentucky.

A library that borrows this thesis for use by its patrons is expected to secure the signature of each user.

Name	Date

THESIS

Chris Fitzwater

The Graduate School

The University of Kentucky

2010

FUNCTIONALIZATION OF MULTI-WALLED CARBON NANOTUBES AND THE INTERACTIONS OF MULTI-WALLED CARBON NANOTUBES IN EPOXY COMPOSITES

THESIS

A thesis submitted in partial fulfillment of the
Requirements for the degree of Master of Science in the
College of Arts and Sciences
at the University of Kentucky

By

Chris Fitzwater

Lexington, Kentucky

Director: Dr. Mark Meier, Professor of Chemistry

Lexington, Kentucky

2010

ACKNOWLEDGEMENTS

This thesis is a multi-disciplinary work and in the course of creating it many paths were taken to finally see it to completion. Along this journey I was helped by many people, some of whom were not even chemists! I was fortunate enough to have them in my company to learn from them and benefit from their knowledge and experience. I would like to thank the following people. Carrissa Dowden and Karen Petty, for work on the composites using my functionalized nanotubes. Delphine Franchi, for traveling all the way from France to tediously measure nanotubes with the SEM. John Craddock, for helping me in and around the labs at CAER. Matt Weisenberger, for painstaking trying explain math and engineering aspects of the project. David Jacques, Dali Qain, Terry Rantell, and Rodney Andrews for figuring out long how to make large batches of nanotubes for me to perform synthesis with. Mark Watson, John Anthony, and Jack Selegue for educating me along the way and taking time to answer my questions when I came to your offices. The US Army *Aviation and Missile Research Development and Engineering Center* for shelling out the bucks to make the project happen.

Most of all I would like to thank my advisor, Mark Meier. He has taken me under his wing and instructed me for a great deal of years. Despite his busy schedule with work and family he always went out of his way to ensure my education was being nurtured and my knowledge of chemistry was expanding. He even waited for me for 2 years when I was deployed to Baghdad, Iraq in support of Operation Iraqi Freedom. Not only did he wait for that long time he was patient with me when I returned and helped me pick up the pieces of my life inside and outside of the lab. Mark, for that I am truly grateful; you went above and beyond what most advisors would do for a graduate student.

TABLE OF CONTENTS

LIST OF TABLES

LIST OF FIGURES

Chapter 1

Carbon Nanotubes: A Unique Filler

Carbon nanotubes are arguable one of the most interesting and most recently discovered allotrope of carbon. Since Iijima's article that was published in 1991 in *Nature* describing helical microtubules of graphic carbon has spawned a large field of research that is multidisciplinary and ever growing.[1] Although it is disputed if Iijima or Bethune first discovered and identified an actual carbon nanotube, it cannot be argued that there is a great deal of interest in this particular field of nanotechnology.[2-5] Since the discovery of carbon nanotubes there has been an exponential growth of patents and articles published in this field.[6] Demands for carbon nanotubes in 2009 were estimated to reach $250 million globally and $10 billion by 2020.[7] In response to this larger chemical companies such as Bayer plan to make large-scale production plants.[8] Compared to other materials such as plastics, this field of research is still young however; carbon nanotubes are not new nanostructures. Carbon nanotubes have been found in 17th century Damascus swords and it is suggested that these nanostructures contributed to the strength of the sword.[9] Although these swords were created without the blacksmith knowing what a carbon nanotube was, it was one of the first examples of filler being used to improve the overall properties of the material.

In today's ever-growing field there is increased interest in carbon nanotube composite materials. Carbon nanotubes have an elastic modulus of 1 TPa, which is close to diamond, a tensile strength of 10-100 times that of steel, thermal stability up to 2800°C, and electric-current carrying capacity 1000 times that of copper[10]. All of the multiwalled carbon nanotubes (MWNTs) used in the course of this project were

generated at the CAER (Center of Applied Energy Research) using the following method developed by Rodney Andrews, David Jacques, Dali Qain, and Terry Rantell.[11]

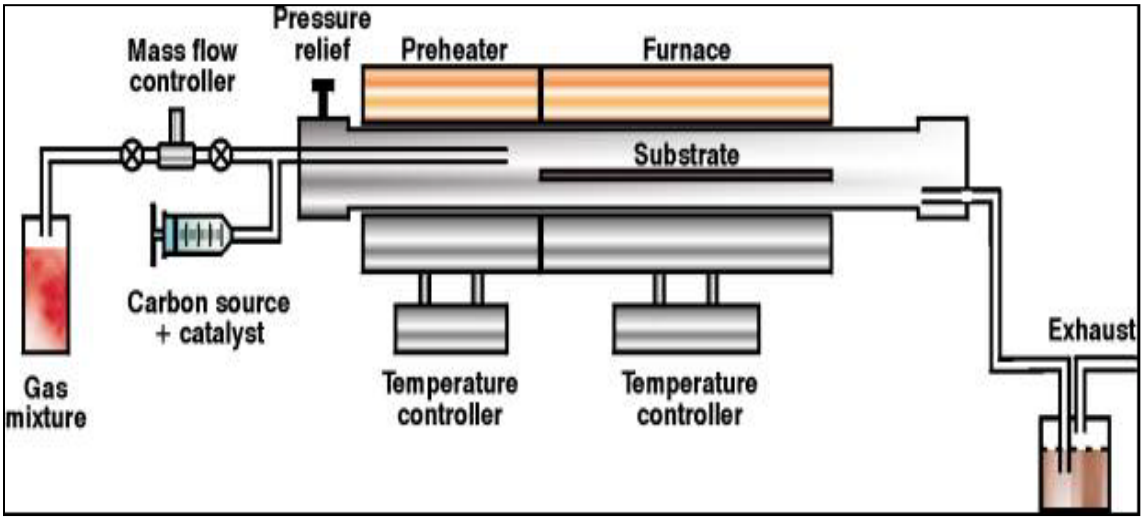

Figure 1-1 Diagram of Chemical Vapor Deposition (CVD) process utilized at CAER to produce MWNTs.[11]

Ferrocene and xylene vapor are carried by an inert gas into a furnace where the ferrocene decomposes and deposits iron nanoparticles onto a quartz substrate. Once the Fe catalyst is deposited, growth immediate occurs as hydrocarbons decompose and facilitate carbon nanotube growth. Reaction conditions have changed for this process over time as refinements have made for more uniform nanotube production.

Despite having all of these interesting and unique properties carbon nanotubes can still be manipulated as other commonplace fillers, such as carbon black. It can be mixed and added to a variety of polymers and processed in similar fashion to that of carbon black. However, in order to harness the full potential of carbon nanotubes in polymer composites, the underlying chemistry and interactions between the carbon nanotube and the polymer matrix must be in investigated. It is the goal of this research project to investigate how chemical modification of MWNTs affects the interaction with a

bisphenol A based epoxy matrix, specifically how functionalization affects nanotube dispersion and the viscosity of the resulting composite resin. Before desirable improvements can be made in the conductivity and mechanical strength of MWNT/epoxy composites, stronger interactions between the exterior of the carbon nanotube and the epoxy matrix must be made. This is no different from that with other fillers, in that covalent bonds must be made in large appreciable amounts before useful load transfer can occur.[12]

Selective chemical modification of solid fillers like carbon nanotubes is a multidisciplinary task. MWNTs are heterogeneous, insoluble and conductive in nature, prohibiting the use of many of the common identification and characterization techniques a chemist is accustomed to using. Our approach is to use synthetic routes and reactions that have been shown to be effective when applied to small aromatic molecules. After chemical modification of the nanotubes, MWNT/epoxy composite samples can be fabricated and the physical, mechanical, and electrical properties of the samples can be compared to those measured from similar composites made with unfunctionalized MWNTs. The results of this comparison will reveal the impact that our chemical pre-treatments had on the MWNT/epoxy interaction. While these comparisons do not prove that covalent bonds are formed to the surface of the carbon nanotube, they indicate that a particular chemical pre-treatment helps the MWNT/epoxy perform in a manner *consistent* with the intended chemical transformation of the nanotube surface. The following work will describe various chemical pre-treatments of MWNTs and how these pre-treatments change the viscosity and conductivity of the composites. Viscosity is of key interest since a composite resin must be able to flow if it is to be used to make an injection molded part

or drawn as a fiber. Conductivity is also a key property, since it is correlated to one of the ways electrical magnetic interference (EMI) shielding is improved.

In the following chapters, the functionalization of MWNTs is examined, characterized, and quantified. Once this basis and justification of our synthetic methodology is established greater detailed is elaborated upon of how these functionalized MWNTs interact within an epoxy matrix. Metal dopants in combination with functionalized MWNTs are also examined for they affect the conductivity of nanotube-epoxy composites. Before any of these studies are explained, the fundamental properties of raw MWNTs in epoxy are explored.

Chapter 2

Epoxy Composites: Designing Properties on a Molecular Level

The chemist's interaction with any material composite is to manipulate or tune the materials at the molecular level in order to reach a desired effect or property. The material composite system that we investigated was an epoxy/nanotube composite. Epoxy is an important engineering resin, noted for its toughness, rigidity, and resistance to chemicals. The epoxy system that was used (and here after referred to plainly as "epoxy") is commercially available EPON 826 resin[13] (primarily bisphenol A (**1**), nadic methyl anhydride (NMA, an isomeric mixture of (**2**) and EMI-2,4 (2-ethyl-4 methylimidazole (**3**) initiator.

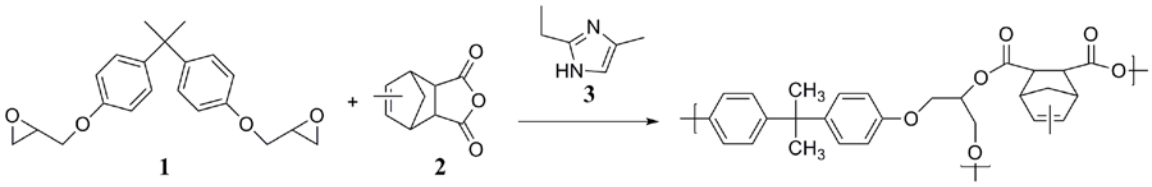

Figure 2-1 Curing mechanism for EPON 826 and NMA

The focus of this work was to investigate how chemical pretreatment of MWNTs would affect the viscosity and resistivity of the epoxy/nanotube composite. Epoxy by nature is a non-conductive polymer. By adding MWNTs as filler to the epoxy we hope can endow the composite system with electrical conductivity and improved mechanical strength. Mechanical strength improvements improve the toughness and durability of the material. Electrical conductivity is useful for static dissipation and electromagnetic interference shielding. The key properties that were investigated were the viscosity, dispersion, and resistivity of the composite material. Rheology, in conjunction with electrical conductivity testing data, helps to identify how specifically the nanotubes are interacting with the polymer matrix.

The interactions between nanotube and polymer matrix in the liquid phase can be quantified by using rheology to assess how well the mixture flows. By looking at a simple feature as how "thick" or "runny" the liquid mixture is shows how well the surface nanotubes are interacting with the polymer. Volume loadings of the nanotubes also dictate how viscous the mixture is as larger and larger amounts of nanotubes are forced to interact with one another. Resistivity and photos taken using microscopy techniques reveal how nanotube and polymer matrix interacts after curing to a solid composite material. Both of these techniques indicate how well dispersed the nanotubes are, and a good dispersion is required in order to form percolating integrated networks within the 3 dimensional polymer matrix. Before going into great detail about the characterization techniques used, the mixing methods must be addressed.

Mixing Methods: What is practical and consistent?

Mixing is a key element of creating a composite material with specific qualities. The three mixing tools that have been utilized during this project are a planetary Thinky mixer, Silverson shear mixer, and an Exakt 3-roll mill.

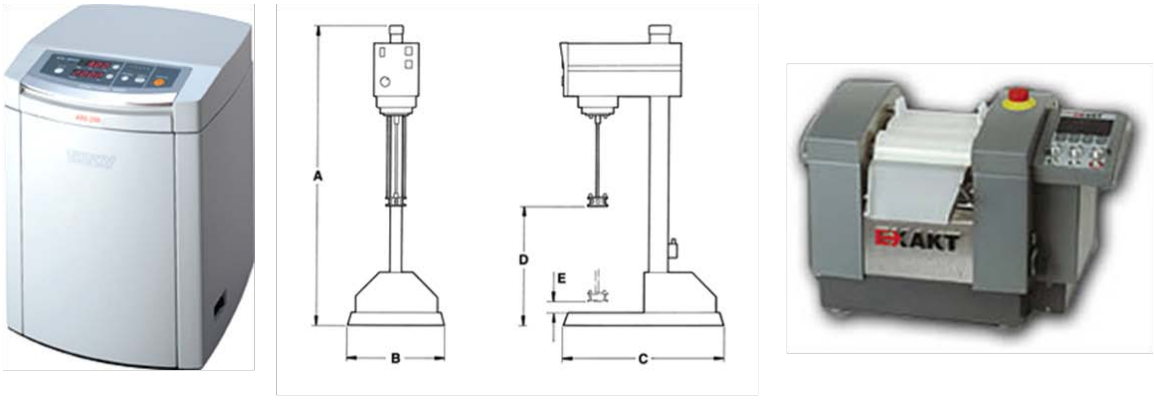

Figure 2-2 a) Thinky ARE-250 mixer[14] b) Silverson LR4 shear mixer[15] c) Exakt 80E 3-roll mill.[16]

The Thinky mixer rotates a sample in the same way the earth revolves around the sun. The sample rotates in a while it revolves in a circular fashion in the mixer at high speeds which causes a centrifugal force that presses the liquid down and out against the outer wall of the container.[14]

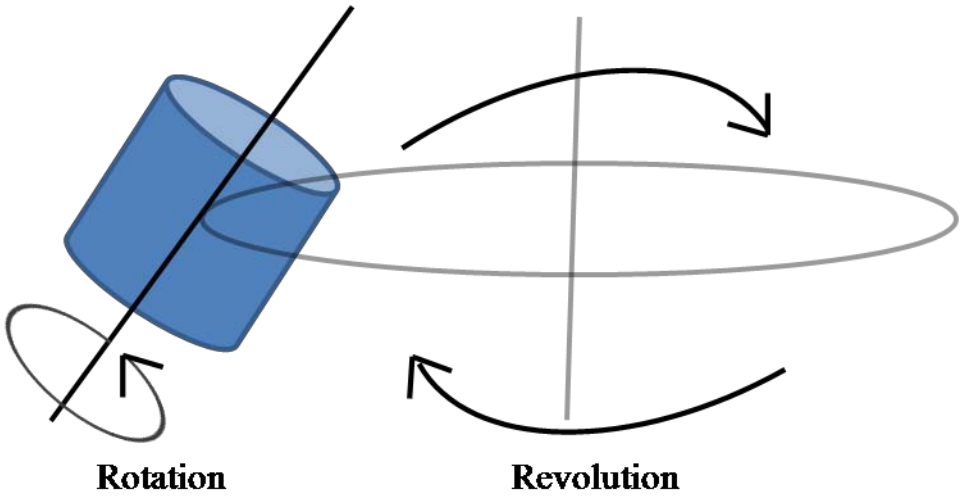

Figure 2-3 Diagram of how a sample moves in Thinky planetary mixer.[14]

This is an attractive method for mixing low viscous mixtures that do not contain dense or heavy fillers. A timeline diagram below shows the cross sectional mixture of two colored clays and how centrifugal forces mix the colored clays together into a homogeneous mixture.

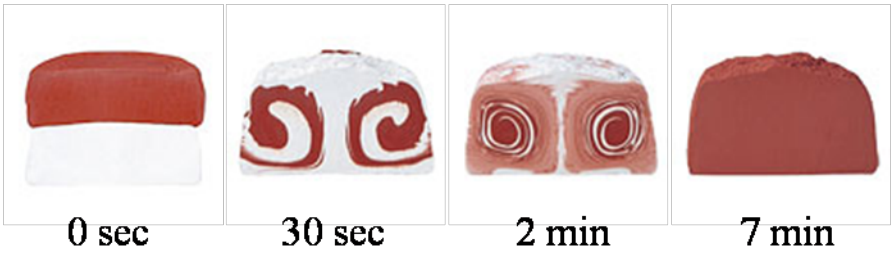

Figure 2-4 Diagram showing timeline of mixing two colored clays into a homogeneous mixture.[17]

This method of mixing is useful on a small scale with a liquid that is not dense or very viscous. MWNT/epoxy composites at loadings of 1% volume loading or above are viscous and do not flow under their own weights making it difficult to obtain a homogenous mixture using the THINKY mixer alone.

The Silverson shear mixer mixes materials in 4 stages which circulates the liquid thru a high shear field. This method is useful for mixing conventional liquids, but given the nature of our filler it can be assumed that the high shear field is damaging the nanotubes as they pass thru the mixer.

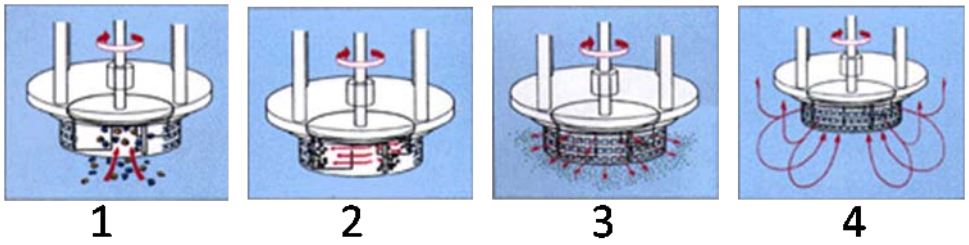

Figure 2-5 The 4 stage mixing process used by the Silverson shear mixer.[18]

The Silverson mixer first draws up the liquids from the bottom of the container into the workhead in a suction fashion. Once in the workhead the liquid is mixed under centrifugal forces between the rotary blades and the inner wall of the stator. Then the liquid is forced out of the workhead under high hydraulic shear forces. Once forced out of the workhead the liquid travels at a high speed towards the sides of the container while new liquid is drawn up from the bottom of the container repeating the process.

This process is more effective at mixing MWNT/epoxy composites than the THINKY mixer. Unfortunately, drawing the nanotubes into the workhead and forcing them out of the stator causes considerable damage to the nanotubes in this high shear field. This method also is not uniform, especially if using a container that is larger than

the shear head of the mixer, where the filler is not uniformly drawn up into the workhead and properly mixed through out the liquid.

The last mixing method that was used for the majority of the mixing processes for this project is the 3-roll mill. The 3-roll mill uses rollers spinning at three different speeds with a micron sized gap between the rollers to exposes material to a high shear field as it passes through it.

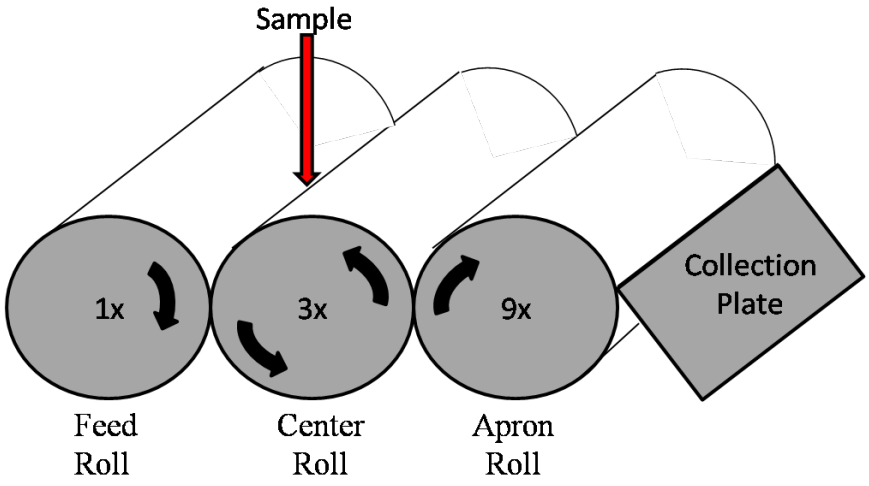

Figure 2-6 of 3-roll mill roller speeds and direction.

The shear strain rate for the first and second gaps is as follows[19];

$$\dot{\tau}_1 = \frac{r(\omega_2 - \omega_1)}{t} = \frac{2}{9}\frac{r\omega_3}{t}$$

$$\dot{\tau}_2 = \frac{r(\omega_3 - \omega_2)}{t} = \frac{2}{3}\frac{r\omega_3}{t}$$

where r, t, and ω represent the radius of the roller, the gap distance and the angular speed of the roller. If increased shear stress is desired then the gap can made smaller or the speed of the rotation of the rollers can be increased. As we will see later increasing shear stress can cause damage to the nanotube. Of all of the above methods the 3-roll mill is most effective for obtaining a uniform homogenous mixture for MWNT/epoxy

composites. Variations in the speed, number of passes and gap distance all play an integral part on the final product of the composite material.

In order to assess the homogeneity and properties of these MWNT/epoxy mixtures viscosity and IR reflectance microscopy were used. These methods are not typical instrumentation for a chemist, however given the material science nature of these projects, both were key tools in quantifying and identifying differing properties of the various MWNT/epoxy composites investigated during this project.

Rheology: How does high aspect ratio filler affect a composite?

Rheology is not a standard tool that is used by most organic chemists. The most common and simple rheological tool that we use every day is our tongue. When we drink water it flows easily into our mouths and travels down our throats into the stomach. Now if we eat something like peanut butter or taffy you notice that is much thicker or viscous and doesn't flow right down into the throat without a concerted effort. The rheometer is much like a smart tongue that uses counter torque to measure how well liquid mixtures flow when a shear force is exerted upon them. For this project it has been an integral part of understanding how chemical modification of a nanotube affects its interaction within the epoxy matrix. A brief explanation is needed before moving forward with results. The viscosity of a material can be characterized macroscopically as how well it will flow or pour.

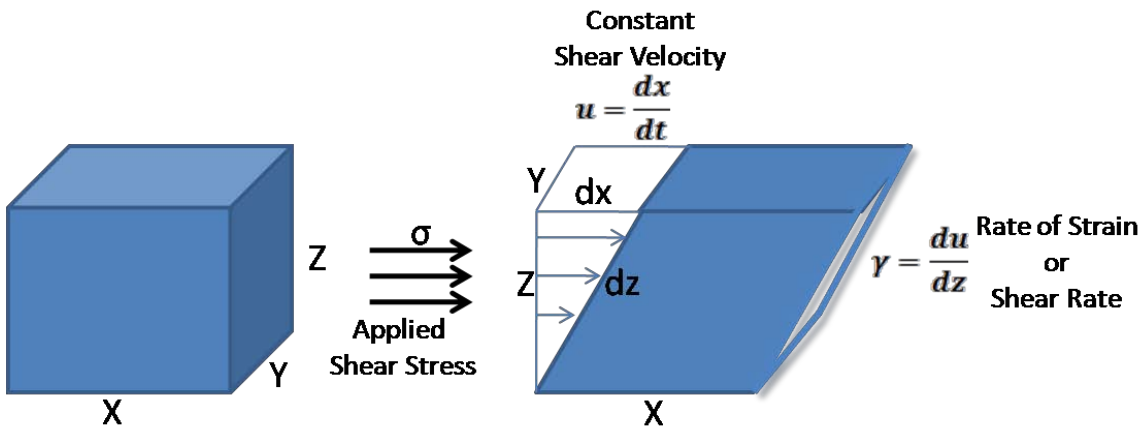

Figure 2-7 Deformation of a 3 dimensional liquid[20].

This example shows an external force is applied to a liquid. The force applied over an area of liquid is known as the shear stress (σ). Once a force is applied over an area of the liquid, the liquid then deforms. If the shear stress is kept constant, then constant shear velocity can be measured as the deformation along the x axis over a period of time. In turn, the rate of strain (or shear rate) can be measured at the constant velocity divided by the change in length of the z axis. For Newtonian liquids, such as water, the shear stress and the shear rate are linearly related with the coefficient of viscosity (η).

$$\sigma = \eta\gamma$$

This equation accurately describes most of the relationships of stress, strain, and time, over a range of response for most materials. There is a wealth of data that can be obtained from various rheology experiments, however we focused on viscosity as a means for quantifying how well a chemical pretreatment of the nanotubes has improved its interfacial interactions with the polymer matrix.

Including carbon nanotubes as filler in a composite has the prospect of improving the mechanical properties, electrical and thermal conductivities, and EMI shielding properties. These improvements come at the cost of the viscosity increasing

dramatically, thus decreasing its processability and potential material application. In order to overcome this problem, improved interfacial interactions between nanotubes and polymer matrix must be achieved in order to overcome the Van der Waals' interactions between nanotubes. Increased nanotube-nanotube interactions lead to agglomerations and poor dispersion throughout the polymer matrix.

Nanotubes used as filler will inherently increase the viscosity the polymer due to their aspect ratio. Glass fiber filler has an aspect ratio ~1500[21] at most, and single wall carbon nanotubes have been grown extremely long to have an aspect ratio of 28,000,000[22]; however multiwalled carbon nanotubes have an aspect ratio ~1000. Aspect ratio is key factor in determining how a filler increases the viscosity of the polymer system. Einstein first proposed that for dilute suspensions of buoyant rigid spheres with non-Brownian motion in a Newtonian liquid is described by the equation below[21].

$$\eta_r = 1 + \alpha_E \phi$$

$$\eta_r = \frac{\eta_S}{\eta_0}$$

The relative viscosity of the suspension η_r is equal to the ratio of the viscosity of the suspension (polymer with filler) η_s, to the viscosity of the suspending medium (polymer) η_0. The relative viscosity is related to amount of filler by Einstein's constant α_E = 2.5 multipled by volume fraction of suspended particles ϕ. This relationship works for simple rigid spherical fillers, but it becomes more complex as the nature of the filler is changed. For filler that is rod-like as are carbon nanotubes, Einstein's constant changes to the following equation below.[21]

$$\alpha_E = \left[\frac{r_a^2}{6(ln2r_a - 1.8)}\right] \sin^4\theta \sin^2 2\psi$$

Einstein's constant greatly changes when the geometry of the filler is changed, specially related to the aspect ratio r_a. When rod-like filler is used the constant is now related by a ratio of the aspect ratio and the spherical coordinates θ, ψ that give the orientation of the rod within the suspended medium. The main characteristic of this equation is that larger the aspect ratio of a rod like filler is the larger Einstein's constant will be thus the larger the relative viscosity of the suspension will be. It is also known that curved fibers increase the viscosity dramatically compared to rigid straight fibers, and nanotubes are rarely straight and rigid. Carbon nanotubes can be grown aligned and straight, however once processed and manipulated agglomeration occurs and nanotubes become bent and curved. This is due to the ductile nature of nanotubes to undergo Stone-Wales transformations and form pairs of pentagons and heptagons along the structure of the nanotube.[10, 23]

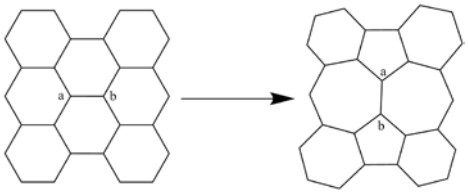

Figure 2-8 Stone-Wales defect showing transition from 6,6,6,6 ring to a 7,5,7,5 ring junction within the skeleton of the nanotube.

These junctions allow for the curvature of the nanotube and add a degree of increased viscosity. High aspect ratio filler, such as nanotubes will increase the viscosity of the polymer they are added to as filler regardless of chemical pre-treatment.[21]

Mixing Techniques: Finding the optimal process

Various mixing processes were used during the progression of this project. Methods were continually refined in light of data and optimization was attempted when possible. Early mixing methods focused on mixing with the Silverson shear mixer; however a majority of the work later focused on mixing with the 3-roll mill. For this study, the nanotubes were mixed into the matrix using a Silverson high-shear mixer.

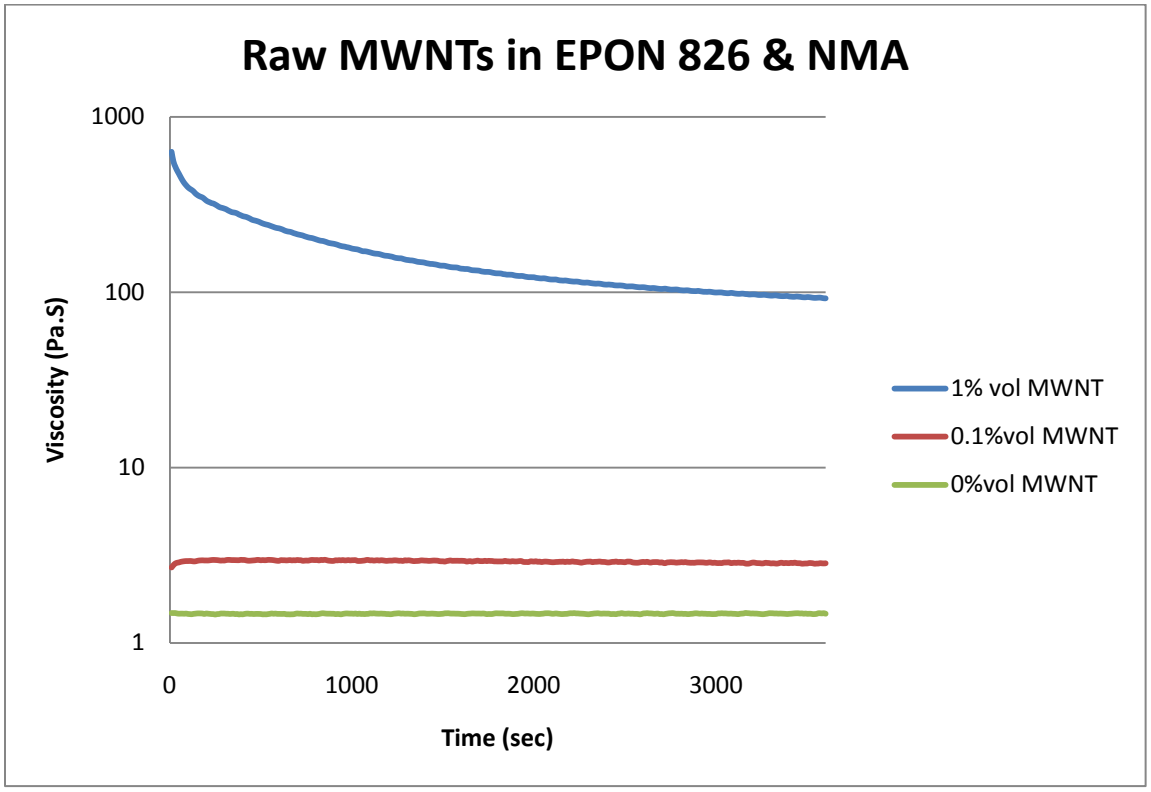

Figure 2-9 Viscosities of raw MWNTs mixed with EPON 826/NMA

In figure 2-9 the results of a series of rheology experiments are shown, in which the shear rate was maintained at a constant shear of $1s^{-1}$. These results show that adding just 1% volume loading greatly increases the viscosity, as would be expected based on the aspect ratio of the nanotubes. The drop in viscosity over time is likely the result of the nanotubes becoming aligned in the shear field. The key point of this experiment is that

the addition of just a small amount of MWNTs to the epoxy causes an exponential increase in the viscosity and that over time in a constant shear field, alignment of the nanotubes will occur.

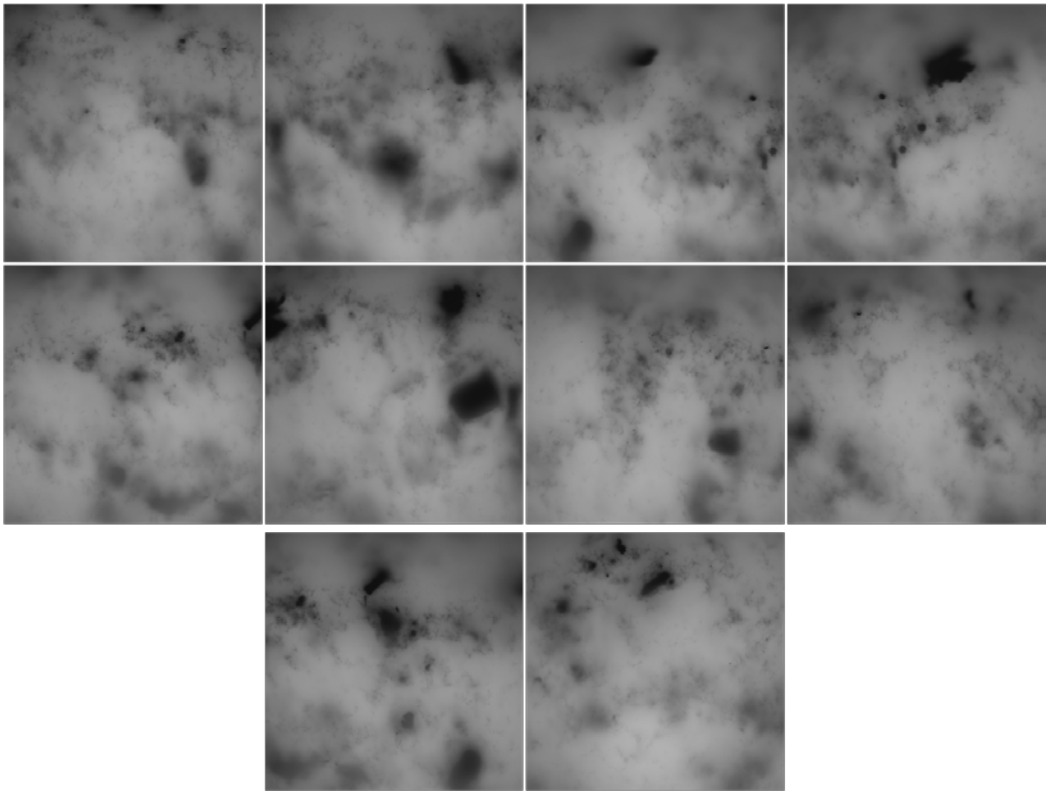

Figure 2-10 Image complied of various UV fluorescence photos taken at 40x mixed using Silverson shear mixer with 0.1% vol loading of MWNTs in epoxy.

UV reflectance microscopy photos reveal at 0.1% vol loading of MWNTs in a nanotube/epoxy resin composite that was mixed using the Silverson shear mixer, that there are many agglomerations that frequently appear through out the cured composite. It was also observable that there was a liquid layer separation between the EPON 826 and NMA after mixing. This will give an inaccurate viscosity reading as the MWNTs typical adhere to the EPON 826 layer making it much thicker while the NMA layer will be runny

and flow. This typical of heterogeneous mixture and improved mixing methods were needed if a uniform MWNT/epoxy composite were to be obtained.

Thostenson et. al have used 3-roll mill to mix MWNT/epoxy mixture to much success.[24] The advantage of using the 3-roll mill is that every part of the mixture passes thru two gaps in the mill. Those gaps can be adjusted down to 5 microns and significant shear forces within those gaps break apart agglomerates. These photos were taken using UV reflectance microscopy on cured MWNT/epoxy samples that were mixed using a 3-roll mill.

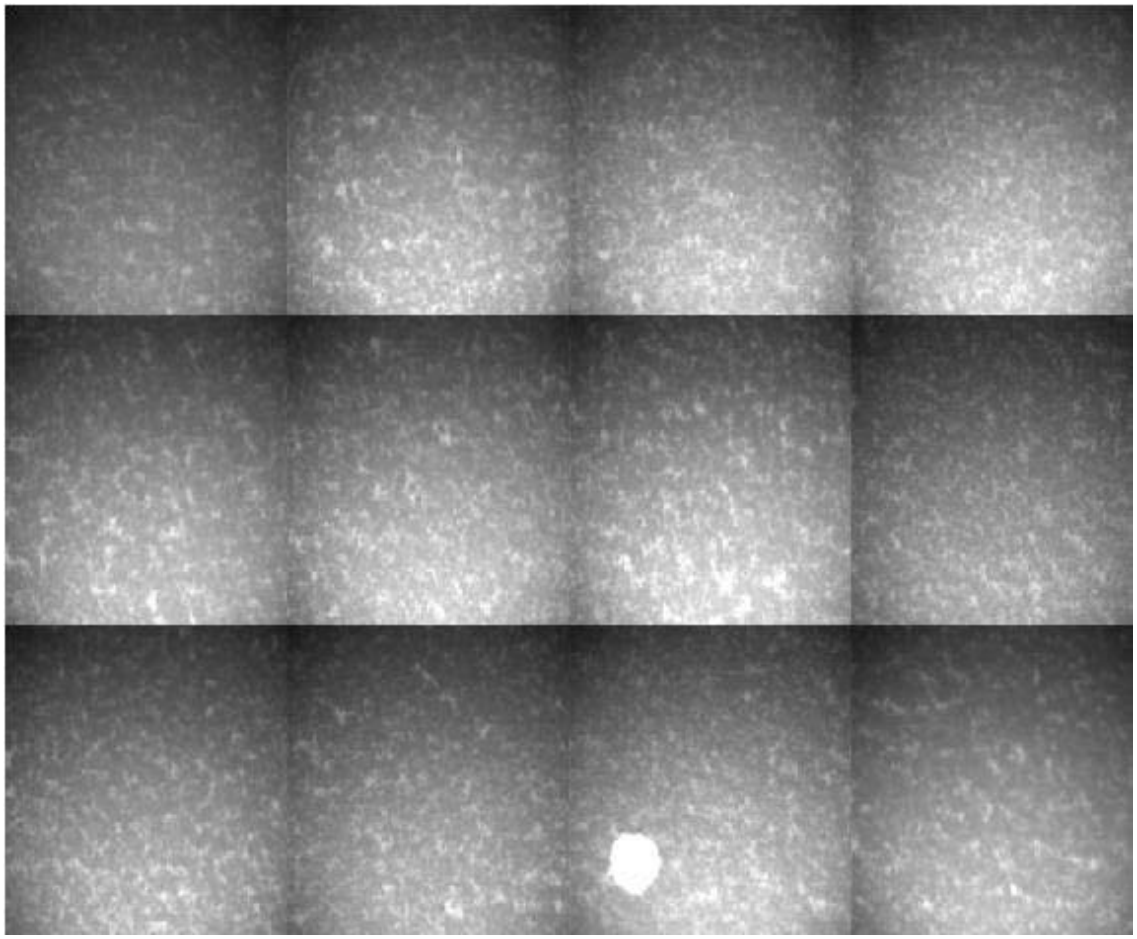

Figure 2-11 Image complied of various UV fluorescence photos taken at 40x mixed using 3 roll method with 1% vol loading of MWNTs in epoxy.

There are far fewer agglomerations when the 3-roll mill is employed to mix MWNT/epoxy composite samples. This method allows for a more homogenous mixture and more accurate viscosity measurements to be taken. As a result, all further rheology measurements were made on samples prepared using 3-roll milling for mixing.

The step that was taken was to accurately determine a proper method for mixing with the 3-roll mill. Long and short methods were employed and a sample was taken after each pass thru the gap of the rollers. Both of the methods are shown below in the two charts.

Long Run

STEP #	#1 ROLL	#2 ROLL	SPEED
1	50	45	200
2	50	45	200
3	25	20	200
4	25	20	200
5	10	5	200
6	10	5	200
7	5	5	250
8	5	5	250
9	5	5	250
10	5	5	250
11	5	5	250

Short Run

STEP #	#1 ROLL	#2 ROLL	SPEED
1	50	40	200
2	25	20	200
3	10	5	200
4	5	5	250
5	5	5	250

Table 2-1 Long (11 passes) and short (5 passes) mixing methods for the 3-roll mill.

A volume loading of 1% MWNTs were used in both methods. From all of the samples taken viscosity was examined as the shear was ramped from 0.001 to 100s^{-1}. UV

microscopy was performed on the final cured composite of each method and a comparisons of the photos is shown below in figure 2-12.

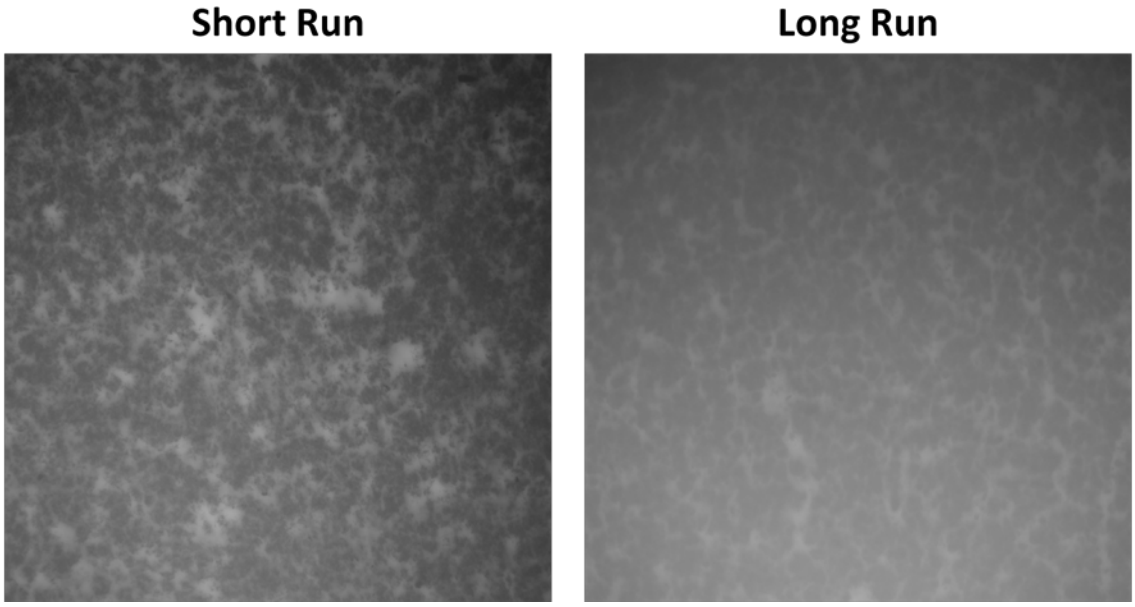

Figure 2-12 Photo comparison the two mixing methods

There is little difference in dispersion of the two mixing methods based on UV reflectance microscopy photos. In addition to this viscosity of each pass thru the 3-roll mill was examined and is shown below.

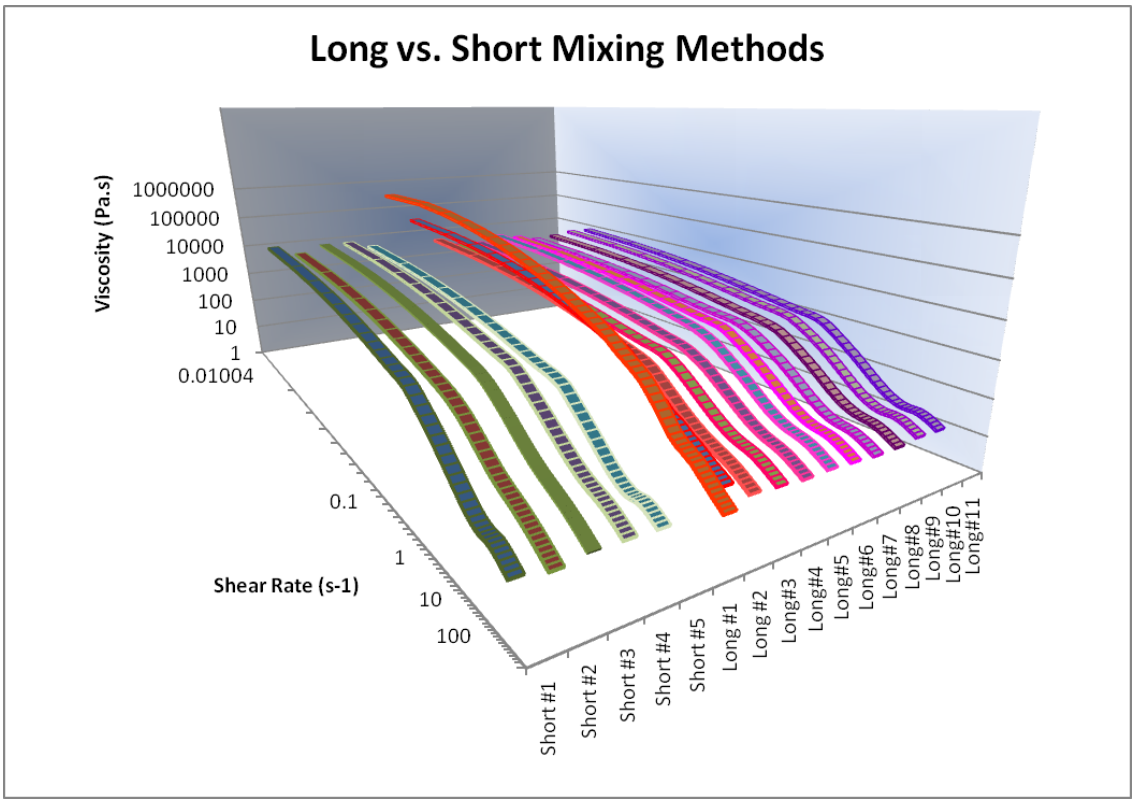

Figure 2-13 Viscosities of each pass using the two 3-roll mill methods. Each ribbon represents a specific pass in the short (green) and long (red) mixing methods. Due to the difficulty of displaying this large amount of overlapping data in 2 dimensions a 3 dimensional graph was chosen.

The results show that there is little benefit from the longer mixing routine as shown in figure 2-13. The viscosity quickly reaches the lowest it will reach after a short number of passes thru the 3-roll mill. Because of the lack in difference between the two methods, the short method was chosen to be used as the standard for mixing MWNT/epoxy composite samples.

Resistivity and Conductivity of MWNT/Epoxy Composites

A manifestation of a good dispersion is a lowering in the percolation threshold at that given volume loading of nanotube, and therefore a lower the resistivity of the MWNT/epoxy composites. This section explains the results of electrical resistivity

testing of the MWNT/epoxy composites. Like graphite, nanotubes, are conductive, but harnessing this ability in a composite is not easily accomplished. The graphene that comprises carbon nanotubes has a twist or chirality which determines the electrical properties of the nanotube.[25, 26] The three types of twists result in tubes known as chiral, arm chair, or zig-zag. The configuration will determine if a nanotube is metallic (arm chair) or semi-conducting (chiral & zig-zag) in nature. This is an issue for composites containing single walled carbon nanotubes if a particular type of chirality is desired for a composite. This is not a problem for composites containing MWNTs as there is typically 40 layers of graphene of various twists within a single nanotube.[11] Li et. al had recently shown that for a single MWNT with a diameter of 100nm that is ~75 walls thick, it had quasi-ballistic electron transport with a low resistance of 34.4 Ω and high conductance of 460-490G_0[27]. Stetter et. al. have shown that inner layers of carbon nanotubes contribute significantly to the conductivity of a MWNT, despite the resistivity that is caused by defects on a particular of carbon nanotube.[28]

MWNTs are potentially useful for their low resistivity and high conductance but in order to achieve a useful MWNT/epoxy composite with useful conductivity, a percolating network of MWNTs has to be formed within the composite. Effective mixing and the volume fraction of MWNTs affect the resistivity of the composite. The 3-roll mixing method has been shown to produce homogeneous samples so the next variable of concern is the volume loading of MWNTs to the epoxy composite. The percolation threshold, or mathematically described as “a filler volume fraction at which an infinite spanning cluster appears in an infinite system”, decreases as aspect ratio is increased.[29] It is shown that weight loadings as low as 0.0025% can achieve the percolation threshold.[30,

[31] Li et. al have also shown that it is essential that the "backbone" of the network be formed and that the aspect ratio of the filler plays a critical role in network formation, as does the waviness of the carbon nanotubes.[29] The curve ratio, or how straight and rigid the nanotube is, also affects the conductivity: more curved nanotubes lead to lower conductivity. This effect also influences the conductivity of the composites, since a majority of the nanotubes are bent or curved. However the volume loadings of 1% are sufficient to overcome morphology issues that may arise and form a percolating network.[29]

To investigate the conductive and network formation in MWNT/epoxy composites the samples made previously were cured, sawn into rectangular samples, polished, and leads were glued on with silver epoxy. The volume resistivities of the samples were tested using the 4 point contact method.

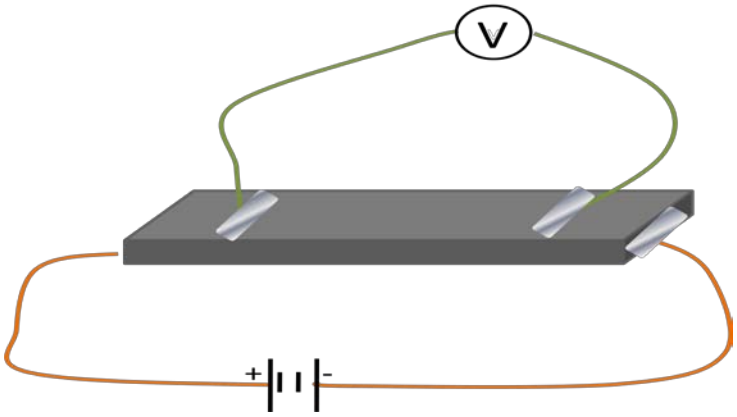

Figure 2-14 Diagram of 4 point resistivity testing.

Using this method, current was passed through the sample and the voltage drop was tested for a section of the composite sample. The follow table has the results for the volume resistivity of the following samples, all of which were performed at 1 volume% MWNT vol loading in epoxy; values averaged over 3 samples.

Mixing Method	**Resistivity (ohm*cm^2)**
Short Mixing Method	100.99
Long Mixing Method	271.94

Table 2-2 Resistivity of 1 vol % MWNT loadings in epoxy using the Short and Long mixing methods.

The results above show that intensive and long mixing process actually increases the overall resistivity of the sample. This was unanticipated, as thorough mixing was expected to result in a better dispersion and a more effective conductive network throughout the sample. After a recent publication by Hoa, stating that mixing methods directly affect the conductivity of MWNT/epoxy composite samples, questions arose about our current mixing method and if it was the optimal choice for mixing.[32] To investigate the effect that the mixing process had upon the nanotubes themselves, MWNT/epoxy mixtures were run thru the 3-roll mill using our short method were washed, filtered, and the MWNTs were collected. These MWNTs were then photographed using SEM and length measurements were taken, and it was found that on average, most MWNTs were the length of ~5 micron, which was the size of the roller gaps of the 3-roll mill on the last two passes. MWNTs at CAER are typical ~25 microns in length.

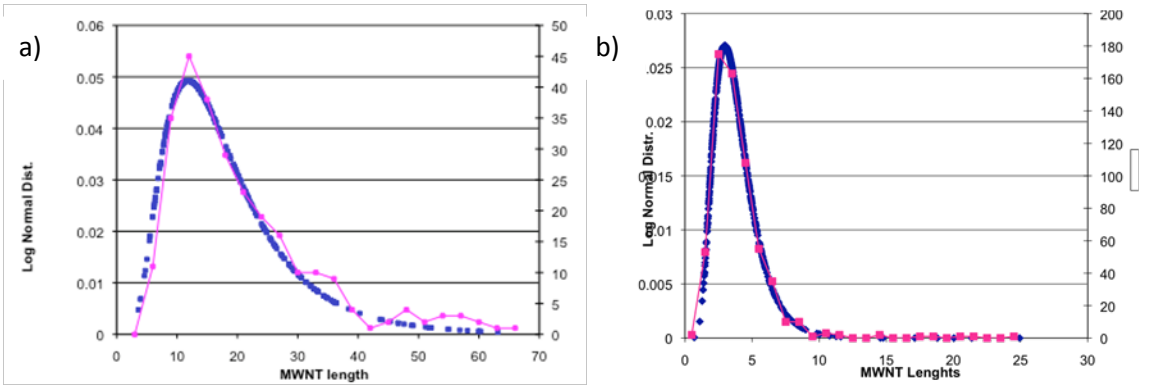

Table 2-3 a) Length distribution histogram of MWNTs measured in microns before 3-roll milling b) Length distribution histogram of MWNTs after 3-roll milling using the standard method. ***Data produced by Delphine Franchi***.

This dramatic shortening of the nanotubes came as a surprise, since Thostensen had reported earlier that using a 3-roll mill to mix MWNT/epoxy mixtures caused little damage to the nanotubes.[33]

Hoa's recent work stated that starting out with nanotubes with a larger aspect ratio would yield a more conductive composite, and that additional speed or excessive passes thru the 3-roll mill produced a less and less conductive composite.[32] It could be assumed that excessive speed and increased number of passes thru the gap damages and reduces the length of the nanotube, as shown with work done using the current standard mixing method. On this basis we devised new mixing methods in an attempt to understand how processing affected the conductivity of the MWNT/epoxy composite. The three new methods are listed below and all speeds were at 100 rpm (apron roller speed) and all the MWNT volume loadings were at 0.5%.

METHOD	A	B	C
1st Pass	50/40	100/100	50/50
2nd Pass	25/20	100/100	25/25
3rd Pass	10/5	50/50	25/25
4th Pass	5/5	40/40	
5th Pass	5/5	25/25	

Table 2-4 Sizes of the gaps are listed by pass as first gap/ second gap in microns.

Method A is the original mixing method, but at a lower speed. Methods B and C use a wider gap than the original mixing method. Viscosity measurements were taken of the composites resulting from these new mixing methods and it was found that each of these new mixing methods resulted in an overall increase in viscosity relative to materials mixed using the original method. This result suggests that an improved mixture resulted as the EPON 826 and NMA layers combine to form a more homogeneous mixture. Typically the nanotubes adhere to the EPON 826 layer better than the NMA layer and this could be attributed preferred aromatic pi bond attraction.

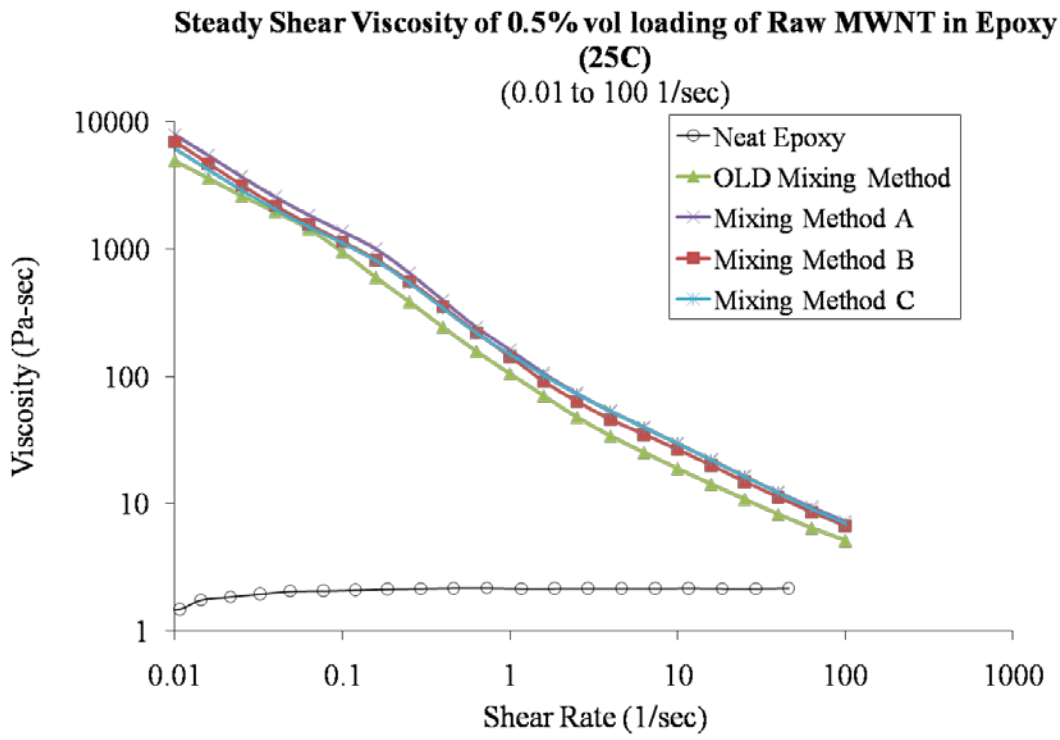

Figure 2-15 Comparison of the viscosity of the last pass of each of the various mixing methods.

This increase in the viscosity is from a more homogenous mixture; previous observations of poorly mixed heterogeneous mixtures show a decrease in viscosity. Samples were taken after each pass thru the 3-roll mill and the viscosity was measured for each. Each of the mixing methods produced a gradual increase in viscosity, showing that there is an improvement in how well the sample is mixed.

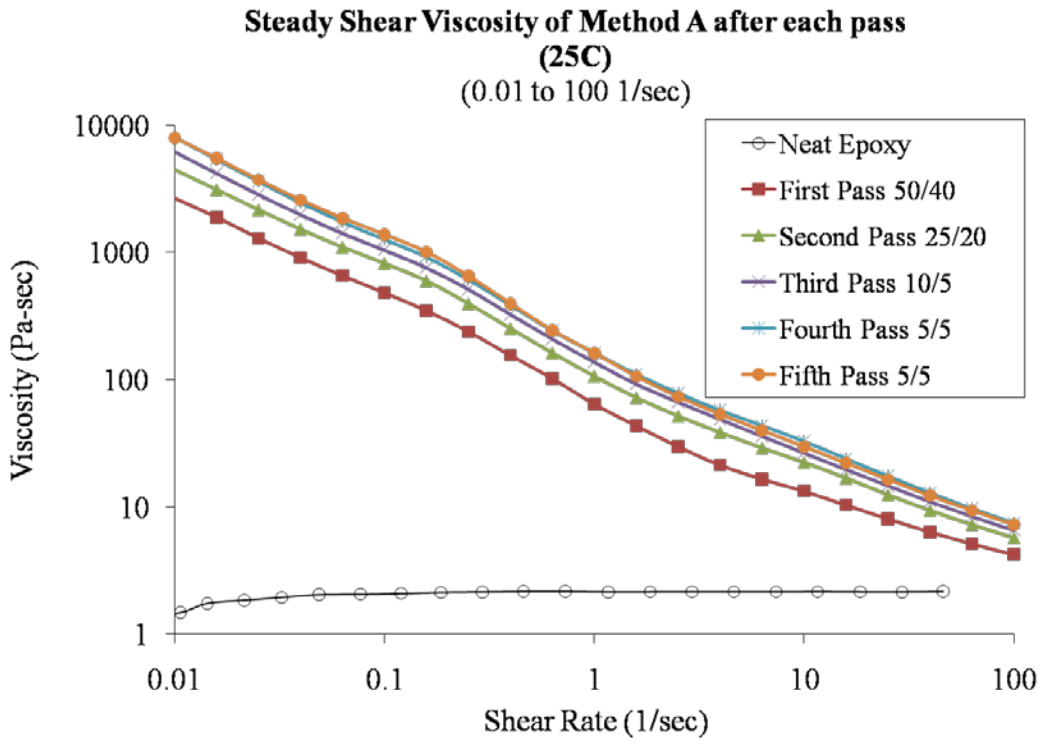

Figure 2-16 Viscosity of each pass for mixing method A.

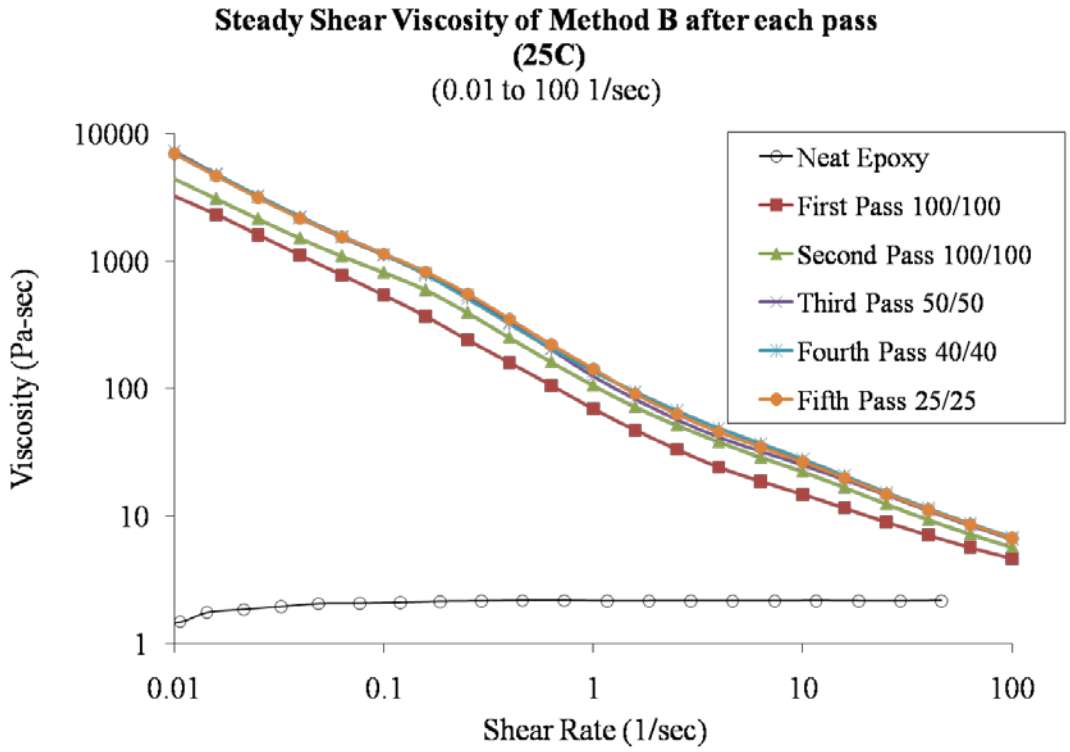

Figure 2-17 Viscosity of each pass for mixing method B.

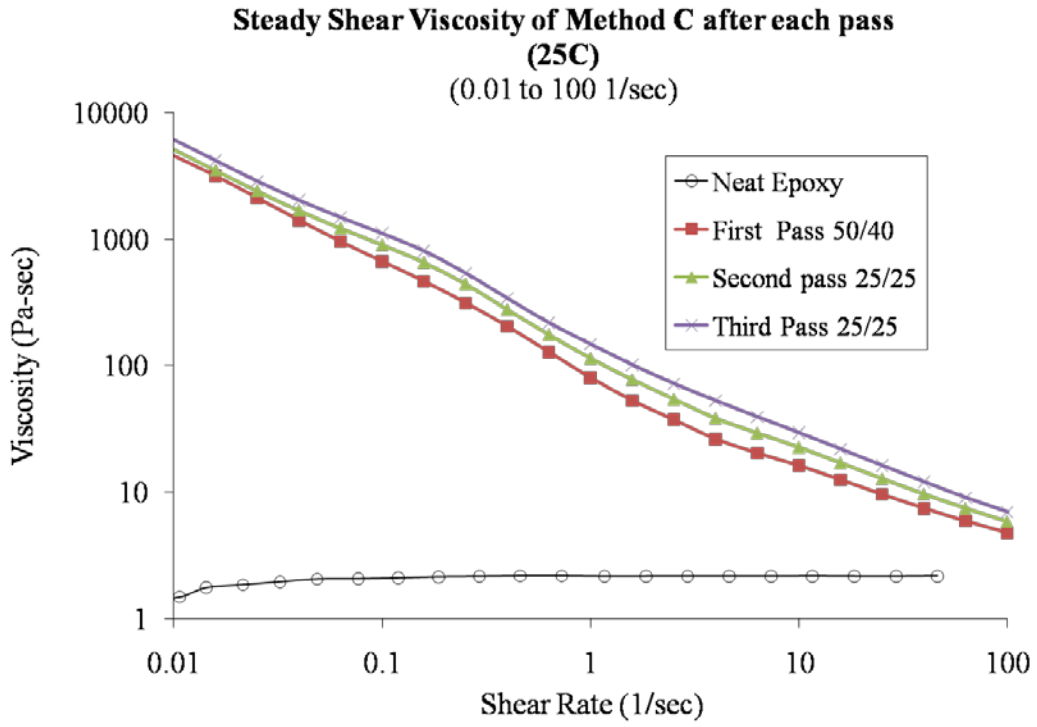

Figure 2-18 Viscosity of each pass for mixing method C.

Photos were taken using UV fluorescence microscopy to quantify how well dispersed the MWNTs were in the epoxy matrix. The images suggest that the least effective of the above mixing methods in table 2-4 was the shortest method C; while the other half of the methods that mixed for a longer number of passes generally produced better dispersions.

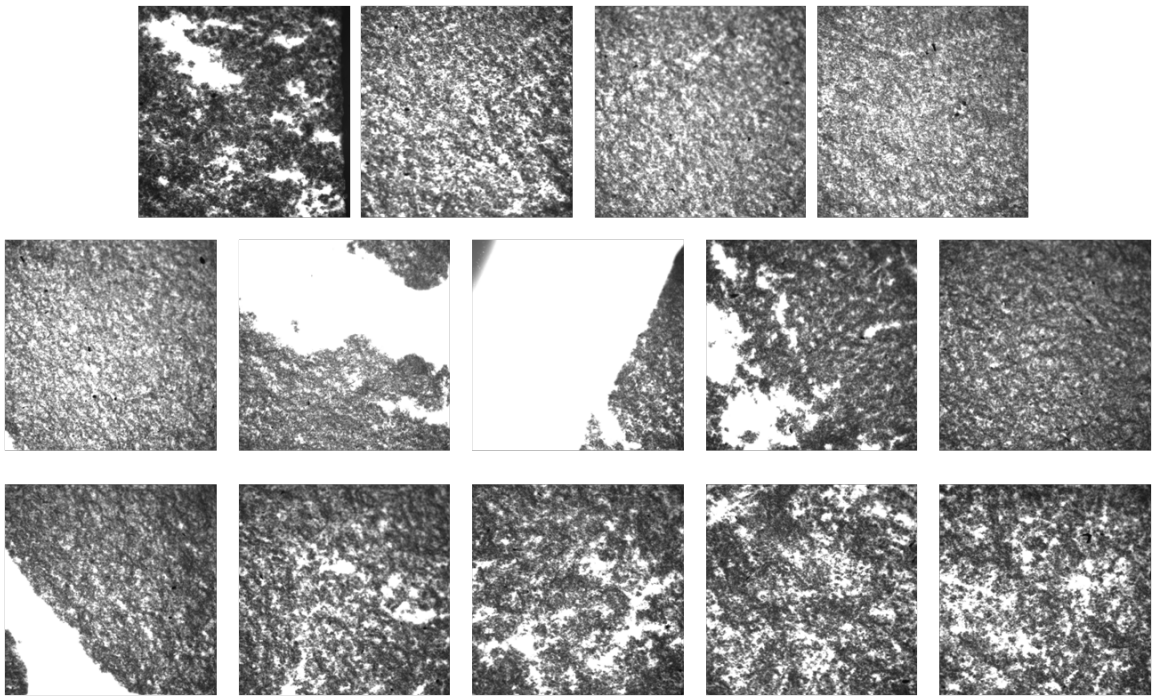

Figure 2-19 Method A UV fluorescence microscopy photos at 20x.

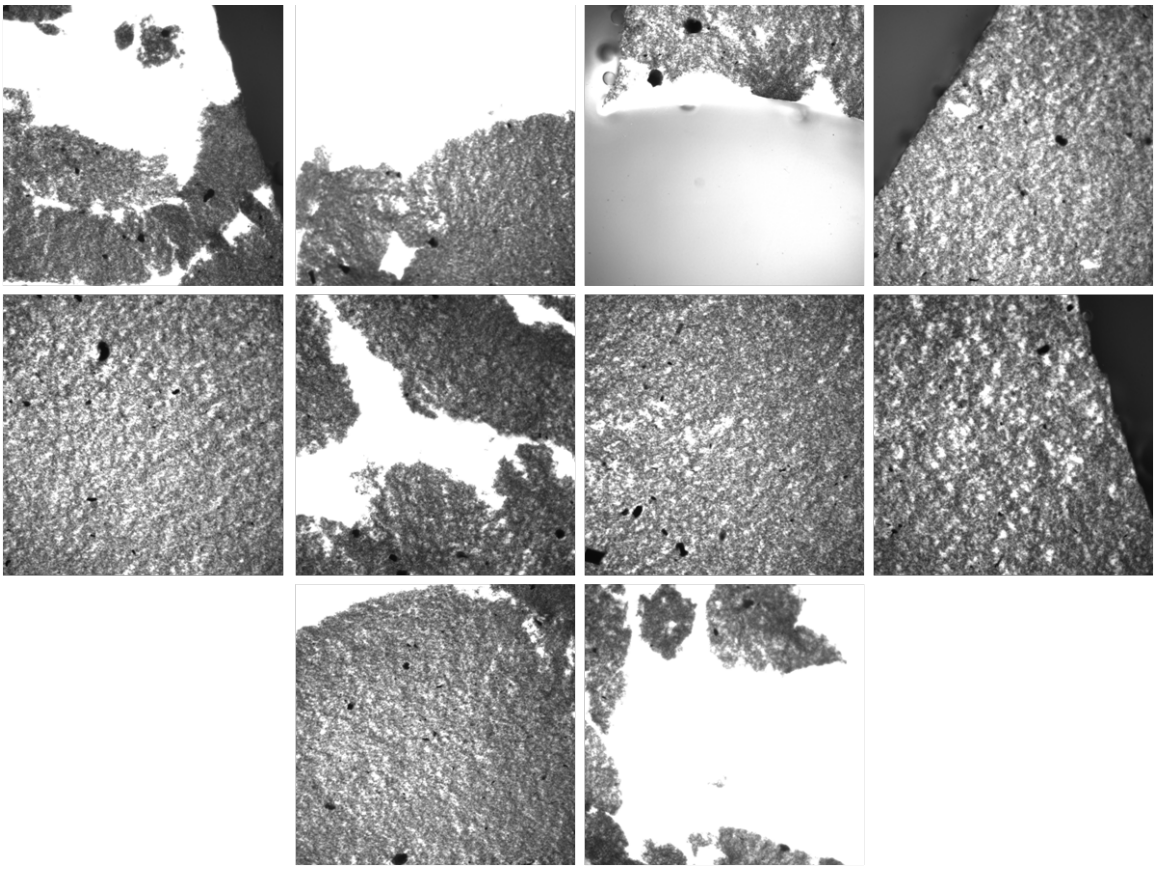

Figure 2-20 Method B UV fluorescence microscopy photos at 20x.

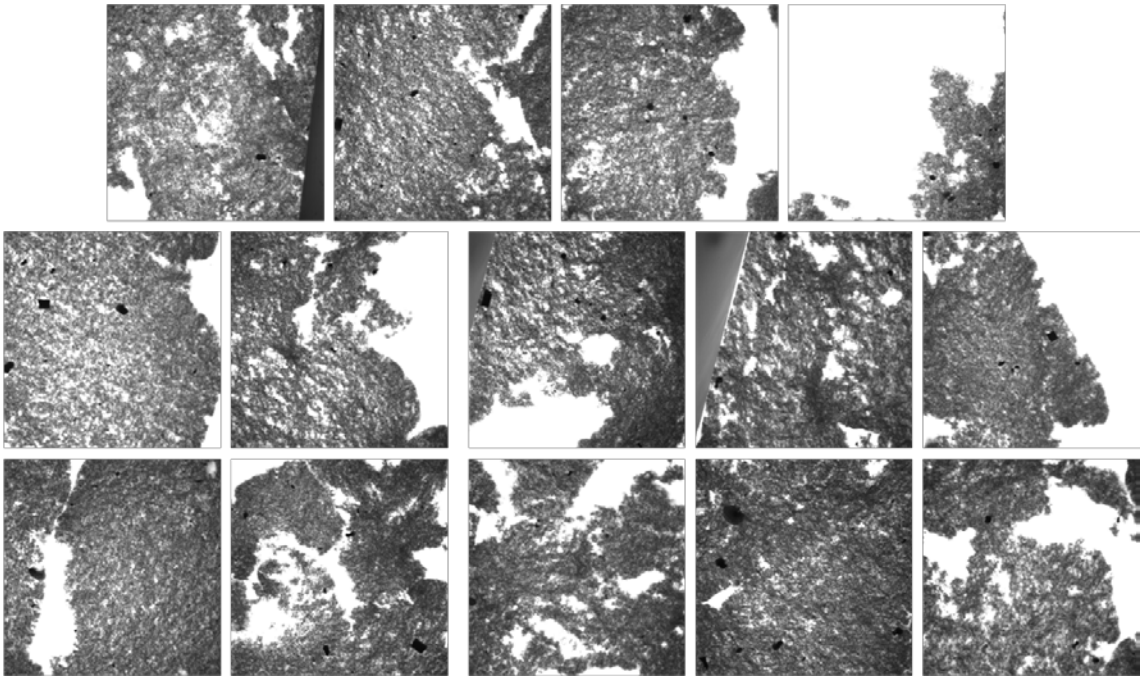

Figure 2-21 Method C UV fluorescence microscopy photos at 20x.

Less intensive mixing leaves small agglomerates of nanotubes that can be easily seen in the photos for mixing method C in figure 20. Regardless of the mixing method used and how well the nanotubes are dispersed, the resulting cured samples show roughly the same bulk resistivity for MWNT/epoxy composites.

Mixing Method	**Resistivity (ohm*cm^2)**
Old Mixing Method	100.99
A	29.53
B	33.81
C	34.88

Table 2-5 Resistivities of revised mixing methods at 100rpm.

All of the new mixing methods that employed a slower speed resulted in composites that were twice as conductive as composites prepared using the original mixing method. This result can be attributed to slower mixing speeds that caused less shear stress to the nanotubes and presumably less damage. By keeping more of the nanotubes intact they retain a higher aspect ratio and are able to form an overall better percolating network.

The next key element of the mixing process that was investigated was the speed at which the mixing took place. Gap distance and angular velocity or the speed of the rollers are key contributors to strength of the shear stress which the nanotubes undergo during mixing in the 3-roll mill.

Resistivity testing on these samples show improvement is gained by lowering the speed. Mixing method C from earlier was examined using the mixing speed of 60 and 30 rpm and compared to previous resistivity results.

Mixing Method **1) 50/50 2) 25/25 3) 25/25**	**Resistivity (ohm*cm^2)**
100 rpm	34.88
60 rpm	25.96
30 rpm	40.85

Table 2-6 Resistivity from 0.5% MWNT vol loading in Epoxy mixed with Method C at various speeds.

There is no clear improvement in resistivity by reducing the speed to lower than 100 rpm. The results are all within a small range of resistivity, indicating a small degree of batch-to-batch variations in the samples. This indicates there is no point to further slowing the rollers and increasing the mixing time because there will be no benefit to the overall improvement of the conductivity of the composite material.

These experiments have demonstrated the relationship between unfunctionalized raw MWNTs in epoxy. Later the relationship between functionalized MWNTs in epoxy will be address under similar conditions.

Chapter 3

The Birch Reduction: Key to a Synthetic Handle

During World War II German pilots were flying at abnormally high altitudes during the Battle of Britain and according to the Polish Underground, the pilots were able to handle the high altitudes because of cortisone injections given to the Luftwaffe fighter pilots. This cortisone was synthetic, made available by German chemists. While corticosteroids have no real effect on the ability of pilots to fly higher, intelligence gathered by the Allies that German submarines were transporting large amounts of bovine adrenal glands from Argentina at the time convinced the British that they needed to find their own steroid alternative.[34] The British wanted an analogous steroid that could be given to their fighter pilots and Robert Robinson at Oxford University tasked his former student Arthur J. Birch to continue his graduate work on steroids to find a British hormone alternative for the Royal Air Force.[35]

Birch's instead of carrying out the steroid work that Robinson wanted, he was trying simple synthetic methods inspired by the work of John and Rita Cornforth and C.B. Wooster. Birch carried out a reduction of anisole in liquid ammonia in the presence of sodium and an alcohol to make β, γ-cyclohexanone.[36]

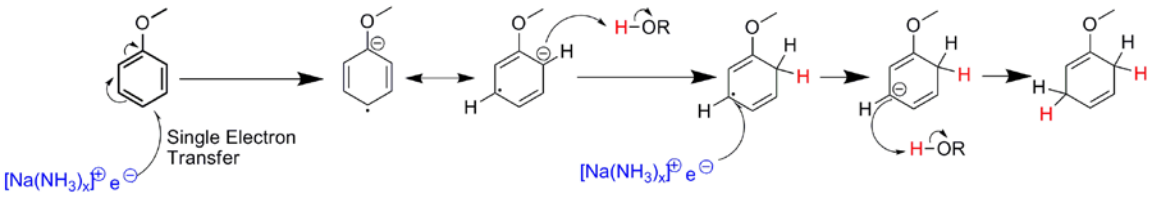

Figure 3-1 Mechanism for Birch reduction of anisole to β, γ-cyclohexanone.[37]

Birch quickly realized the synthetic value of this reaction because it could reduce aromatics partially rather than completely as occurs with catalytic hydrogenation. This

reaction was an essential and useful way to partially reduce estrogenic steroids to androgenic steroids.

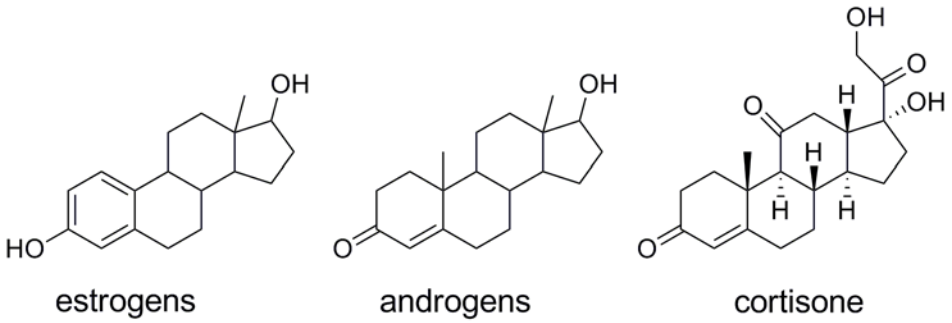

Figure 3-2 Structures of steroids.

The reaction might have been coined the Robinson-Birch reduction were it not that Robinson was infuriated to find out that Birch had been experimenting with solvated metals in ammonia rather a pursuing a traditional synthetic approach for steroids and wanted nothing to do with the publication. This useful synthetic route was later used by Frank Colton to create the first birth control pill, norethynodrel in 1952.[38]

Birch would later carry out a reductive alkylation on 2,5 dihydroanisole in the presence of potassium amide in ammonia with the addition of methyl iodide to produce 3-methyl 2,5 dihydroanisole.[39]

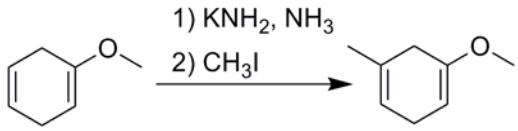

Figure 3-3 Birch alkylation.

It would not be till later that Loewenthal would first demonstrate the single step reductive alkylation of an aromatic compound.[40]

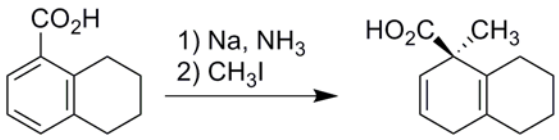

Figure 3-4 Conditions for the first single step reductive alkylation of an aromatic compound.

The formation of a C-C bond using the Birch-derived carbanion in the presence of an alkyl halide is a useful way of installing alkyl groups onto aromatics. In addition to use in small molecule chemistry, this synthetic method can be utilized in nanotube chemistry since a nanotube is essentially just many aromatic rings.

Pekker showed in 2001 that thru metal dissolution in ammonia in the presence of a proton source that "corrugation" of the layers of the MWNT occurs and can interpreted as the formation of sp^3 centers with a new covalent bond to carbon.[41] Pekker's TGA-MS data that shows when their hydrogenated MWNTs are heated under argon, a small mass percentage of hydrogen and methane is released. TEM photos show that a distinct change occurs to the morphology of the layers of nanotubes. Billups in 2004 carried out reductive alkylation of MWNTs using conditions identical to Loewenthal, using alkyl halides ranging from n-butyl iodide to n-dodecyl iodide,[42] producing alkylated MWNTs. Following this lead, Tour has shown that under the same conditions that reductive alkylation occurs on MWNTs with alkyl halides.[43]

Terrones et. al. have also demonstrated that thru aggressive HNO_3/H_2SO_4 oxidation of MWNTs followed by Birch reduction conditions that the tubes are effectively torn open longitudally from end cap to the middle, exfoliating the exterior layer of grapheme.[44] It was also shown that lithium ion intercalation disrupts the inner

graphitic layers of the MWNT with the introduction of hydrogen being covalently bonded to carbons in place of aromatic carbon carbon double bonds.

Lithium intercalation in graphite has been known since the 19th century and analogous similarities can be drawn with intercalation of lithium in MWNTs.[45] The interlayer spacing in MWNTs is ~0.34nm, similar to that of graphite and the size of a Lithium ion is 0.068nm; intercalation within layers of the MWNT is very likely to happen as long as there is an opening from defects in the wall of the exterior nanotube.[46] This theory of intercalation of the lithium ions between graphitic layers is reinforced by recent work by the Meier group showing that when similar Birch reduction conditions are carried out on nitrogen-doped MWNTs that the exterior graphitic shell is torn open to reveal the inner stacked cup features of the N-doped MWNTs.[47] This change to the morphology of the nanotube should allow for covalent bonding at sites other than just edges, defects, or end caps. Using an alkylating reagent of choice, C-C bonds can be formed and further functionalities can be placed on the exterior graphite layer of the MWNTs. Once a C-C bond is made between a MWNT and alkyl halide bearing another functional group, the synthetic chemist has an effective handle from which to do further chemical manipulations, potentially tuning the properties of the MWNT to desired specifications.

The utility of these reductive conditions is that when MWNTs are placed in Li/NH_3 solutions they become charged and repel one another. It is essential to debundle or un-rope agglomerates of nanotubes in order to expose every possible site for functionalization.

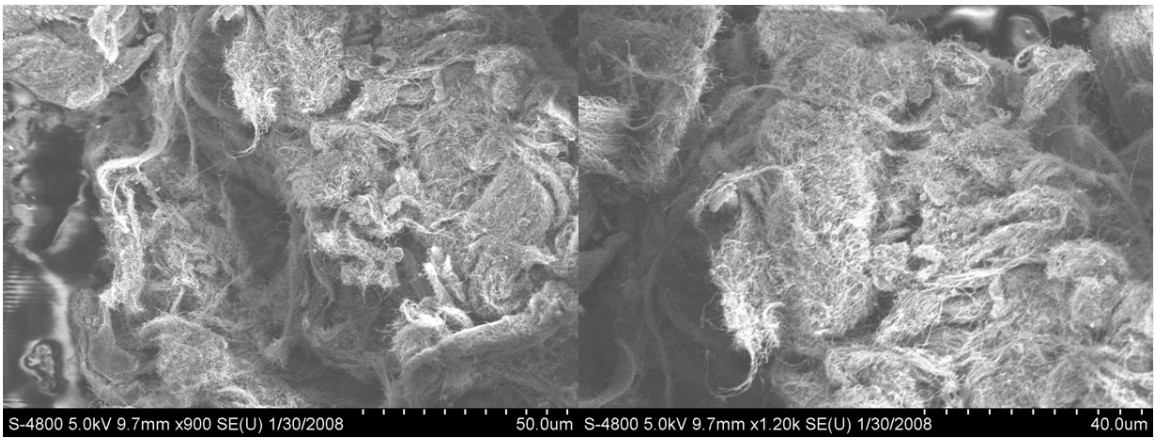

Figure 3-5 SEM photos of agglomerated raw MWNTs.

MWNTs produced at CAER are formed into arrays of nanotubes that aligned vertically into forests, however when they are harvested and scraped from the quartz substrate they tangle and rope unto one another as shown in figure 3-5.

Reductive alkylation conditions can help to disperse MWNTs in solution, and previous work has shown that using alkyl halides can install alkyl groups on the exterior surface of the MWNTs. However, there is significant difficulty in measuring a chemical yield, or measuring the degree to which the MWNTs have been functionalized. The typical tools that a chemist would use to identify and quantify small molecules produced in the lab, such GC-MS, NMR, and LC, are nearly useless in the field of nanotubes where the material is heterogeneous and insoluble. In order to quantify and prove the validity of this synthetic methodology, an experiment was devised in attempts to confront this issue. The most efficient and predictable tool we had at our disposal was the TGA. A dramatic and noticeable change in the weight of the sample as the temperature was elevated was need in order to quantify a mass loss that could translated into how much of alkyl substituent was covalently bonded to the surface of the nanotube. In order to do this an

alkyl group would need to be installed and then further modified to show a predictable weight loss in the TGA dependent on how secondary modifications.

Obtaining a percent yield?

A reductive alkylation was carried on MWNTs using allyl bromide to install an allylfunctional group on the exterior of the MWNTs. These allylated MWNTs (**4**) were then mono (**5**) and di-brominated (**6**).

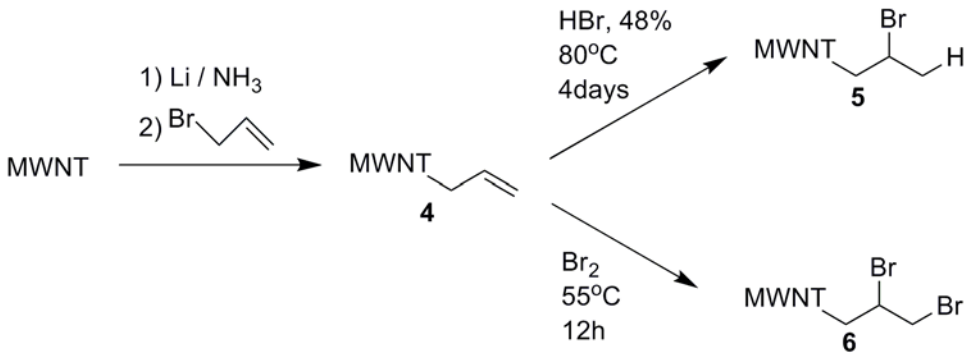

Figure 3-6 Synthetic route to brominated MWNTs.

By carrying out this synthetic strategy the hope was there would be distinct mass loss in the TGA due to the eliminatiion of HBr prior to the combustion of the nanotube. If this could be seen in an appreciable amount, the molar ratio of bromine to carbon could be back calculated to find the extent of functionalization.

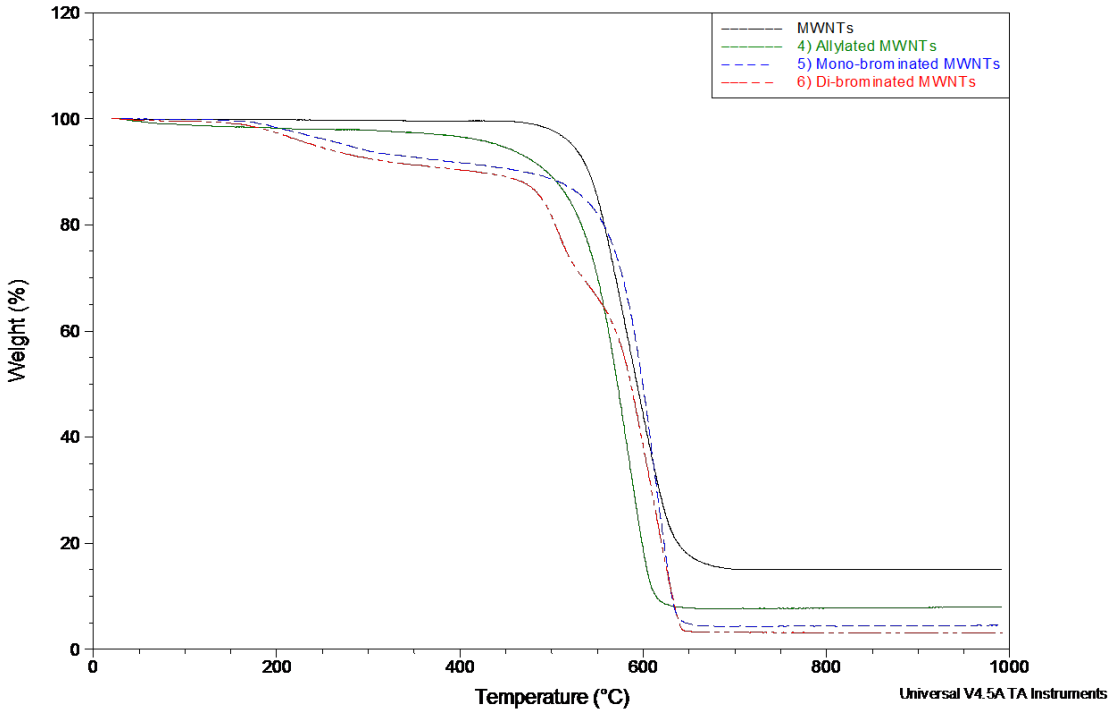

Figure 3-7 TGA of Allylated, mono and di-brominated MWNTs under air, heated at 20° C/min.

The TGA results in Figure 3-7 show that there is a stepped mass loss for both of the brominated MWNTs (**4** and **6**) that is not found with the allylated MWNTs or the raw MWNTs. For the mono-brominated MWNTs (**5**) there is only one mass loss ~200°C and for the di-brominated MWNTs (**6**) there are two mass losses: one at ~200°C and one at 500°C. These mass losses are consistent with loss of 1 eq.of HBr in the case of **4** and with the loss of 2 equivalents of HBr in the case of dibromide **5**.

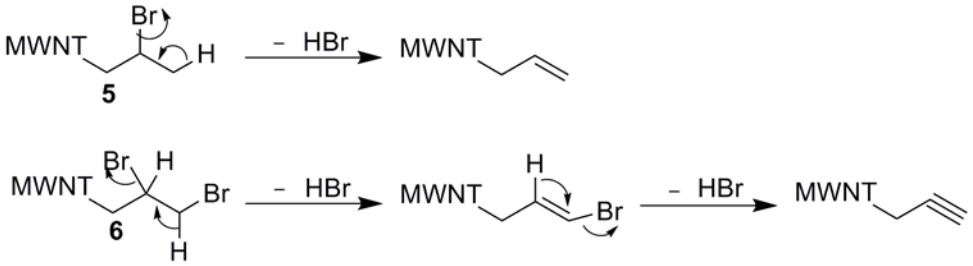

Figure 3-8 Scheme of dehydrohalogenation.

To rule out that these mass losses are from simple combustion of carbon from the nanotube, the samples were run again under the same heating conditions but under an inert atmosphere of nitrogen (carefully scrubbed to remove traces of O_2) in order to rule out any possibility of mass loss due to combustion.

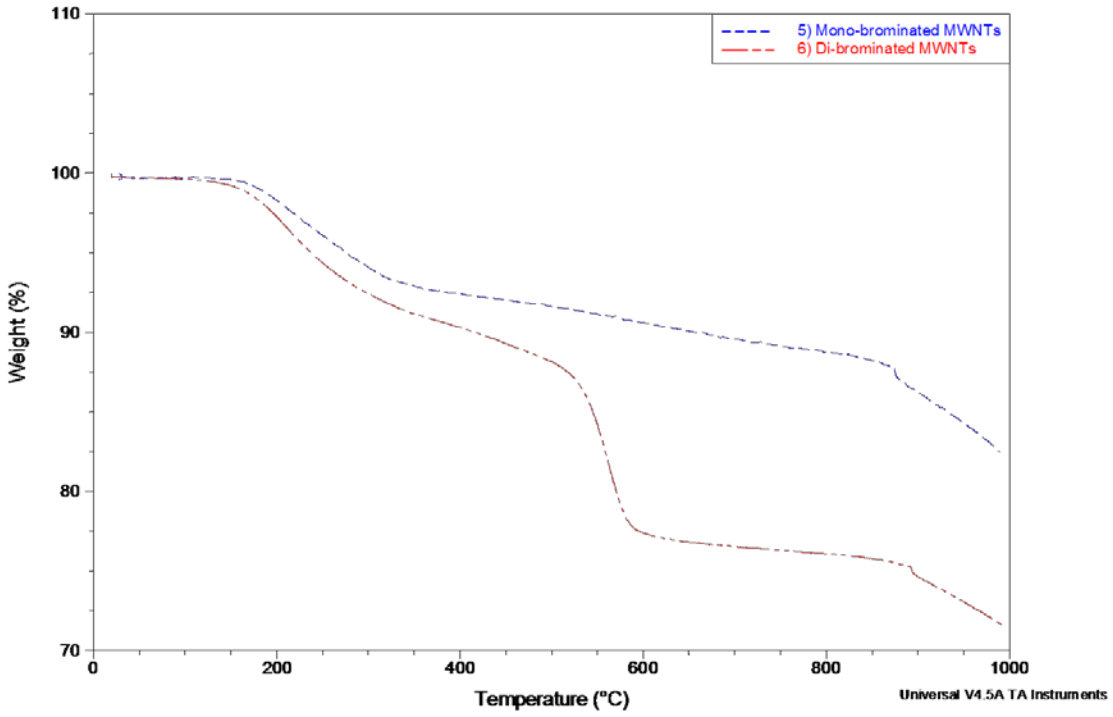

Figure 3-9 TGA of mono and di-brominated MWNTs under N_2, heated at 20° C/min.

Repeating the same experiment under a N_2 atmosphere reveals that the mass loss occurs in the same fashion, indicating that dehydrohalogenation, not combustion, is occurring over this temperature range. There is small amount of mass loss ~900^{o}C, likely due to a small amount of air that the scrubbers on the inline did not remove which is indicative of combustion of the nanotubes.

Maccoll has carried out extensive pyrolysis studies on isopropyl bromide and n-propyl bromide. These extensive kinetic studies show that elimination of HBr and the formation of propene occurs in a homogeneous first order reaction at a temperature range of 300-350 ^{o}C.[48, 49] Thermal decomposition of 1,2-dibromoethane to bromoethene also occurs in this temperature range.[50] These studies were carried out in a different apparatus and at a different pressure from that of the TGA furnace that was used in our experiment; however the observed elimination of HBr occurs in a temperature range that closely matches the temperature range of the first mass loss we observe by TGA. TGA analysis of vinyl chloride polymers show a mass loss and elimination of HCl at a temperature range of 200-300^{o}C.[51] All of these studies indicate that a similar temperature range to that our TGA results for dehydrohalogenation.

To better prove that the mass loss seen in the TGA, a TGA-MS experiment was carried out under N_2. The TGA-MS is similar to that of TGA in that samples are heated in a weigh boat in a heated sealed chamber that has inert gas flow into it and out to a fused silica line to into a mass spectrometer. Gases that evolve from the sample being heated should then be detected by the MS portion of the machine.

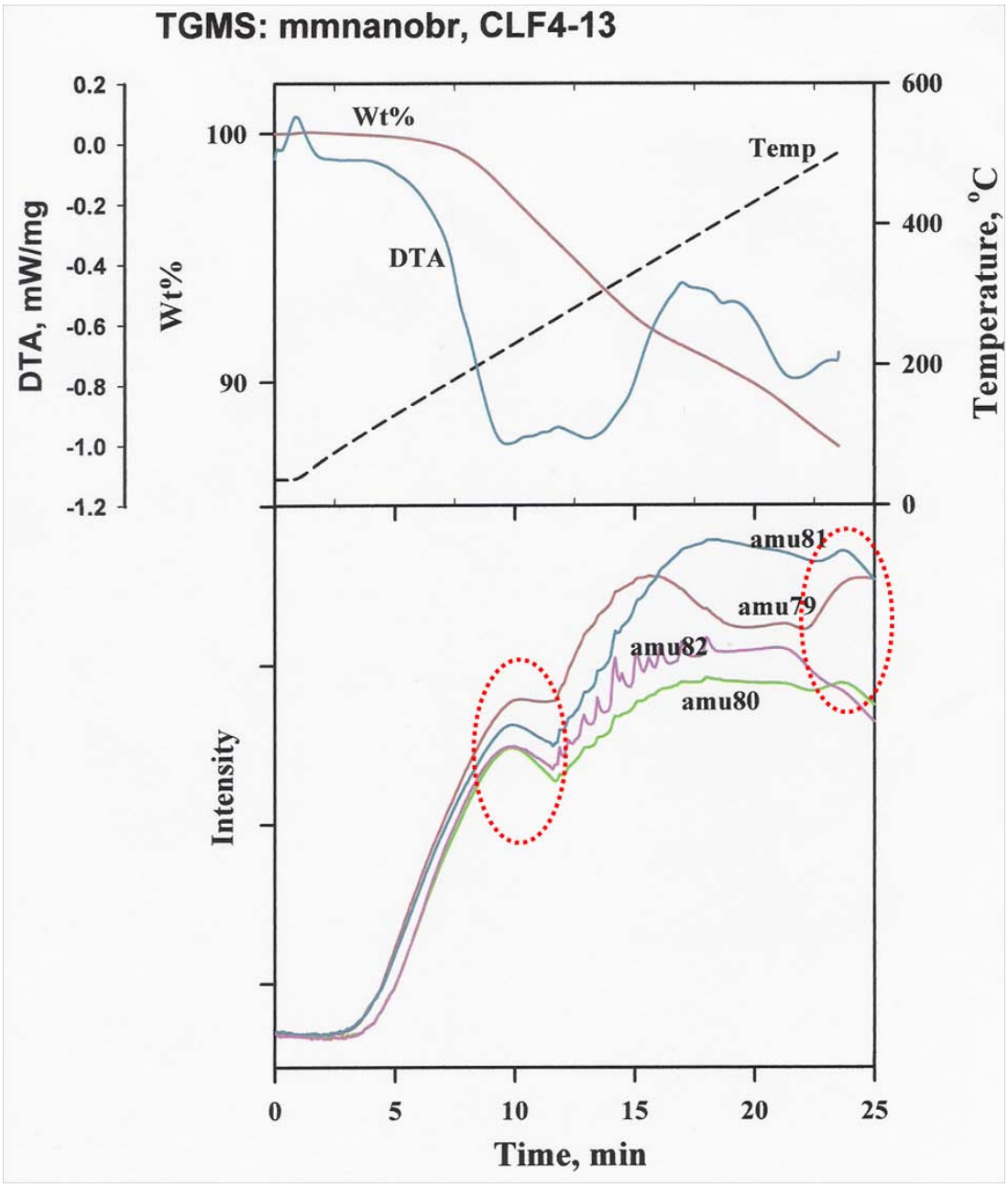

Figure 3-10 TGA-MS of 6) di-bromo MWNTs under N_2 heated at 20°C/min.

The results show that there is corresponding 79/81 amu ion peaks for bromide ions and 80/82 amu ion peaks for HBr at the temperature ranges in which there is mass loss. There is a clear bromine ion peak during the first mass loss, and then at the beginning of the second mass loss there is another ion peak for bromide again, although

unfortunately the temperature range of this experiment did not go high enough to span the second mass loss of HBr.

From the above case of the mono-brominated f-MWNTs, assuming that the mass loss in the TGA is due to elimination of HBr, a molar ratio of carbon to HBr can be back calculated from treating stepped weight loss as a gram weight and then convert it to moles using molecular weights. Also assuming that the MWNT dimensions are 12μm in length and 20nm in width with 7 graphitic layers and that layers are spaced ~0.34nm and a carbon atom width is 1nm, a surface area percentage can be calculated of the exterior layer of the nanotube. Using this percentage of surface area a comparison of the amount of carbon mass loss in the TGA to the functional groups or bromine loss can be made. By using these parameters the 7th exterior layer of the MWNT would encompass about 24% of all of the carbon in the nanotube.

$$11\text{g Br} \times \frac{1\text{ mol Br}}{79.9\text{g}} = 0.137\text{mol Br} = 0.137\text{mol functional group covalently bonded}$$

$$86\text{g carbon} \times 24\% = 20.64\text{g carbon} \times \frac{1\text{mol carbon}}{12.011\text{g}} = 1.72\text{mol carbon}$$

$$\frac{1.72\text{mol carbon}}{0.137\text{mol groups}} = 12{:}\,1 \text{ ratio carbon to functional group}$$

$$\frac{0.137\text{mol groups}}{1.72\text{mol carbon}} \times 100\% = 7.9\% \text{ surface area covered by functional groups}$$

Pekker's data from his TGA-MS experiments on his hydrogenated SWNTs can be used to calculate a similar measurement to validate our results.[41] Pekker's TGA-MS data shows a combination of H_2 and CH_4 to be 1.2% of the total mass of the hydrogenated SWNTs. Pekker later concludes that half of this hydrogen content is actually covalently

bonded, while the other half are intercalated protons based on similar experiment that prepared hydrogenated nanostructured graphite via a mechanochemical method.[52]

$$0.6\ \text{H} \times \frac{1\text{mol H}}{1\text{g}} = 0.6\text{mol H}$$

$$98\text{g carbon} \times \frac{1\text{mol carbon}}{12.011\text{g}} = 8.15\text{mol carbon}$$

$$\frac{8.15\text{mol carbon}}{0.6\text{mol H}} = 13.6\ \text{ratio carbon to functional group}$$

$$\frac{0.6\text{mol H}}{8.15\text{mol carbon}} \times 100\% = 7.36\%\ \text{surface area coverd by functional groups}$$

This is encouraging because the estimates closely match between our work and Pekker's. These experiments validate this methology and synthetic impact that reductive alkylation have on MWNTs. All of the further synthetic manipulations of this project hinge on this first key synthetic step, so emphasis must placed on proving it is carried out in an appreciable amount of functionalization.

Chapter 4

Further functionalization attempts without harsh conditions.

Our previous investigation of the effects of reductive alkylation on MWNTs mass loss at elevated temperature. These results show how a particular functionalized nanotube decomposes at these higher temperatures but doesn't illustrate how these nanotubes would react with one another in epoxy. These interactions can be quantified by how conductive the f-MWNT/epoxy composite. UV fluorescence photograph can capture how f-MWNTs disperse into the epoxy matrix. A simple experiment to quantify these changes is perform reductive alkylations with progressively large n-alkyl halides and show how larger and larger steric bulk affects how functionalized nanotubes interact with one another in the epoxy matrix. A study with similar conditions has been performed previously by Tour.

Tour's work shows that functionalization and the properties of the functional groups affect how nanotubes interact with one another in a solid, felt-like agglomerate of filter cake described as a buckypaper.[53] Tour had previously performed reductive alkylations of MWNTs using alkyl halides of varying chain length, including 1-iodododecane.[54] These resulting dodecyl f-MWNTs were filtered and dried on filter paper into a buckypaper. This dried aggregate of MWNTs was tested for resistivity against a control made from raw MWNTs. The dodecyl f-MWNT bucky papers were found to be five times more resistive than the raw MWNT control. HRTEM photos of a dodeycl f-MWNT show corrugation side wall layers and a clear change from the pristine side walls of raw MWNTs. The electronic structure and aromatic conjugation being compromised is a possible blame for this increase in the resistivity of these functionalized MWNTs.

Tour's experiment simply looked at f-MWNTs touching one another when dried on filter paper without polymer matrix as a medium for the composite. We have performed a set of experiments, that probe how the length of alkyl groups affect nanotube to nanotube interactions and nanotube-resin within an epoxy matrix. A series of functionalized MWNTs were synthesized by performing a reductive alkylation using alkyl halides of various lengths.

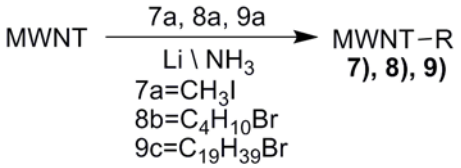

Figure 4-1 Reductive alkylation scheme.

The reductive alkylation of MWNTs with linear alkyl halides with 1, 4, and 19 carbons were carried out to produce (**7**) methyl f-MWNTs, (**8**) butyl f-MWNTs, (**9**) nonodecyl f-MWNTs. Progressively longer alkyl chain lengths were chosen in order to determine the how alkyl groups affect the interactions of the nanotubes within the epoxy matrix. We anticipated that longer alkyl chains should push nanotubes away from one another, essentially breaking up agglomerations and improving nanotube dispersion within the epoxy matrix.

The various alkyl chain f-MWNTs (**7 – 9**) were examined in by TGA under air to characterize them.

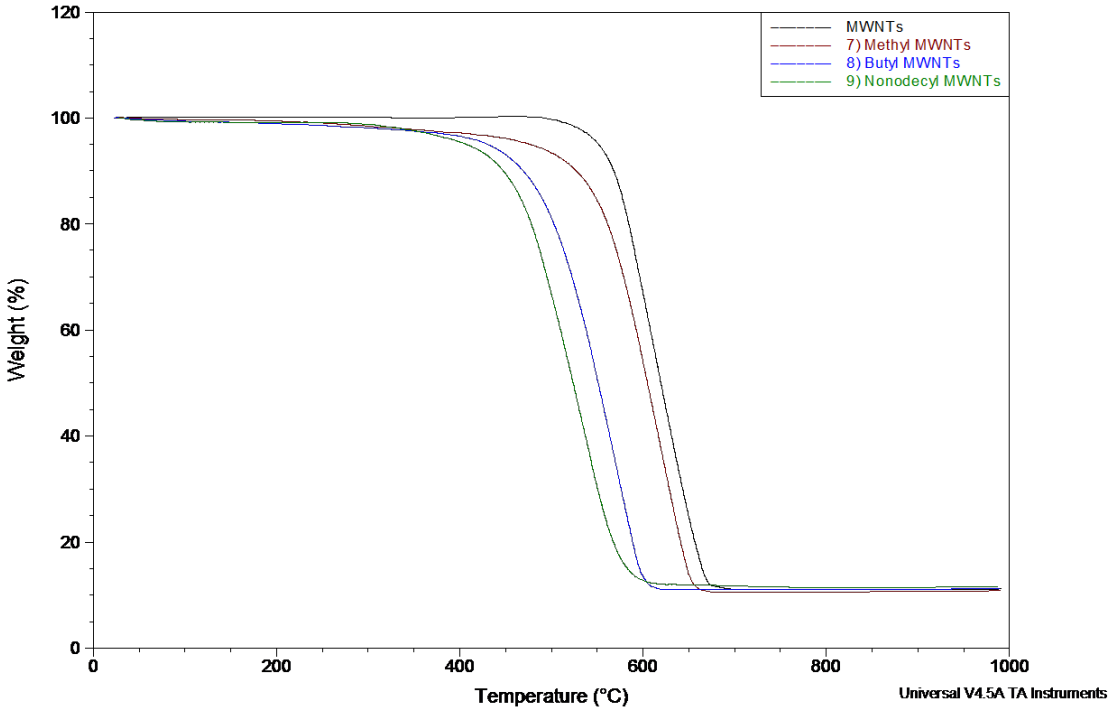

Figure 4-2 TGA comparison of various alkyl chain length f-MWNTs.

The TGA data shows that as the alkyl chain length of the alkyl group is increased, there is an earlier onset temperature of decomposition. This would indicate that are there more available sp^3 hydrogen-bearing carbons on the exterior of the nanotube, facilitating combustion as a better fuel than the typical sp^2 carbon found within the graphitic skeletal structure of the nanotube. Evidence of this functionalization is further reinforced by the viscosity data obtained from 1% vol loading of f-MWNTs in epoxy.

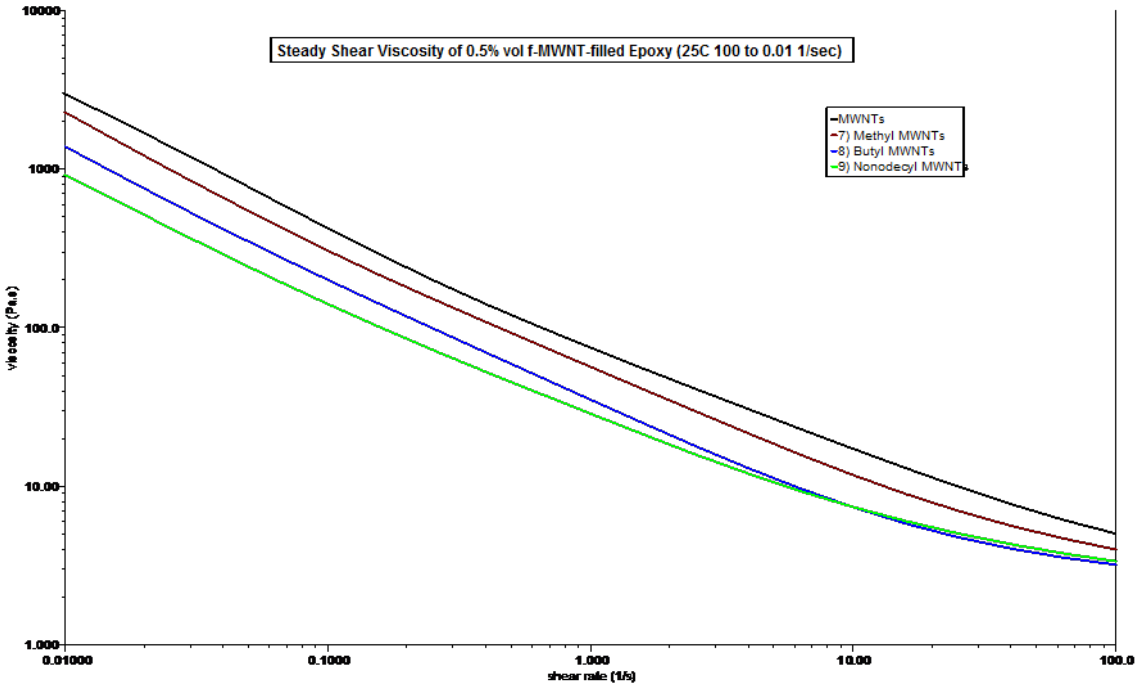

Figure 4-3 Viscosities of f-MWNTs (7 – 9)/epoxy composites, compared to raw MWNT/epoxy composites.

As shown in figure 4-3, longer the alkyl chain functional groups result in a lower viscosity in the MWNT/epoxy composite. Longer alkyl chains provide steric bulk to overcome the van der Waals interactions between nanotubes, forcing deagglomeration and improved wetting within the epoxy. Using UV fluorescence microscopy, photos were taken of each of the composites to evaluate the quality of the dispersion.

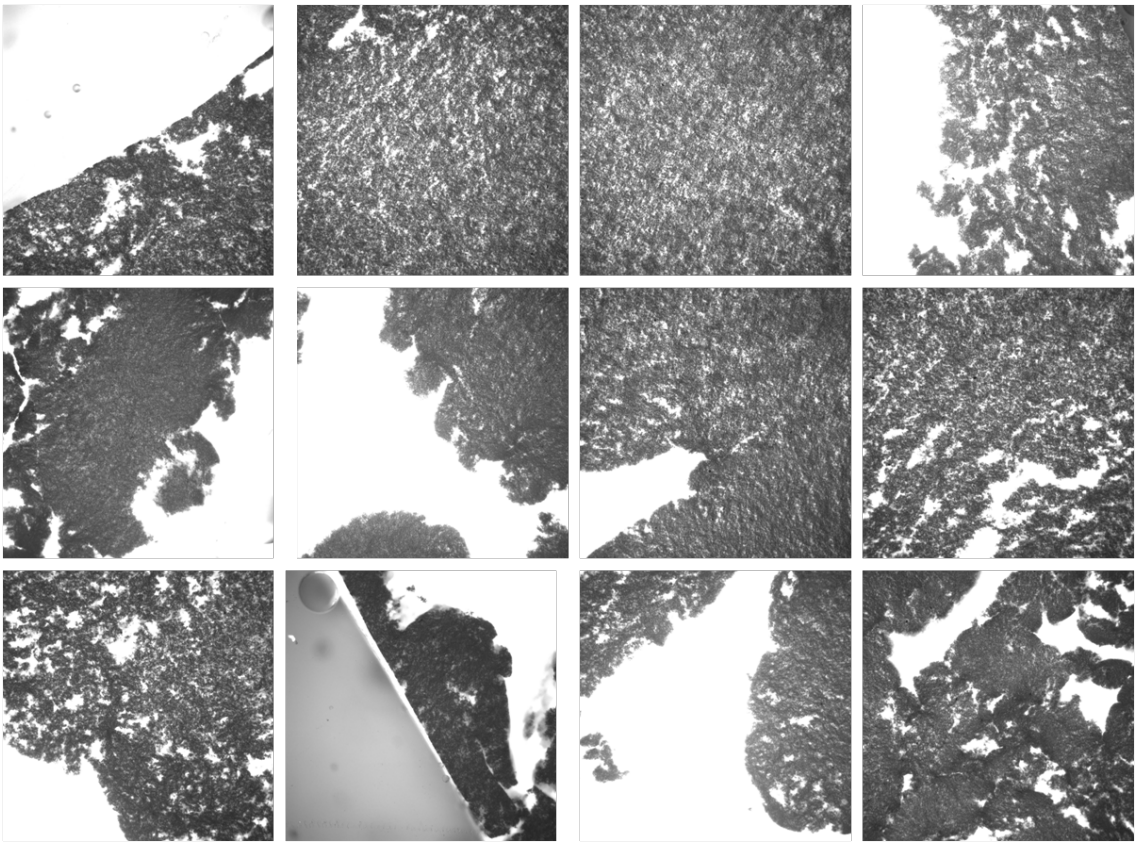

Figure 4-4 UV fluorescence microscopy photos of 0.5 vo%l loading MWNTs in epoxy at 20x magnification.

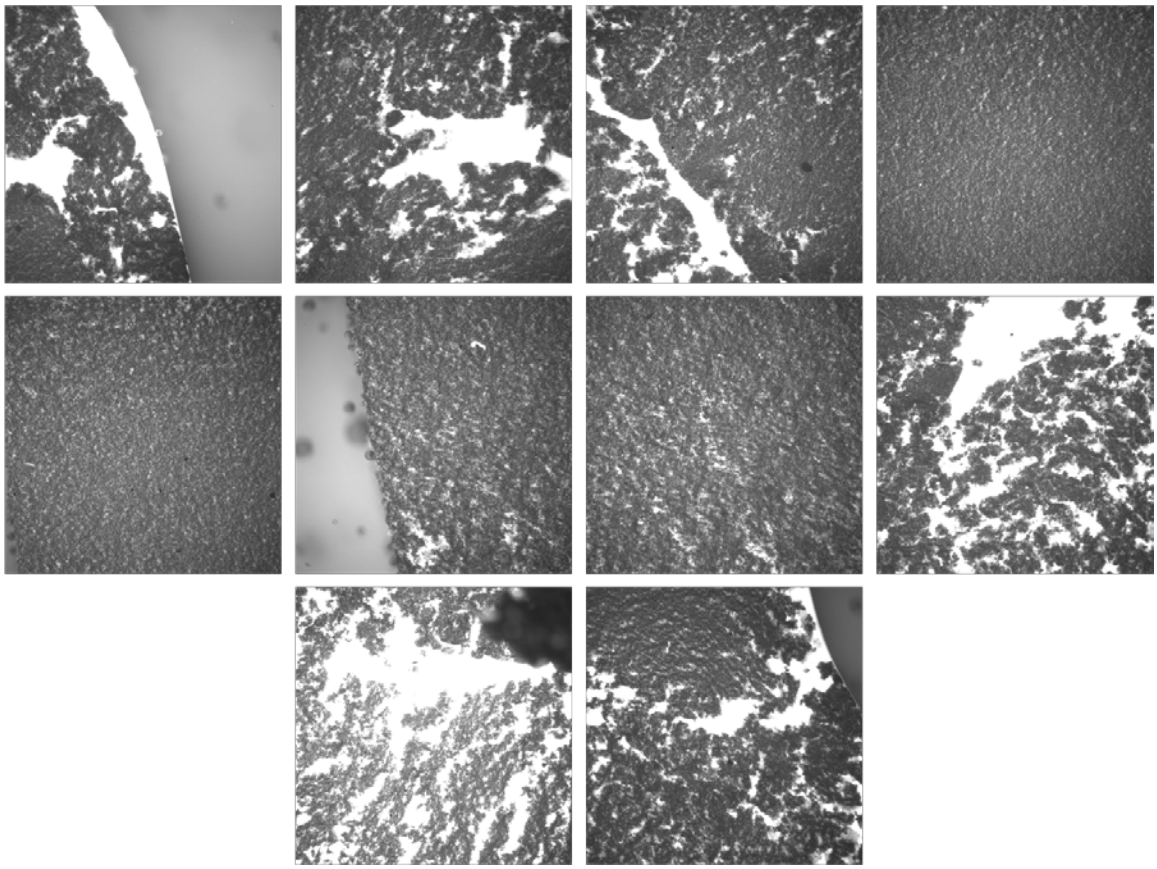

Figure 4-5 UV fluorescence microscopy photos of 0.5vol% loading of methyl f-MWNTs (7) in epoxy at 20x magnification.

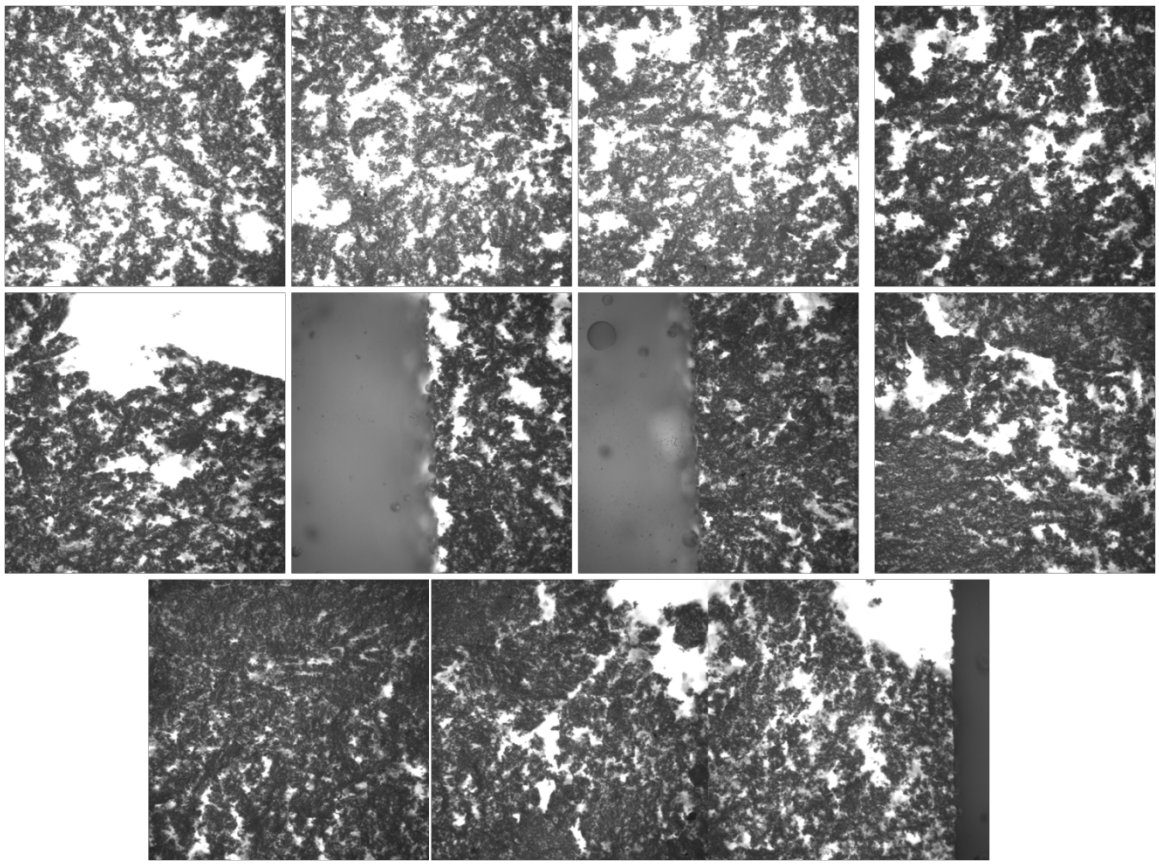

Figure 4-6 UV fluorescence microscopy photos of 0.5 vol% loading butyl f-MWNTs (8) in epoxy at 20x magnification.

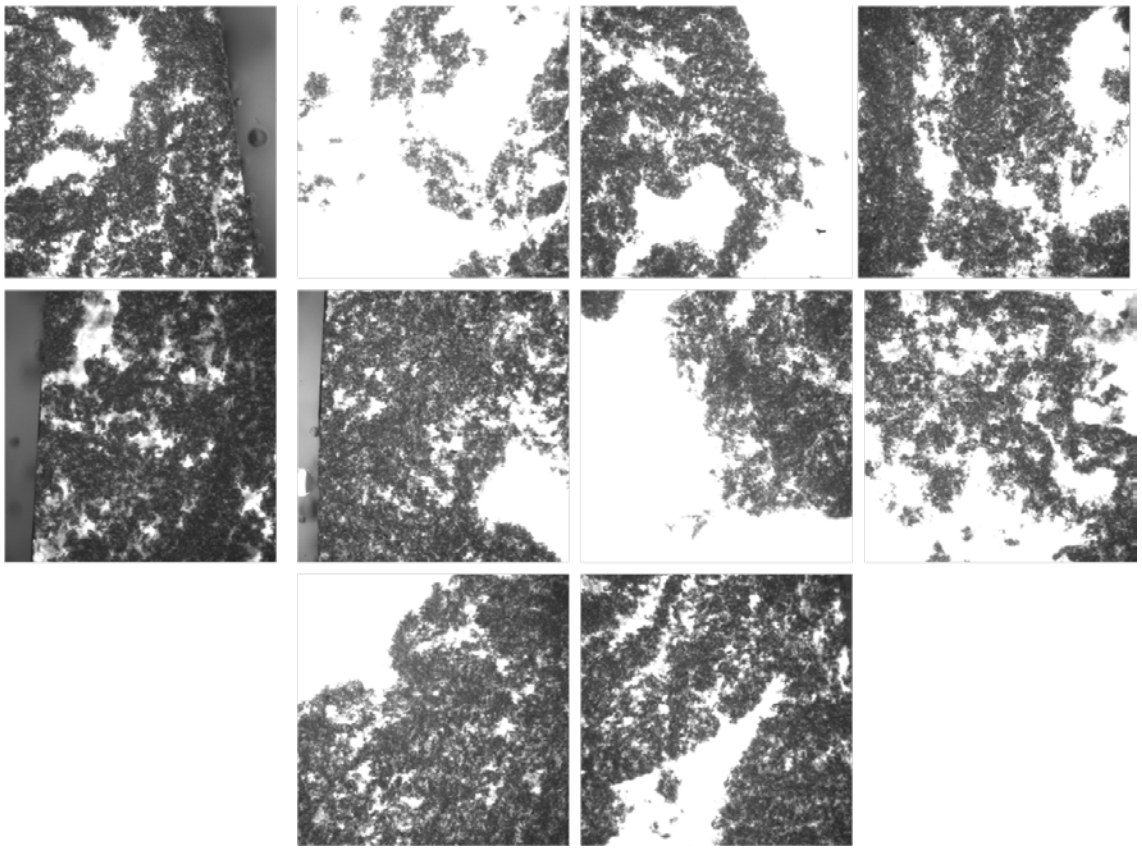

Figure 4-7 UV fluorescence microscopy photos of 0.5 vol% loading of nonodecyl f-MWNTs (9) in epoxy at 20x magnification.

The UV fluorescence microscopy photos show increasing chain length of the alkyl functional groups increases the frequency of nanotube voids within the epoxy matrix. The nonodecyl f-MWNTs clearly have large areas of epoxy free of any nanotubes. This ocular method of determining dispersion is not precise by any means but the viewer can judge that last set of photos is a less homogeneous dispersion than the previous sets of photos.

The lack of nanotube-nanotube interaction is further reinforced by the resistivities of the f-MWNT/epoxy samples. The photos reveal that as the alkyl groups grow longer in chain length, that the dispersion of the f-MWNTs within the epoxy becomes worse.

The raw MWNTs and the 1- and 4-carbon long alkyl f-MWNTs have fairly good dispersion with some voids. When the alkyl chain is extended to 19 carbons, it is obvious that the nanotubes are no longer dispersed evenly throughout the matrix and there are large voids where no nanotubes are present. This poor dispersion affects the overall percolation of the composite samples since the pathways for current travel now have been reduced, thus increasing the resistivity of the sample. The impact of the functionalization becomes apparent from the resistivity data shown in table 4-1.

Sample at 0.5 vol% loading in epoxy	**Resistivity (ohm*cm^2)**
Raw MWNTs	52.99
7) Methyl MWNTs	138.20
8) Butyl MWNTs	492.93
9) Nonodecyl MWNTs	14939.20

Table 4-1 Resistivities of varying alkyl chain length f-MWNT/epoxy composites at 0.5% vol loading.

Again a trend emerges: the longer the alkyl chain functional groups are, the higher the resistivity. As mentioned before, the steric bulk of the alkyl groups adversely affects dispersion. Improved interaction between the epoxy matrix and the nanotube leads to overall poor nanotube-nanotube interactions and this increases the contact resistance at these junctions where is it essential for electrons to be able to move from one nanotube to the next in order to permit percolation throughout the composite.

Chapter 5

Using Functionalization to Improve Dispersion.

As previously mentioned high aspect ratio fillers, such as carbon nanotubes, increase the viscosity of polymer composites greatly. In order to overcome this processing hurdle a functionalization of the nanotubes must be carried out to improve the wetting and dispersion of the nanotubes within the epoxy. To achieve improved interactions between a nanotube filler and the epoxy matrix, we have investigated the use of functional groups that will interact with the epoxy and anhydride components before and during the resin curing step. By introducing a carboxylic acid functionality onto the surface of the MWNTs, we hoped to improve the interactions between the surface of the MWNTs and the polymer matrix, as well as to create an opportunity for the formation of covalent bonds between the nanotubes and the matrix.

The route in which this was achieved was by a dissolving metal reduction of MWNTs, followed alkylation with ethyl bromoacetate to produce ester f-MWNTs (**10**). Following the reductive alkylation, the ester f-MWNTs (**10**) were saponified to produce carboxylic acid f-MWNTs (**11**).

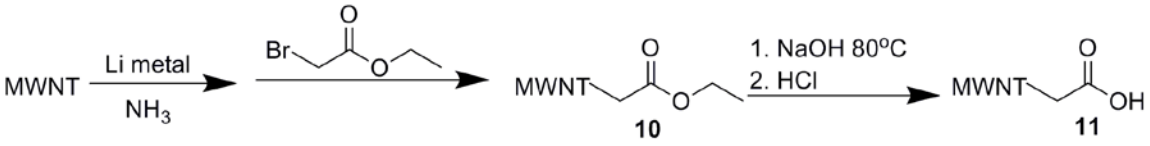

Figure 5-1 Synthetic route to functionalize MWNTs with carboxylic acid functional groups.

Once carboxylic acid functional groups decorate the exterior of the MWNT, the carboxylic acid can act as a nucleophile that can open the epoxide rings and the anhydrides within the resin mixture.

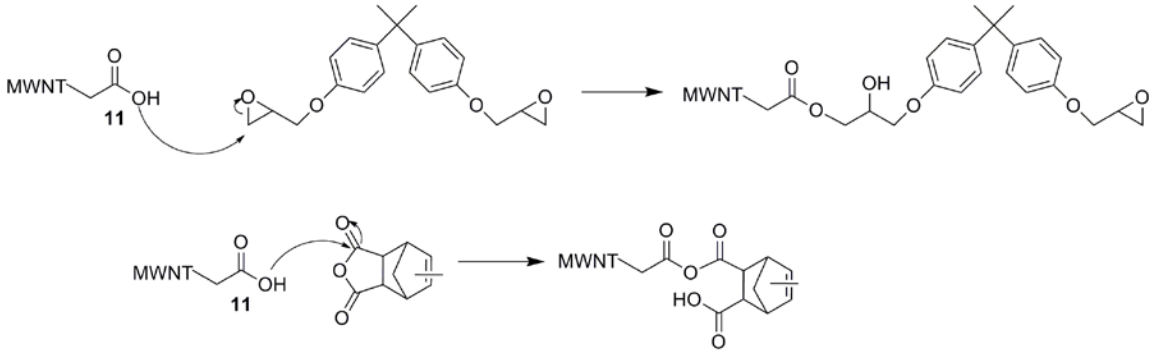

Figure 5-2 Examples of carboxylic acid reactions with epoxide rings and anhydrides.

By improving MWNT-polymer interactions, the dispersion of nanotubes within the composites should be improved. By adding carboxylic acid functional groups that will have an affinity for the polymer matrix, it will overcome the van der Waals interactions between nanotubes which cause roping and agglomeration. Functionalization has observable differences in the properties of the MWNTs as shown from TGA data.

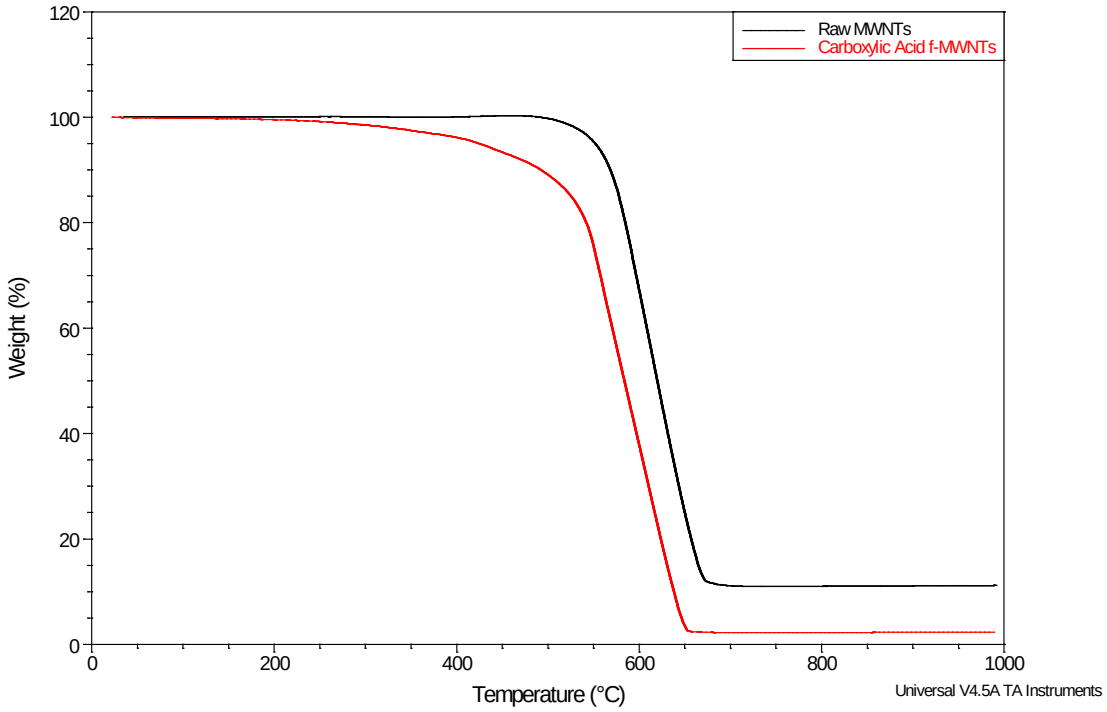

Figure 5-3 TGA comparing raw MWNTs (black line) vs. carboxylic acid f-MWNTs (11, red line) .

The TGA data does not show evidence of covalent carbon to carbon bonding on the exterior surface of the MWNT, however it does show a change from the starting raw MWNTs to that of carboxylic acid f-MWNTs (**11**). The amount of noncombustable residue is reduced from about 10% to near 0%, consistent with loss of residual catalyst during the various reactions involved in installation of the carboxylate group. The oxidative stability of the sample is also reduced and this is reasonable, as non-graphitic carbon has been added (the $–CH_2CO_2H$ group) and some graphitic regions of the MWNTs have been converted to non-graphitic, sp^3 carbon. This TGA data, in conjunction with further epoxy/MWNT composite data, provides indirect evidence of covalent bonding to the exterior of the nanotube.

Viscosity data of epoxy composite with 1% volume loading MWNT shows that it is less viscous than a composite with raw MWNTs at the same loading.

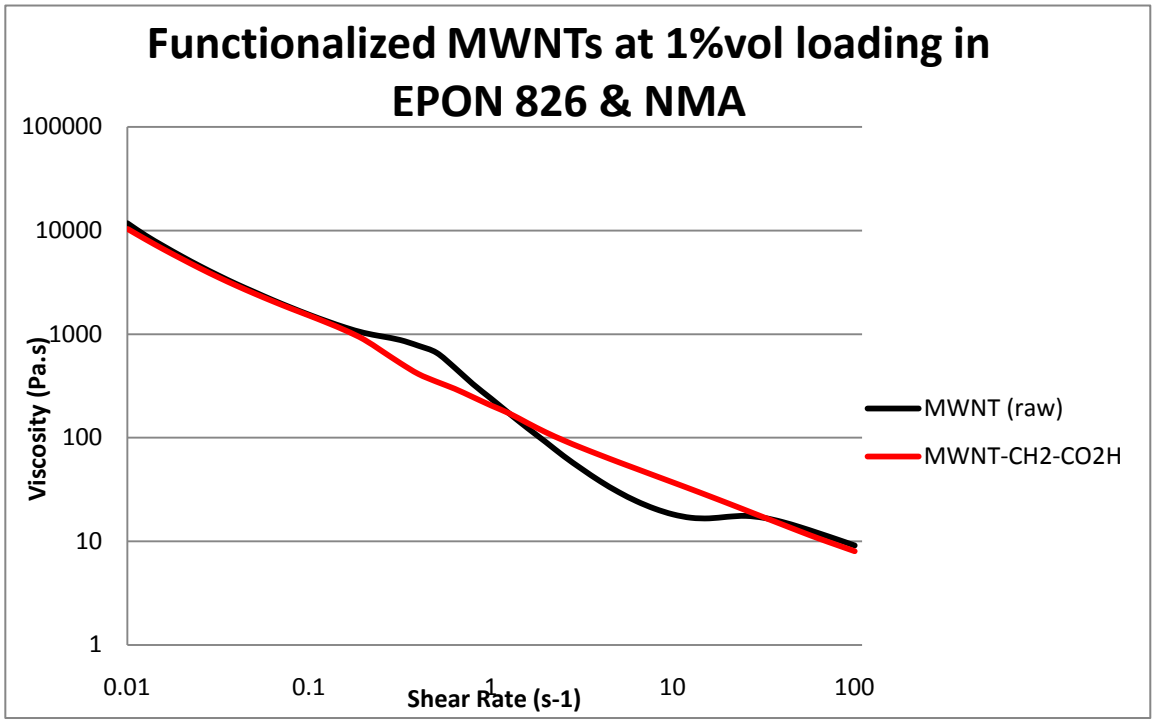

Figure 5-4 Comparison of the viscosity of epoxy resin composites containing 1 vol% raw MWNTs (black line) and 1 vol% carboxylic acid f-MWNTs (red line).

MWNTs have a natural tendency to form tangles and agglomerates after they have been harvested from quartz substrates used in production. We believe that the observed decrease in viscosity of the composite material is due to deagglomeration of MWNT bundles and their subsequent alignment within the shear field of the parallel-plate geometry used for these measurements. Dispersion photos taken with UV fluorescence further demonstrate a change in the properties of these f-MWNTs from those of raw MWNTs.

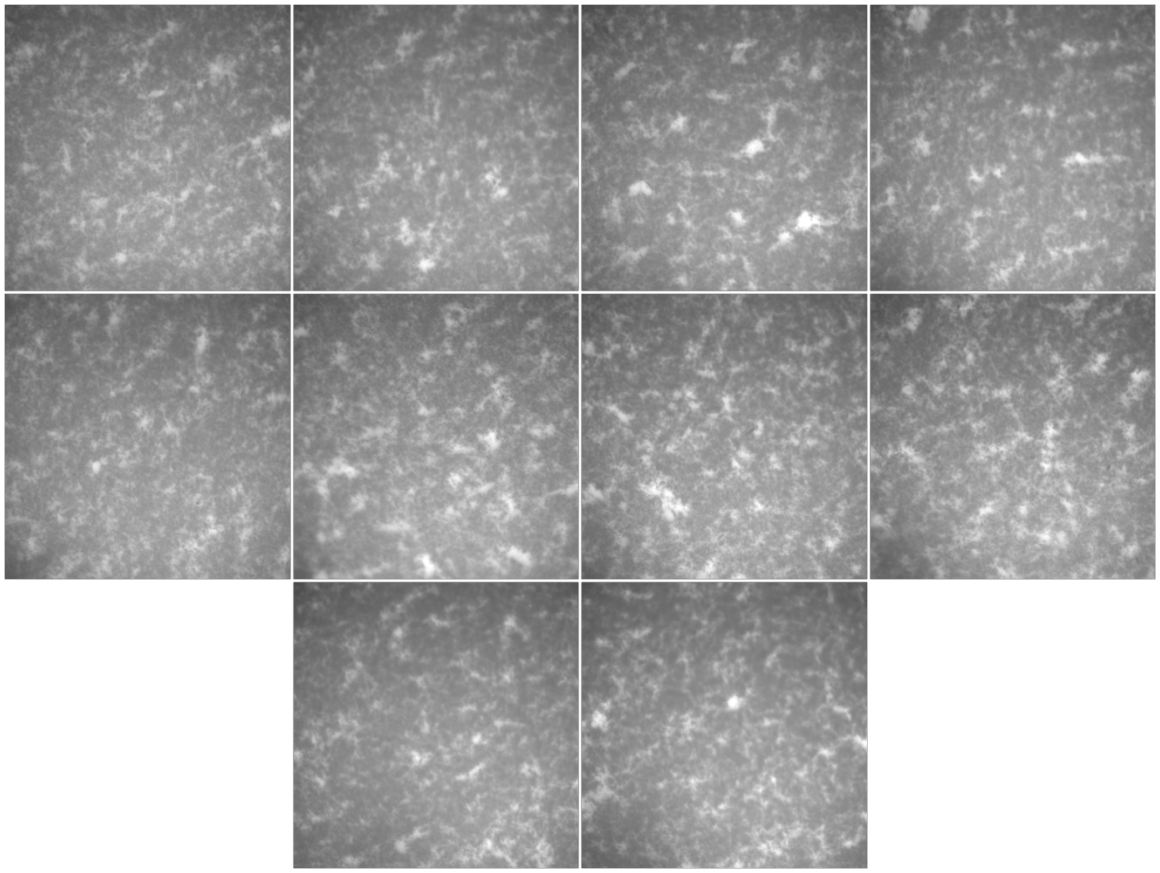

Figure 5-5 UV fluorescence microscopy photos of 1 vol% loading of carboxylic acid f-MWNTs (11) in epoxy at 40x magnification.

These photos, although taken at 40x instead of the typical 20x as seen previously, show a good dispersion of f-MWNTs within the epoxy. This continues to built upon the lower viscosity results indicating little or no large agglomerates of nanotubes throughout the epoxy matrix. The benefit of decreased viscosity of the epoxy/MWNT composite appears to come at the cost of the conductivity of the sample. By overcoming the favorable van der Waals interactions between nanotubes, by introducing steric bulk of functional groups and enabling better interactions with the epoxy matrix via the carboxylic acid, resistivity is increased due to a reduction in the number of intimate contacts between nanotubes.

Sample at 1% vol loading in epoxy	Resistivity (ohm*cm^2)[a]
Raw MWNTs	100.95
Carboxylic Acid f-MWNTs	950.08

Table 5-1 Resistivities of Raw MWNTs vs. carboxylic acid f-MWNTs at 1% vol loading in epoxy composites mixed using "Short mixing Method".

[a]Measured using the 4-point method.

Another property of carboxylic acid f-MWNTs that could be responsible for both the decreased viscosity and conductivity of the composites is a decrease in the aspect ratio of the nanotubes. The length of the nanotube may be decreased due to breakages from mechanical stirring, from harsh acidic or basic conditions that cause damage to the overall morphology of the nanotubes, or from shear in the process of mixing MWNTs into the epoxy. The latter seems unlikely, as the raw MWNTs were mixed into the resin in the same manner as were the f-MWNTs. The saponification step, used to convert the ester (**10**) to the carboxylic acid (**11**), includes using strong base at elevated temperatures and this may cause a significant change to the aspect ratio of the nanotubes. Treating nanotubes to harsh acidic conditions using H_2SO_4/HNO_3 at elevated temperatures has been shown to shorten the nanotubes[55-57] and to decorate the exterior of the tube with phenolic, aldehyde, and carboxylic functional groups.[57] It has also been shown that by performing harsh acidic treatment to the MWNTs followed by subsequent Birch reduction conditions that the nanotubes are sliced opened.[58] Tour has recently found that treating MWNTs with H_2SO_4 followed by $KMnO_4$ and heat, led to the nanotubes longitudinally unzipping to form sheets of graphene.[59] Galiotis recently published a report showing that mild oxidative treatment of MWNTs with H_2O_2/NH_4OH improved

the conductivity of the MWNT/epoxy composite because of the removal of amorphous carbon. However harsh acid treatment damages nanotubes and lowers conductivity.[60]

This extensive precedence for changes in the morphology of the nanotubes from harsh oxidative treatment suggests that the saponification treatment could change the length and diameter of the nanotubes. One member of our group (Delphine Franchi, an exchange student from the University of Dijon) has performed an extensive SEM-based size measurement study of raw MWNTs and f-MWNTs, using the carboxylic acid f-MWNTs described above. She found that following the aforementioned synthetic route, the aspect ratio of the carboxylic acid f-MWNTs is about half that of raw MWNTs. Hoa has shown through an extensive study of varying nanotube length in nanotube/epoxy composites that the aspect ratio has a direct affect on the conductivity of a composite, consistent with our length measurements (Table 2).[32]

Type of Nanotube	**Aspect Ratio**
Raw MWNTs	602
Carboxylic acid f-MWNTs	345

Table 5-2 Aspect Ratio of Raw MWNTs vs. carboxylic acid f-MWNTs. ***Data produced by Delphine Franchi.***

Decreased conductivity of the MWNT/epoxy composite was an unforeseen and undesirable effect of the functionalization route. The initial goal had been to achieve improved dispersions and lowered viscosity of the composite material by improved interactions between nanotube and epoxy, and it appears that we achieved one of these goals at the expense of the other.

Another practical application that is affected by conductivity is electromagnetic interference (EMI) shielding. The EMI shielding effectiveness of a material is dictated mainly by 3 mechanisms; reflections, absorption, and multi-reflections. Reflection is performed ideally by a metal sheet that uses interactions between mobile charge carriers and incoming EM waves.[61, 62] Absorption is dependent on the thickness of the material and is improved greatly if the material has electrical or magnetic dipoles to interact with EM waves.[61] The last mechanism is multi-reflections, which are multiple reflections that occur within the layer of shielding material. The EMI shielding capability of a material is decreased if the shielding layer is thinner than the skin depth of the material. This can be ignored if the shield is thicker than the skin depth. Skin depth is defined as the depth of shielding material to attenuate 1/e of the waves, or roughly 37% of the EM waves. Skin depth (δ) is related to the relative permeability (μ) of the shielding material, the frequency (*f*) of the waves, and the conductivity (σ) of the shielding material as shown in the formula below.[63]

$$\delta = \frac{1}{\sqrt{\pi f \mu \sigma}}$$

The standard for this measurement usually compared to the skin depth of copper, and attenuation ~9dB is considered the skin depth of copper, and typically if the shielding material absorbs more than 10dB than mutli-reflection shielding can be ignored. Mutli-reflection shielding becomes important at low frequencies, which are predominately magnetic.

Multiple studies have been conducted on EMI shielding capabilities of MWNT/polymer composites.[64-72] Until the discovery of carbon nanotubes, metal-coated carbon fibers or steel fibers used in polymers were practically the only option for EMI

shielding for polymer composites.[73, 74] These methods however were not viable options on an industrial scale because the required loading of filler made this material cost inhibitive. Shielding of 30 decibels (dB) effectively blocks 99.9% attenuation of EM radiation and is considered acceptable for industrial applications.[75, 76] Using both raw MWNTs and carboxylic acid f-MWNTs, MWNT/epoxy plates were prepared with the MWNTs or f-MWNTs at various volume loadings. These plates (roughly 20 cm diameter and 0.7 mm thick) were cured and sanded to a uniform thickness of ~ 0.5 cm. The plates were then tested to over a frequency range of 300 MHz to ~ 1 GHz in order to determine the overall effectiveness of the filler as an EMI shielding material.

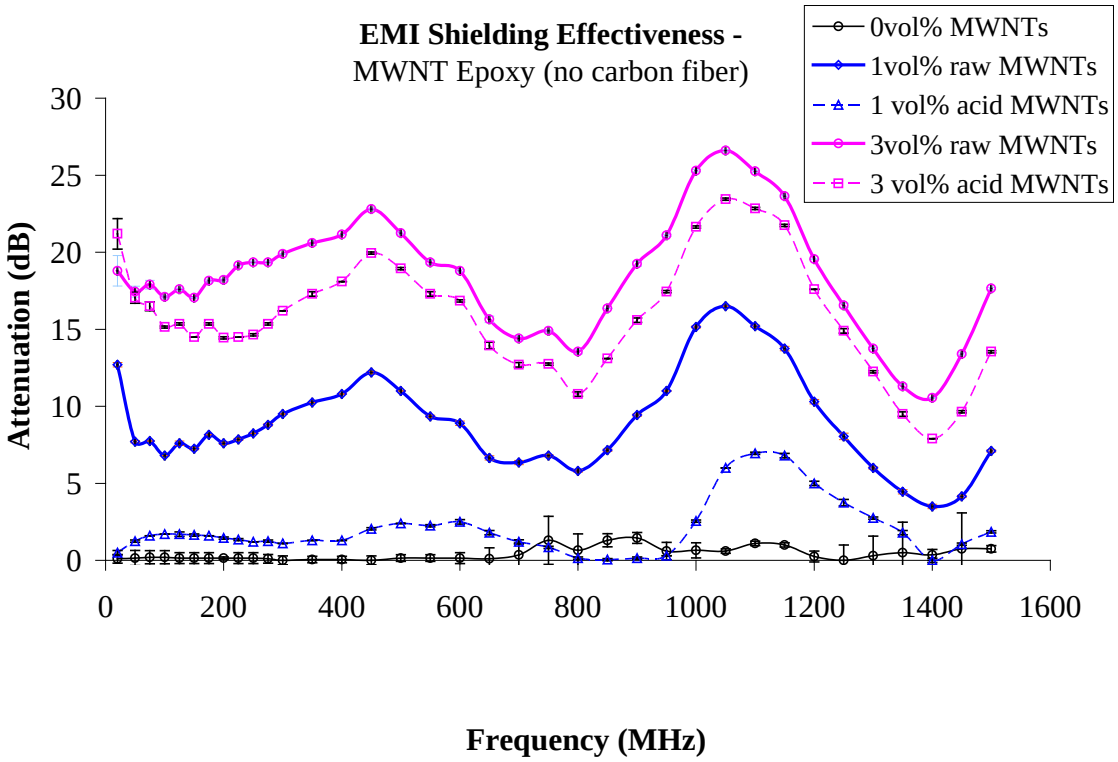

Figure 5-6 EMI shielding of epoxy/MWNT plates made with 0, 1, 3% volume loadings with raw MWNTs and f-MWNTs. ***Data measured by Carissa Dowden.***

A trend emerged that correlated with our viscosity and conductivity data is that carboxylic acid f-MWNTs (**11**) performed poorly as an EMI shielding material compared to raw MWNTs. At the higher loading of 3 volume % loading there is a smaller difference in the effectiveness of both, however both still are below the required 30 dB for practical industrial applications.

Sundararaj recently publish EMI shielding results of MWNT/PP(polypropylene) composites and found that the more conductive the material was the more effective of a EMI shield it was.[67] Composites at varying loadings of MWNTs showed that conductivity increased as loading was increased and in turn the EMI shielding effectiveness was increased. The thickness of composite samples was also investigated and showed that as thickness was increased absorption played a greater role than reflection in EMI shielding. MWNTs are thought to ineffectively shield through multi-reflections because of their diameters are much smaller than the skin of the composite material, however this was shown to be overcome by effective absorption and reflection.

In addition to these results further functionalization was carried out. The carboxylic acid f-MWNTs (**11**) were converted to an acid chloride functional group by way of heating the f-MWNTs in thionyl chloride neat.

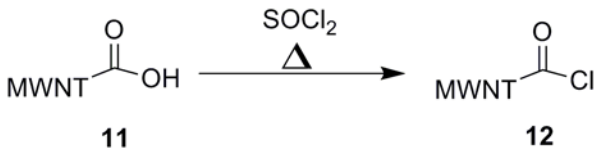

Figure 5-7 Conversion of carboxylic acid functional group to acid chloride functional group.

The acid chloride f-MWNTs (**12**) synthesis was carried out to the have an acyl functional group that would increase interaction with the epoxy matrix. By having a good leaving

group in the chloride the various nucleophiles in the epoxy can easily displace it and afford these f-MWNTs with improved dispersion in the epoxy matrix.

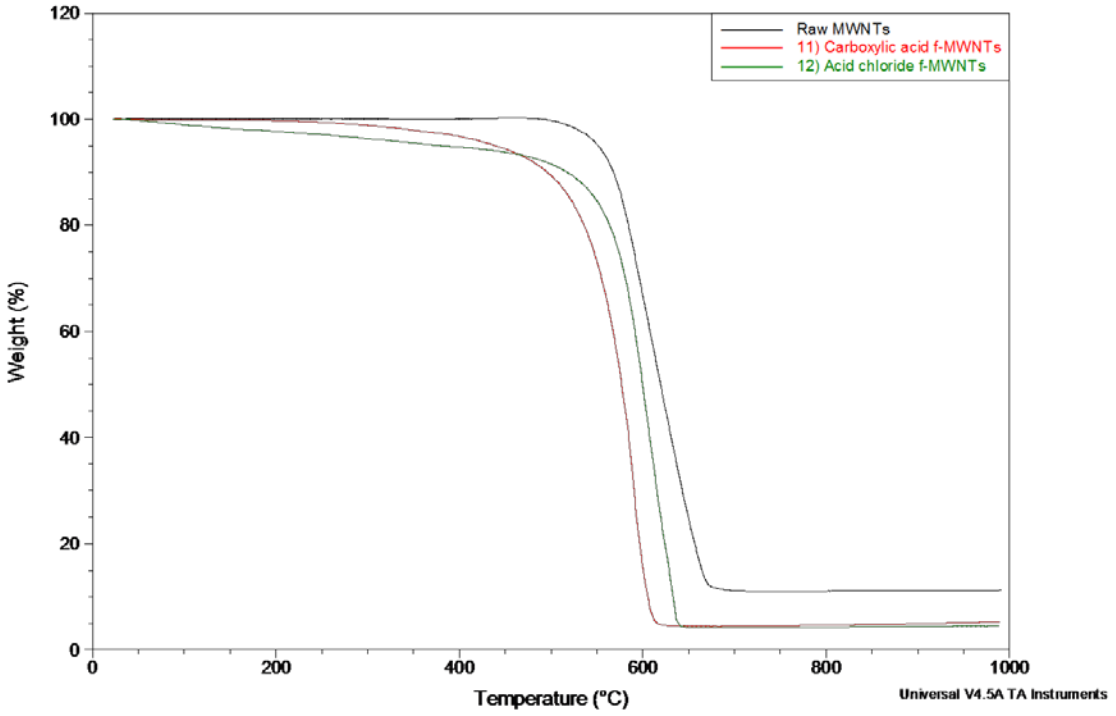

Figure 5-8 TGA comparing raw MWNTs (black line), carboxylic acid f-MWNTs (red line), and acid chloride f-MWNTs (green line) .

TGA analysis shows after converting the carboxylic acid f-MWNTs (**11**) to acid chloride f-MWNTs (**12**) there is an increase in the onset temperature of decomposition. This can be attributed to the addition of a covalently bonded halogen to the nanotube by way of the acid chloride functional group. This trend was observed previously after brominating the MWNTs (**5** and **6**). The clearly indicates a change from the previous functionalized starting material. Dispersion photos also indicate a change in the interaction of the f-MWNTs and the epoxy matrix.

The acid chloride f-MWNTs (**12**) have a lower viscosity at lower shear rates. This could be attributed to improved wetting because of the ease of nucleophiles to displace the chloride of the acid chloride functional group.

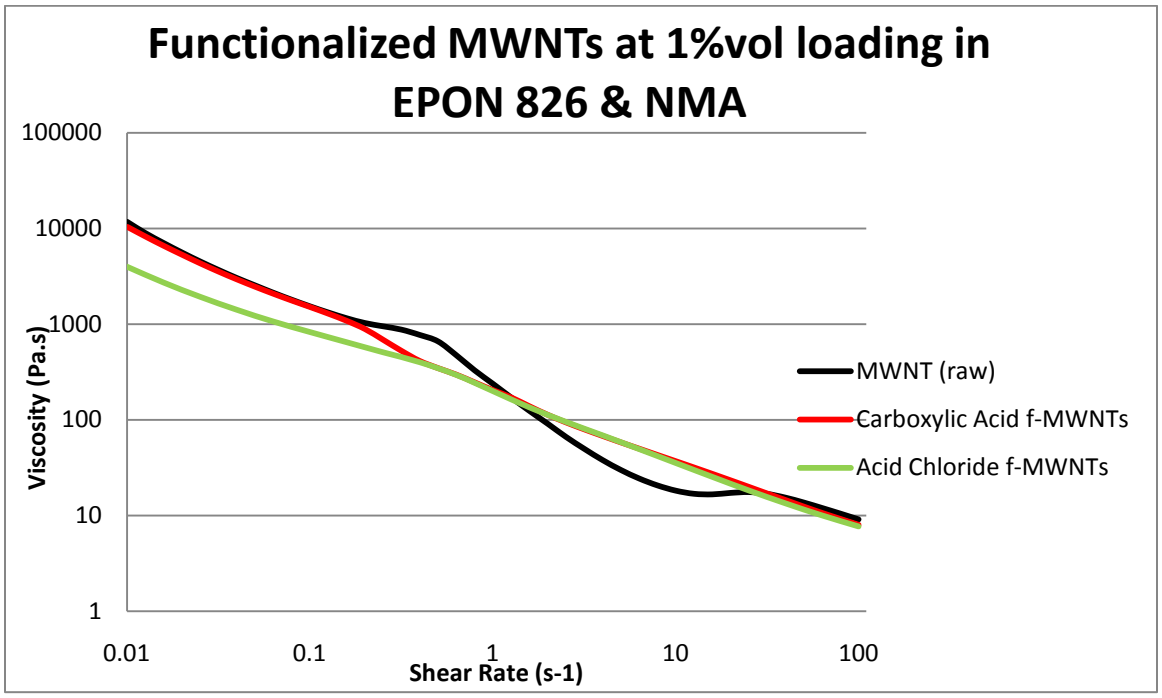

Figure 5-9 Comparison of the viscosity of epoxy resin composites containing 1 vol% raw MWNTs (black line), 1 vol% carboxylic acid f-MWNTs (red line), and 1 vol% acid chloride f-MWNTs (green line)

Higher shear rates indicate that as all the nanotubes align in the direction of the turning plate that the viscosity is relatively the same regardless of the type of functionalization. The dispersion of the acid chloride f-MWNTs (**11**) is slightly different from the carboxylic acid f-MWNTs (**12**), as indicated by UV fluorescence microcscopy.

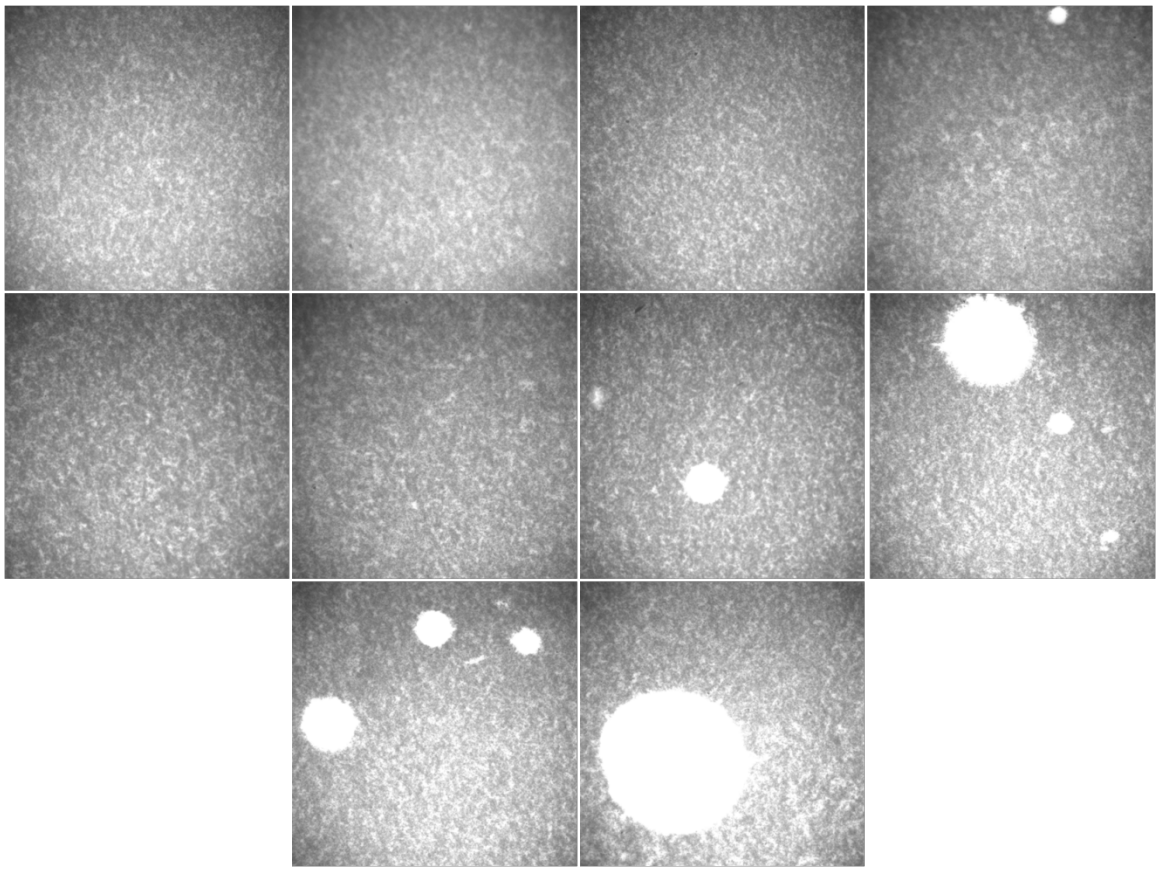

Figure 5-10 UV fluorescence microscopy photos of 1 vol% loading of acid chloride f-MWNTs (12) in epoxy at 40x magnification.

These dispersion photos show that in general there is good dispersion of the acid chloride f-MWNTs (**12**) into the epoxy, but there are distinct well rounded voids of nanotubes periodically throughout the sample. The interesting thing about these nanotube voids is that they are uniquely circularly and well shaped as opposed to the random appearance of voids that are seen in raw MWNT/epoxy composites. Resistivity data further illustrates the properties of this type of functionalization.

Sample at 1% vol loading in epoxy	Resistivity (ohm*cm^2)[a]
Raw MWNTs	100.95
Carboxylic Acid f-MWNTs	950.08
Acid Chloride f-MWNTs	565.15

Table 5-3 Resistivities of Raw MWNTs vs. carboxylic acid f-MWNTs and acid chloride f-MWNTs at 1% vol loading in epoxy composites mixed using "Short mixing Method".

[a]Measured using the 4-point method.

There is a drop in the resistivity of the acid chloride f-MWNTs (**12**) compared to the carboxylic acid f-MWNTs (**11**). This indicates that there is an improved network of nanotubes within the epoxy that lowers the percolation threshold. This could possibly be attributed there still being some carboxylic acid functional groups present that act as a nucleophile and attach the acid cholide site and bring the nanotubes closer. Or perhaps there is less charged repulsions because there no longer being any possible carboxylate anions present in the epoxy matrix.

Achieving good conductivity of the composite material is indicative of the charge carriers needed to interact with EM waves, and our current route of functionalization of nanotubes lowers viscosity of the composite but at the cost of conductivity and EMI shielding effectiveness. These results led to speculation as to what damage the strong base treatment has done to the nanotubes. TGA data showed evidence of some effect of the saponifcation on raw MWNTs without an ester functional group.

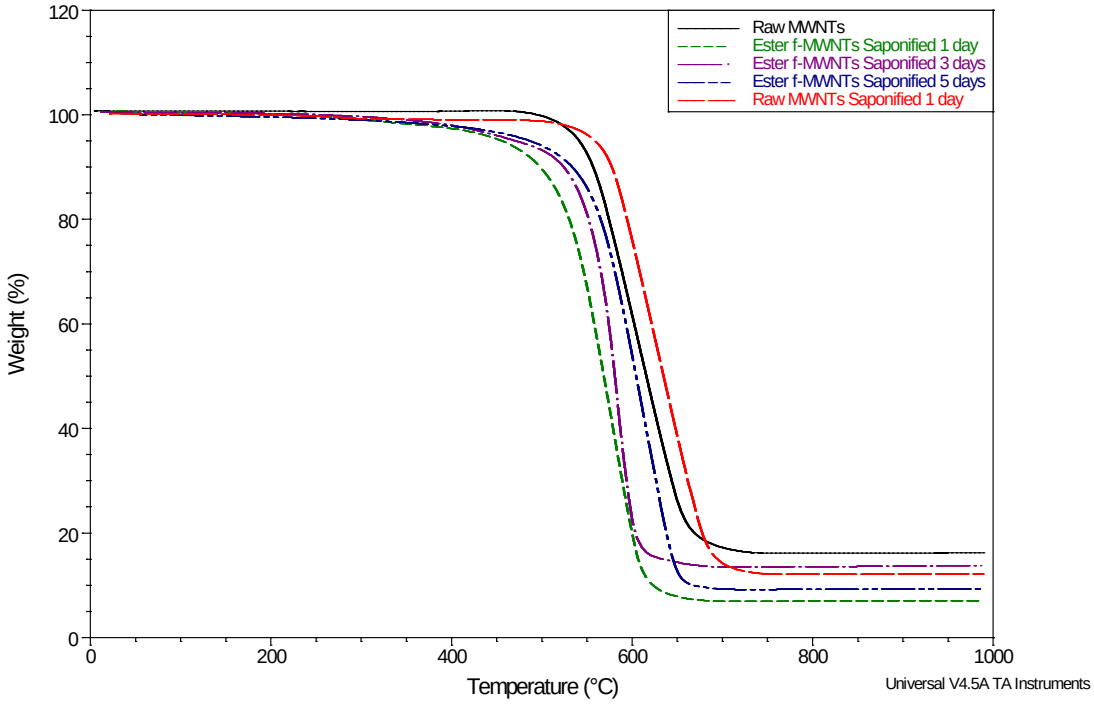

Figure 5-11 TGA comparison of various Ester f-MWNTs and Raw MWNTs saponified over various reaction times.

TGA results show that the longer the ester f-MWNTs are exposed to saponfication conditions, the higher the onset temperature of decomposition is raised. This also occurs for raw MWNTs exposed to saponification conditions. The effect that strong base and heat have on raw MWNTs could be similar to that H_2SO_4/HNO_3 treatment of nanotubes, in that aldehyde, phenolic groups are installed afterwards.[57] An increase in the number of surface functional groups that contain oxygen may make it more difficult for the nanotubes to combust, raising the onset temperature of decomposition. In addition to this data, extensive diameter measurements by using SEM indicate that the diameter of MWNTs is decreased when exposed to saponification conditions for one day.

Sample	Diameter (nm)
Raw MWNTs	46.35
KOH w/heat treated MWNTs	30.21

Table 5-4 Diameter comparison of Raw MWNTs vs. KOH treated MWNTs. ***Results produced by Delphine Franchi.***

The saponification step has raised questions as to what occurs during this treatment to the MWNTs. Decreased conductivity of epoxy/MWNT composites could be attributed to the damaging of the nanotubes, to decreased contacts between nanotubes as there is improved nanotube-polymer interactions, or a combination of the both effects. To improve nanotube-nanotube interactions while improving wetting with the polymer matrix, a modification must be achieved that improves nanotube to nanotube connections and still obtains a dispersion that is better than that found with raw MWNTs in epoxy.

In an attempt to solve to this problem, complementary functionalities were used in an attempt to increase nanotube to nanotube contact while maintaining a good dispersion within the polymer matrix. By coupling carboxylic acid f-MWNTs (**11**) to choline chloride using 1-ethyl-3-(3-dimethylaminopropyl)-carbodiimide (EDC), we produced choline f-MWNTs (**13**), a functionalized MWNT bearing a permanent positive charge**.** By forming the conjugate base of the carboxylic acid f-MWNTs (**14**) we produced a functionalized MWNT with a permanent negative charge. This gave us MWNTs with two oppositely charged functional groups installed on the exterior.[77]

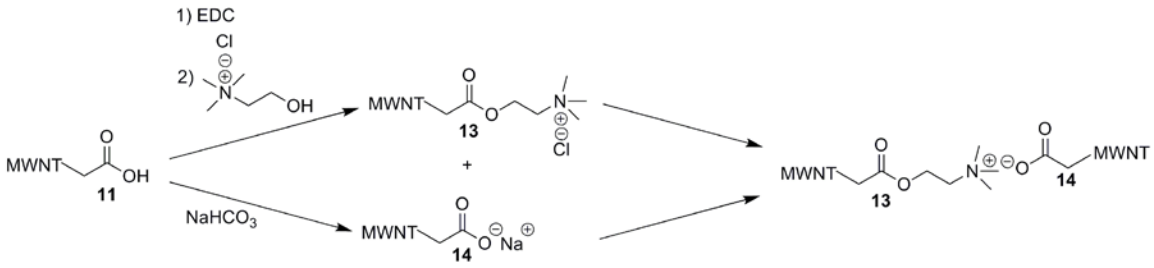

Figure 5-12 Scheme of orthogonal functionalities.

By having opposite charges, we hoped that the nanotubes would be attracted to each other, producing more nanotube-nanotube conjunctions to enable current travel and improve conductivity of the epoxy/MWNT composite. Unfortunately there is little improvement to the conductivity when epoxy/MWNT composites are made of half choline f-MWNTs (**13**) and conjugate base f-MWNTs (**14**).

Sample at 0.5% vol loading in epoxy	**Resistivity (ohm*cm^2)**
Raw MWNTs	34.88
Carboxylic acid f-MWNTs (**11**)	98.97
Choline f-MWNTs (**13**) and Conjugate base f-MWNTs (**14**)	92.75

Table 5-5 Resistivities of Raw, Carboxylic Acid, and Choline f-MWNTs at 0.5% vol loading mixed using Method C.

The lack of improvement in the conductivity of the composite samples could be due to an inefficient coupling reaction that did not have a high yield, or that the nanotubes were damaged to begin with after undergoing saponification. However, it is also likely is the possibility that there are insufficient charges on these nanotubes to bring about the desired conducting network. Future orthogonal functionality approaches may still be able to result in an improved dispersion and conductivity within epoxy/MWNT composites.

Chapter 6

Metal Doping: An Alternative Approach to Optimization of Conductivity in Epoxy/MWNT Composites.

Metal dopants may be able to improve the conductivity of epoxy/MWNT composites, higher than what has been produced from optimal processing alone. By adding various copper compounds, we hoped that we could achieve improved conductivity as a result of the very nature of metals being excellent charge carriers. Copper has a conductivity of 59.6×10^6 S/m and a resistivity of 17.2 nΩm.[78] Copper is not the most conductivity metal but it is a near second to silver at a much lower cost, which makes it an attractive metal dopant. By doping the epoxy/MWNT composites with a small amount of copper we hoped to find gains in conductivity and EMI shielding without large costs in viscosity.

The three types of copper that were used to dope the epoxy/MWNT composites were dendritic copper powder, electrolytic copper dust, and copper phthalocyanine. However, processing these various types of copper into the composites posed some technical issues. Mixing metallic copper with the planetary mixer would cause the dense copper particles to crash to the bottom of the container, and as a result the planetary mixer had to be avoided when making composites doped with copper. The size of the copper particles compared to the size of the gap between the rollers of the 3-roll mill was an issue also because damage that could be caused to the machinery during mixing. The average particle size of the dendritic copper powder is 3 μm, but the average particle size of the electrolytic copper dust was unknown. SEM photos were taken (figure 6-1) and we found that the average size was around 50 μm, which is larger than the smallest gap size used in mixing method C. However mixing the electrolytic copper dust caused no damage to the roller and was the composite was mixed with ease.

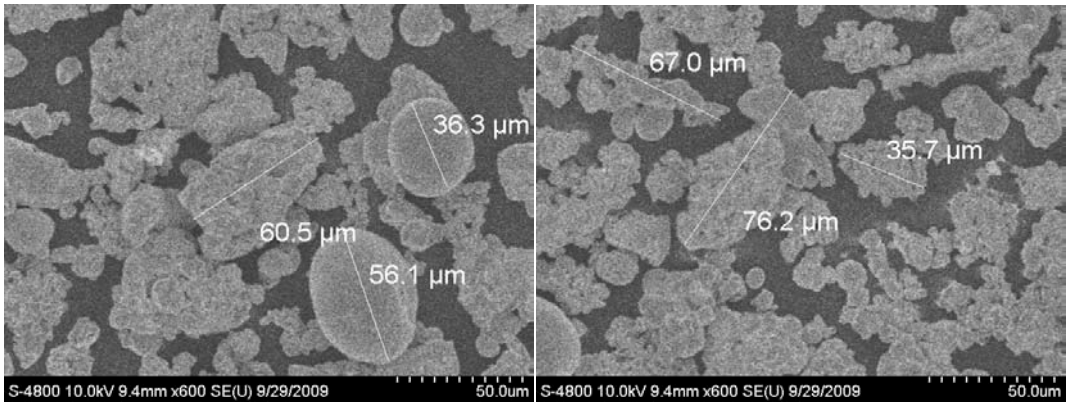

Figure 6-1 SEM photos of electrolytic copper dust.

After mixing the various copper dopants into the epoxy/MWNT composites, viscosity measurements were taken to assess how much of impact these copper particles had on the viscosity of the mixture. The viscosity results show that by adding these copper dopants that typically there is only a slight increase in the viscosity of the composite.

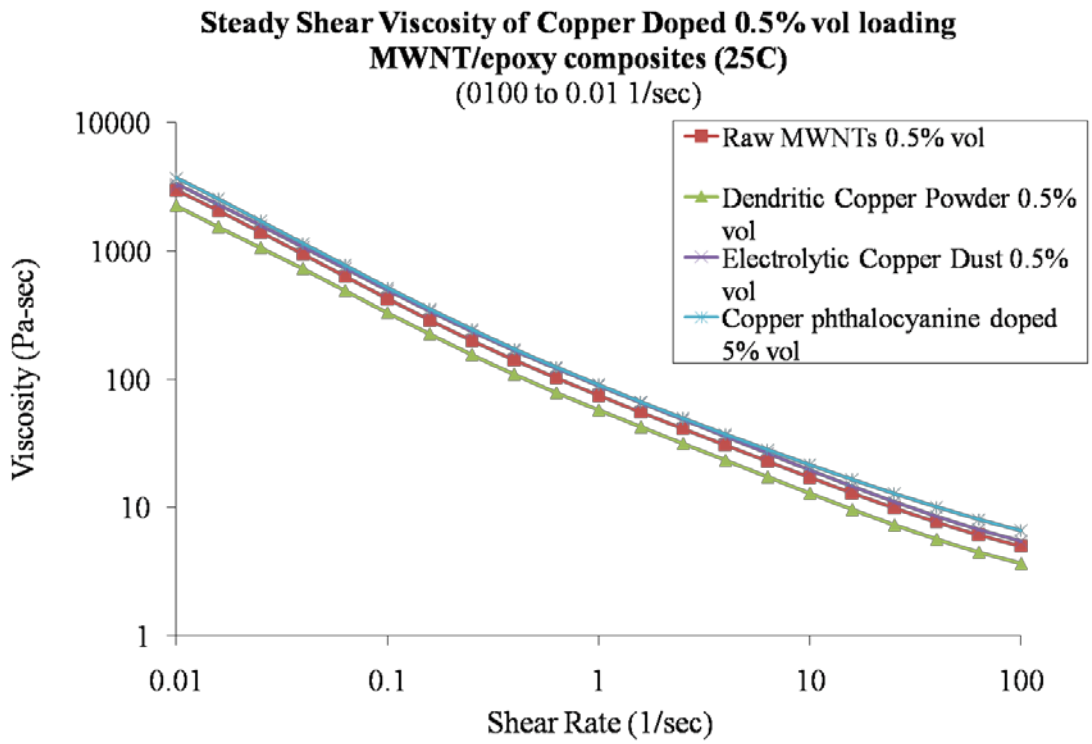

Figure 6-2 Viscosity graph of Copper doped 0.5% vol loading MWNT/epoxy composites using a 100 to 0.01s^{-1} shear ramp at 25°C.

To examine the dispersion of copper and MWNTs, photographs were taken using UV reflectance microscopy. One difficulty with the traditional grayscale photography used with earlier photos is that it did not show different shades of color between the MWNTs and the copper. However, we took some of the photos without a grayscale color filter in an effort to differentiate between the agglomerations of MWNTs and copper.

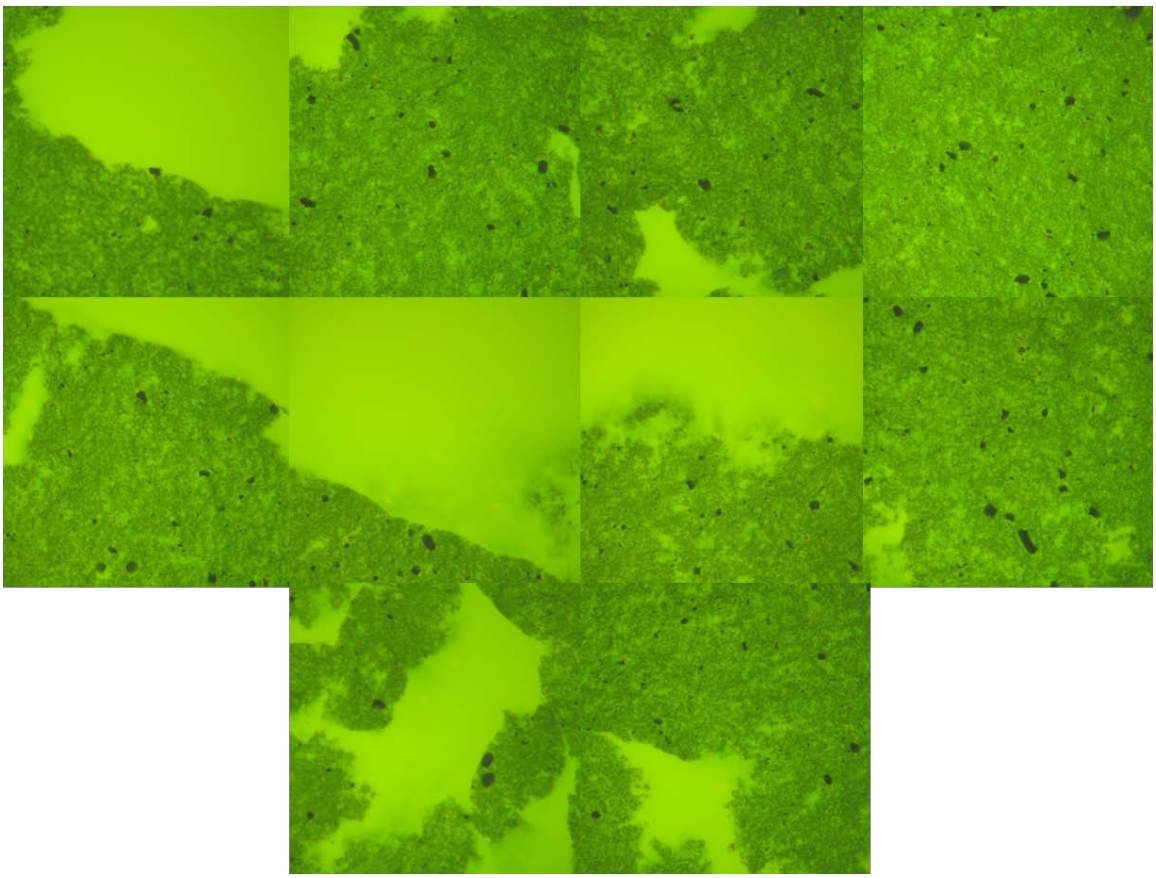

Figure 6-3 UV reflectance microscopy photo taken at 20x of 0.5% vol dendritic copper powder, 0.5% vol MWNTs/epoxy composite with no color filter.

Identifying where the dendritic copper powder is in these photos is difficult at best, but the 3μm particle size is probably why it is difficult to image or see any agglomeration.

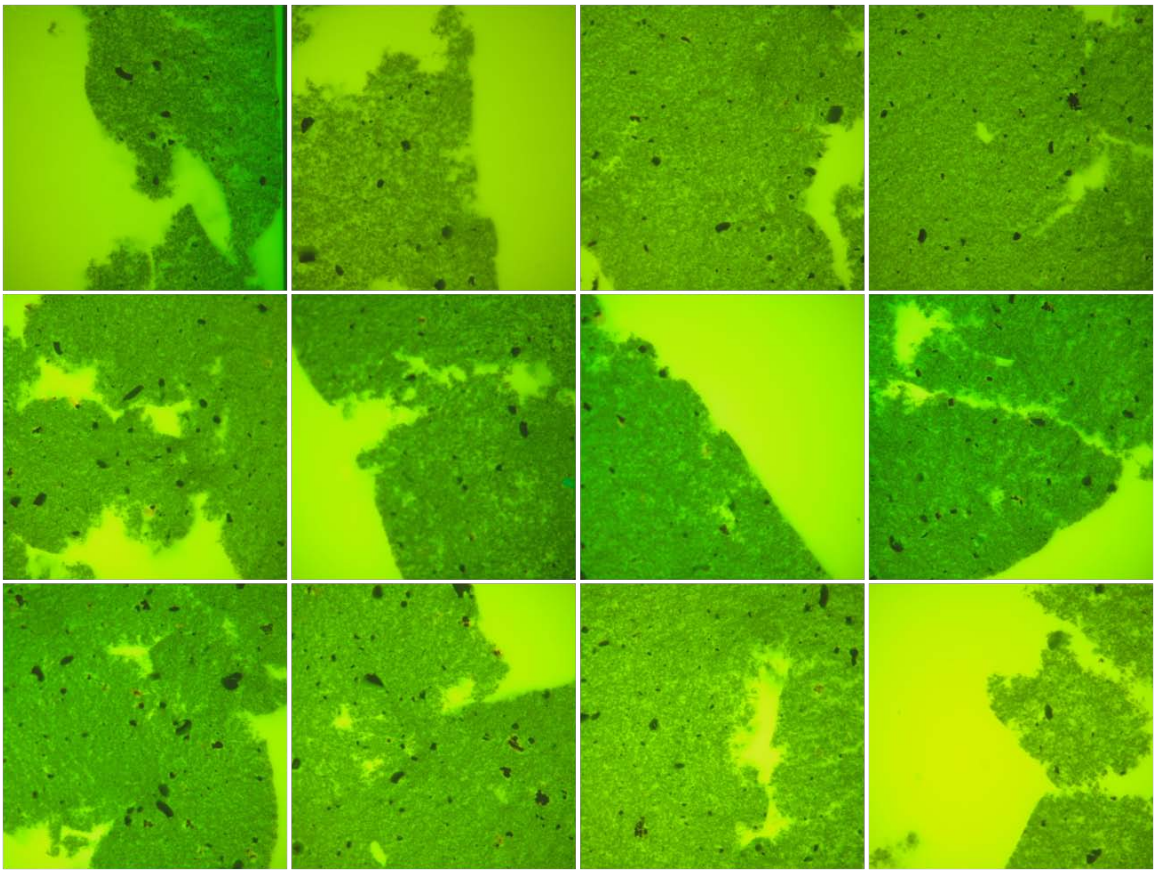

Figure 6-4 UV reflectance microscopy photo taken at 20x of 0.5% vol electrolytic copper dust, 0.5% vol MWNTs/epoxy composite with no color filter.

The UV fluorescence photographs from the electrolytic copper dust show very dark chunks that are spread intermittently throughout the composite. Upon closer inspection of these agglomerates, a copper hue color is observed.

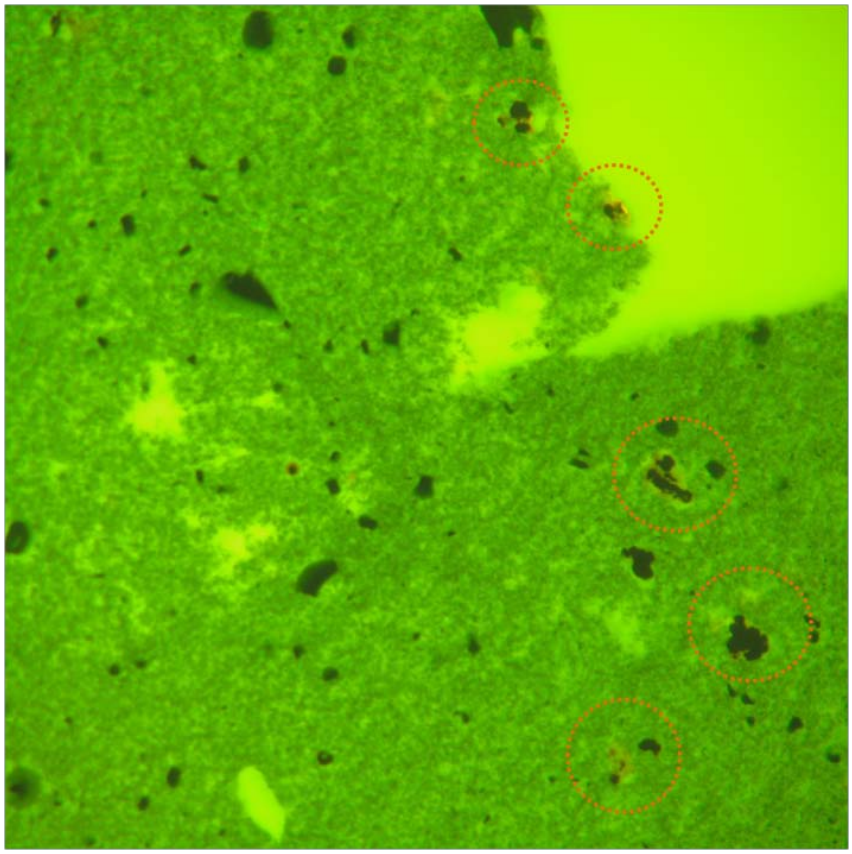

Figure 6-5 Enlarged UV reflectance photo at 20x of 0.5% vol electrolytic copper dust, 0.5% vol MWNTs/epoxy composite with no color filter with copper hued color outlined.

This observation suggests that these black agglomerates are large deposits of electrolytic copper dust within the composite or a mixture of copper and MWNT agglomerates.

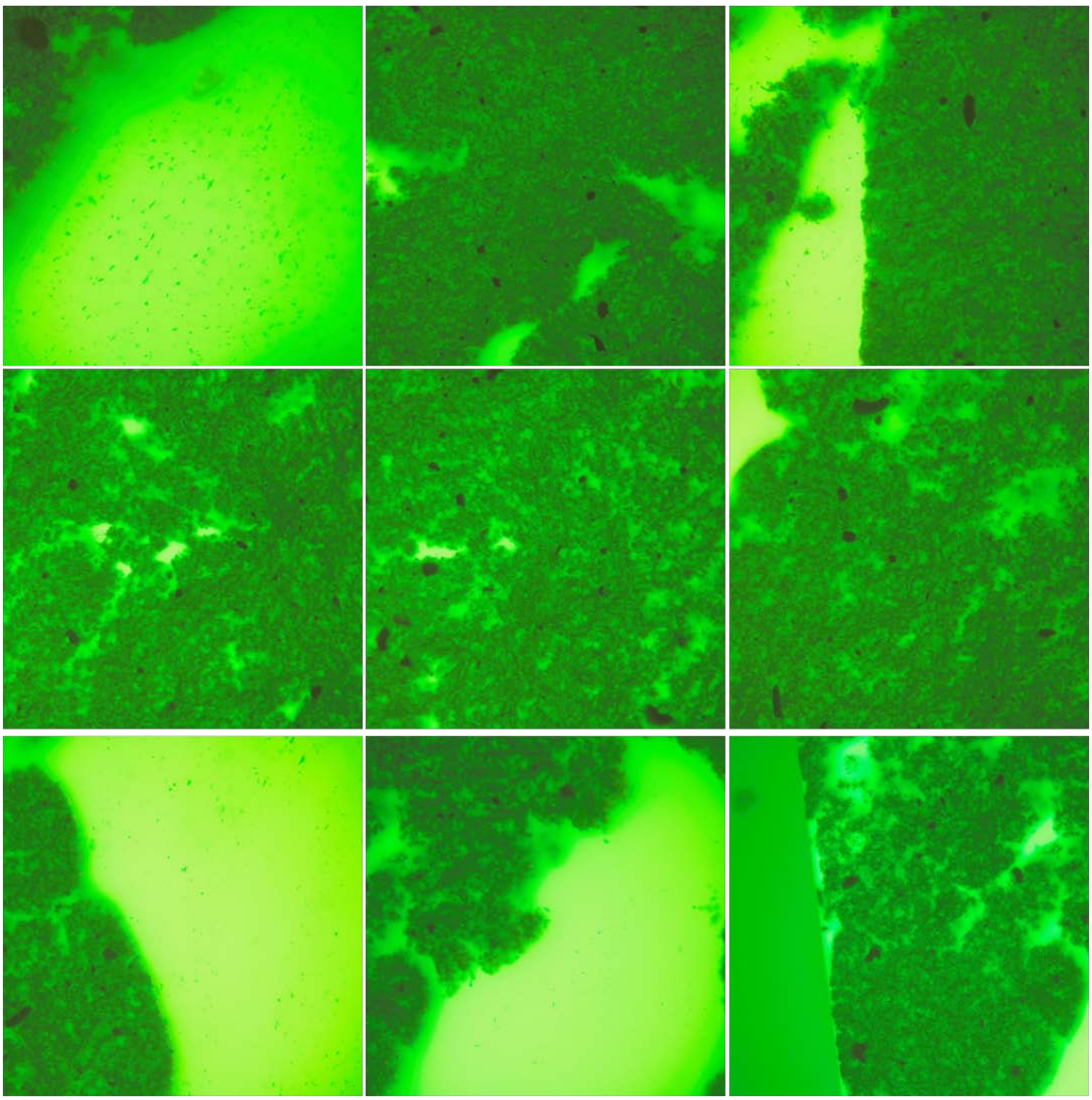

Figure 6-6 UV reflectance microscopy photo taken at 20x of 5% vol copper phthalocyanine, 0.5% vol MWNTs/epoxy composite with no color filter.

Photos taken of the copper phthalocyanine doped composites indicate no obvious signs of agglomeration other than MWNT agglomerations. This is not surprising, as bulk metal should provide more contrast than isolated metal complexes. There are signs of possible copper phthalocyanine agglomeration dispersed evenly throughout the epoxy.

All told, these dispersion photographs do not provide a clear indication of which copper compound is dispersed with more uniformity than the others.

Resistivity data was also taken of each of the copper doped epoxy/MWNT composites.

Sample at 0.5% vol loading in epoxy	**Resistivity (ohm*cm^2)**
Raw MWNTs	34.88
Dendritic copper powder at 0.5% vol	37.40
Electrolytic copper dust at 0.5% vol	36.45
Copper phthalocyanine at 5% vol	70.08

Table 6-1 Resistivities of various copper doped 0.5% vol MWNT/epoxy composites all mixed with mixing method C.

The resistivities of the copper doped epoxy/MWNT composites suggest that at this small volume loading there is little benefit from adding copper. The copper phthalocyanine doped composite shows a higher resistivity than any other samples, and this suggests that the copper pthalocyanine prevents contact between nanotubes. These results show that is there is no benefit from doping the composite with copper, at least in composites that are already highly conductive. Noticeable improvements may be observable if copper is used to dope an epoxy/MWNT composite that had a poor conductivity to begin with, such as composites using the carboxylic acid f-MWNTs **(11)**. The next series of results show the viscosities, dispersion photographs, and resistivity of copper doped 0.5% carboxylic acid f-MWNT/epoxy composites.

The viscosity results show that there is a reduction in viscosity when the composite is doped with the various coppers. This could be attributed to the carboxylic

acid functionality having some interaction with the copper through coordination that allows the nanotubes to slide past one another as they the exteriors are decorated to some degree with copper.

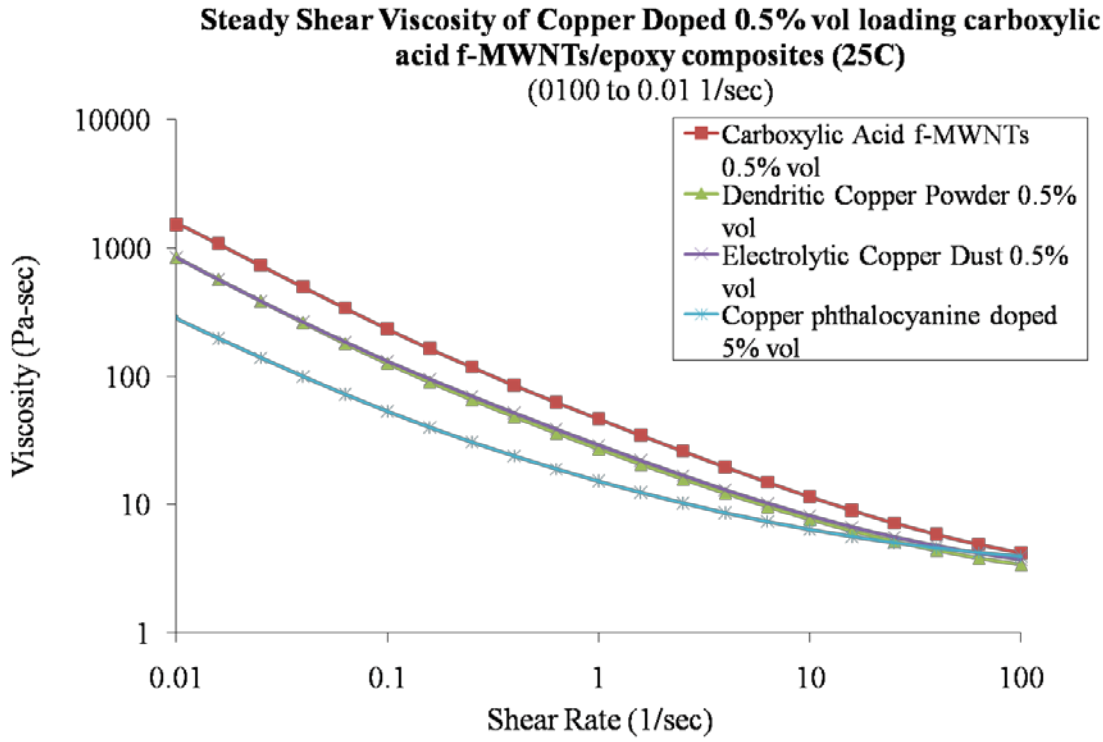

Figure 6-7 Viscosity graph of Copper doped 0.5% vol loading carboxylic acid f-MWNT/epoxy composites using a 100 to 0.01s^{-1} shear ramp at 25°C.

Dispersion photographs were taken of the electrolytic copper dust and copper phthalocyanine doped carboxylic acid f-MWNT/epoxy composites. The dendritic copper doped composites were riddled with voids throughout the sample and could not be used proper resistivity samples. Many attempts were made to adjust the processing to remove these voids that appeared during the curing process, but without success. It is still not fully understood why these smaller sized 3µm copper particles caused this problem, while the larger ~50µm sized copper particles found in the electrolytic copper dust did not.

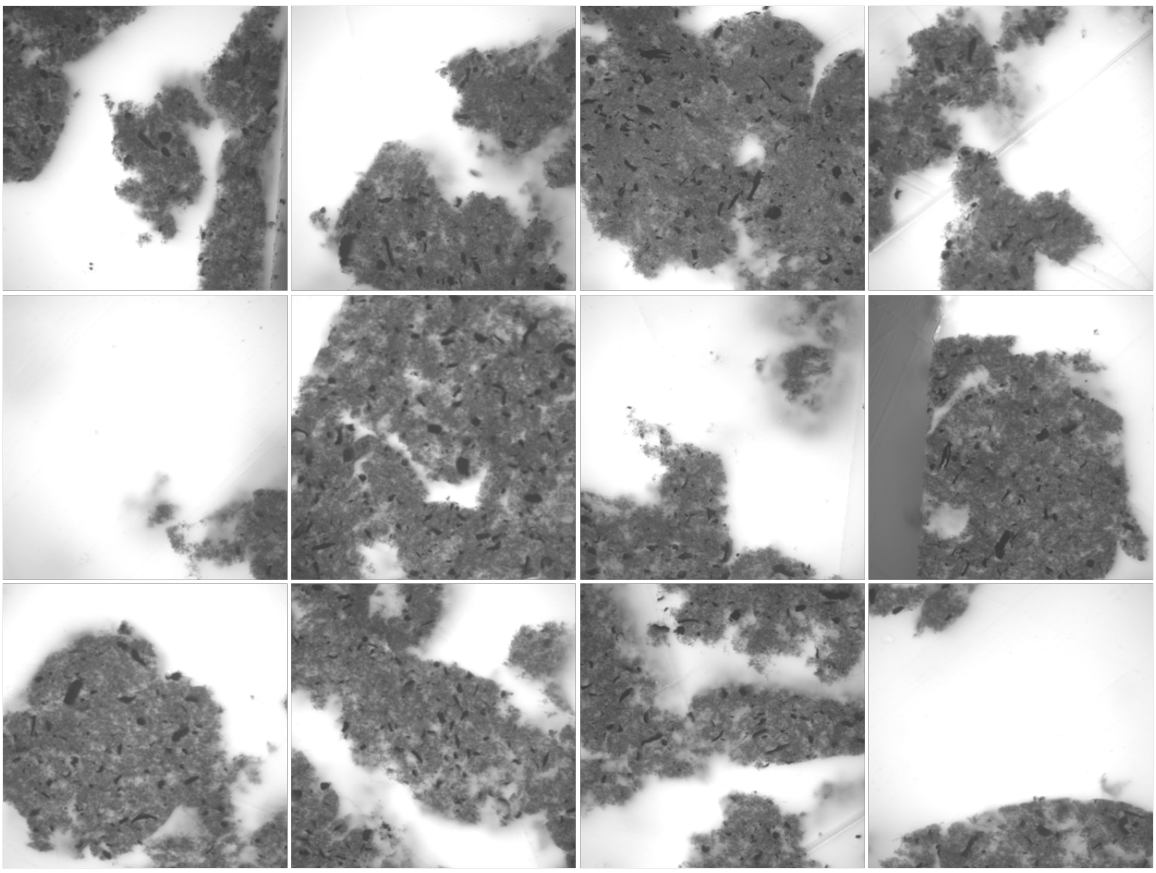

Figure 6-8 UV reflectance microscopy photo taken at 20x of 0.5% vol electrolytic copper dust, 0.5% vol carboxylic acid f-MWNTs/epoxy composite.

Dispersion photographs (Figure 6-8) of the electrolytic copper dust doped carboxylic acid f-MWNT/epoxy composite that there is a severe degree of agglomeration of the nanotubes and the copper. There are many voids in this sample, regions free of nanotubes, indicating that the lower viscosity reflected a poor dispersion, and the low viscosity permits additional agglomeration to occur during the curing process. The dark black streaks indicate copper agglomeration within the networks of nanotubes.

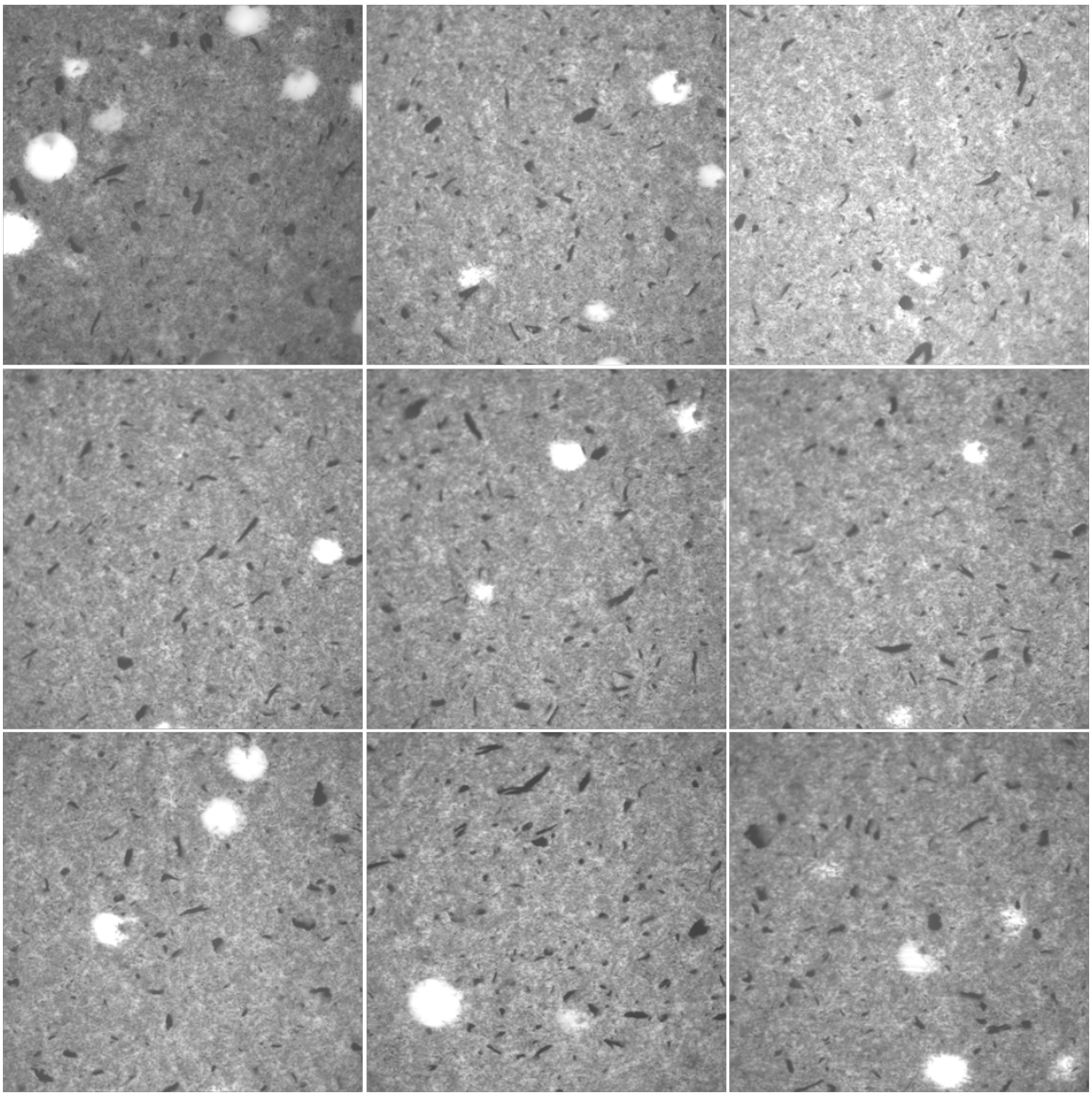

Figure 6-9 UV reflectance microscopy photo taken at 20x of 5% vol copper phthalocyanine, 0.5% vol carboxylic acid f-MWNTs/epoxy composite.

Dispersion photographs of the copper phthalocyanine doped carboxylic acid f-MWNT/epoxy composite (Figure 6-9) show a good dispersion of MWNTs, with small voids and agglomerations that could be nanotubes or copper phthalocyanine. Overall this sample looks particularly good because of the minimal amount of epoxy voids within the composite sample. Unfortunately, resistivity data reveals that regardless of how well

dispersed the nanotubes appear to be dispersed in this composite, it performs the most poorly as a conductive material.

Sample at 0.5% vol loading in epoxy	**Resistivity (ohm*cm^2)**
Carboxylic acid f-MWNTs	98.97
Dendritic copper powder at 0.5% vol	Data could not be obtained.
Electrolytic copper dust at 0.5% vol	268.92
Copper phthalocyanine at 5% vol	23,599.43

Figure 6-10 Resistivities of various copper doped 0.5% vol carboxylic acid f-MWNT/epoxy composites all mixed with mixing method C.

The resistivity results show that by doping carboxylic acid f-MWNT/epoxy composites with various copper compounds that the conductivity is lowered instead of raised. Lower conductivity indicates that a less effective conducting network is formed. The lowered viscosity of these samples relative to composite prepared with raw MWNTs suggests that there are fewer nanotube to nanotube interactions when these various copper particles are included in the mixture. It is unclear why this would be the case. The copper doping experiments as a whole are a disappointment, since there is little or no improvement in the overall conductivity of the composite samples. Future studies would probably need a simple volume loading experiment with raw MWNT/epoxy composites to determine how much copper needs to be added before there is a clear impact on the overall conductivity of the composite.

Chapter 7
Conclusions and way Forward

A majority of this research project had a considerable focus on material science. The chemistry behind our synthetic approaches to functionalize MWNTs was only one small aspect of the project. This multi-disciplinary project has involved many different facets of chemistry, physics, material science, and material engineering. The evolution of this project has shown how important composites properties can reflect a particular functionalization of a nanotube. Until analytical methods are developed that can assess the degree of identification of functional groups installed onto the nanotube there will be no better way to judge a percent yield or purity of a particular synthetic route used on nanotubes.

Although the primary focus of my project was to explore the chemistry that could be successfully performed on nanotubes, a considerable amount of time was invested in developing an understanding of processing methods for MWNT/epoxy composites. As demonstrated in previous publications and by our own mixing studies; how a composite is mixed can ultimately determine how well it will perform.[30, 31, 79] Optimization and consistency of the processing methods will benefit future composite studies performed at CAER.

Our initial concept of functionalization was that by decorating the exterior surface of the MWNTs an improved dispersion would occur in the polymer matrix and through this improved network of nanotubes, a lower percolation threshold and improved conductivity would be obtained for the composite material. Improved dispersions and lower viscosities permit greater manipulation and processing applications, but unfortunately we found that decreased electrical conductivity plagued these composites.

Improving wetting of nanotubes with the polymer matrix came at the cost of the nanotube to nanotube interactions that are essential for forming the multiple contacts and pathways required for electrons to travel effectively through the insulating polymer. These studies on the correlation between viscosity and resistivity have clarified their relationship in these MWNT/epoxy composites; however the goal of gaining sufficient electrical conductivity to facilitate an EMI shielding material that is higher than 30dB was not obtained.

Metal doping also proved to be ineffective in improving the conductivity of MWNT/epoxy composites. This could be due to having an inappropriate type of copper compound or from using an inappropriate processing methodology, although we examined a number of variations of each. Difficulties with obtaining homogeneous and void free composites also proved to be a major hurdle for copper doping to be a viable technique. If the processing method could be refined or another type of copper used, such as copper nanorods, an increase in conductivity of the composites might be achieved.

With the knowledge that the reductive alkylation is a viable and reliable route to functionalized MWNTs, further synthetic routes and materials projects can be pursued. The allylated f-MWNTs could be used as a filler in poly(methyl methacrylate) (PMMA) composites being studied at CAER.

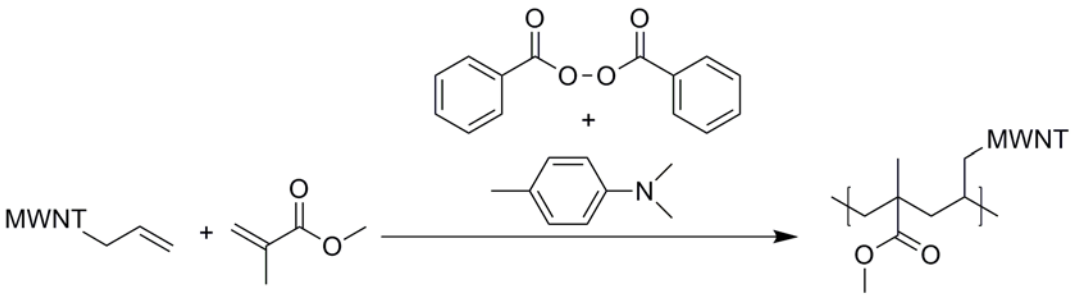

Figure 7-1 Scheme of free radical polymerization of allyl f-MWNTs and methyl methacrylate.

By forming covalent bonds into the polymer matrix, load should be effectively transferred to the MWNTs, increasing the modulus and fatigue life of the composite and making it a longer lasting, stronger material for medical and other applications. Additionally allyl f-MWNTs could be used with many different monomers in free radical polymerization for better nanotube integration into the polymer matrix. The allyl f-MWNTs can further be manipulated to form epoxides that could then be used to covalently bond into the epoxy network during curing.

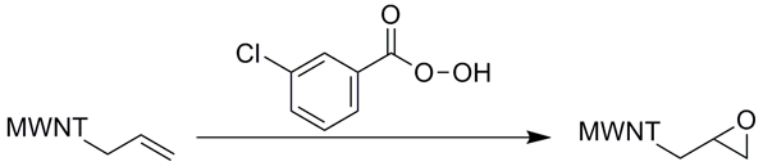

Figure 7-2 Epoxidation of allyl f-MWNTs.

Again, by forming covalent bonds from the exterior of the MWNTs into the polymer matrix, improved load transfer and increased modulus can be achieved.

The reductive alkylation does not only install vinyl groups onto the nanotubes, but acetylene groups can also be covalently bonded to the exterior of nanotubes. Using propargyl bromide in similar reductive alkylation conditions, a progargyl functionality can be covalently bonded to the nanotube. The propargyl group could then be used in

further manipulations, such as Diels-Alder or click chemistry, to attach additional functional groups and to build upon the surface of the MWNTs in an effective manner.

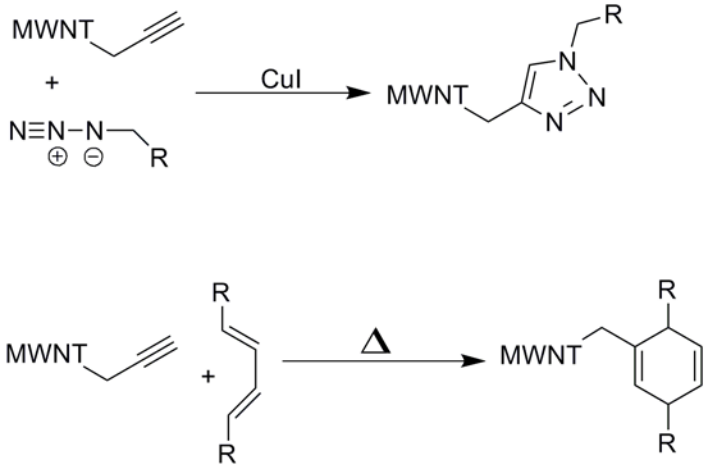

Figure 7-3 Scheme showing manipulation of propargyl functional group using cycloadditions.

These cycloadditions allow for chemical manipulations using relatively mild conditions that would not damage the structure of the nanotube. A variety of possibilities are possible with these cycloadditions, depending on the substituents on the adducts.

Since the carboxylic acid f-MWNTs proved to be damaged from harsh saponfication conditions, a reductive alkylation with bromoacetic acid would produce a carboxylic acid f-MWNT (**11**) under mild conditions. These structurally intact functionalized nanotubes could then be used for further material applications.

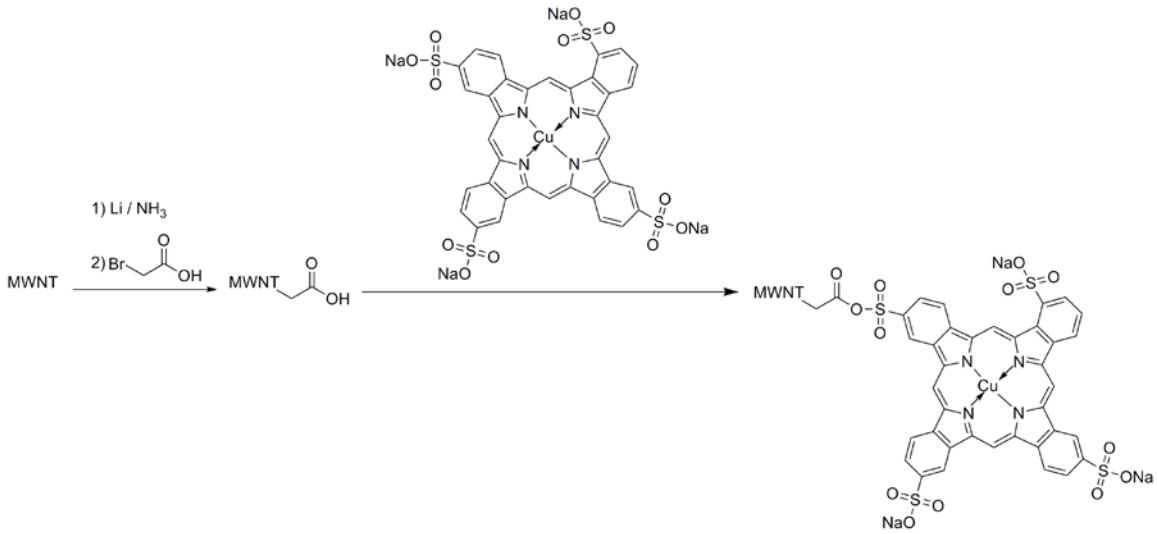

Figure 7-4 Coupling of copper phthalocyanine tetrasulfonic acid tetrasodium salt to surface of MWNT.

Decorating the exterior of the MWNTs with copper phthalocyanine tetrasulfonic acid tetrasodium salt produces a useful molecule to be can used in photovoltaics.[80, 81] In addition to this, the carboxylic acid f-MWNTs (**11**) can be coupled with antibodies or amino acids to form molecules useful in a variety of biosensor applications.[82]

There are a vast number of applications and materials that can uilize functionalized carbon nanotubes. As instrumentation advances, the chemistry that can performed on carbon nanotubes will only become more robust and refined as more complete chacterization can be achieved. Until that time, bulk properties of materials that contain carbon nanotubes will be the only form of assessment to quantify functionalization of carbon nanotubes. The future holds much promise in this unique nanostructure.

Experimental

All MWNTs were obtained from the Center for Applied Energy Research using a xylene/ferrocene feedstock under the VGE S-31 batch conditions.[11] All reagents for functionalization were obtained from Sigma-Aldrich. EPON 826 and NMA (nadic methyl anhydride) were obtained from Miller-Stephenson, while EMI-2,4 (2,4 ethyl methylimidazole) was obtained from Sigma-Aldrich. All TGA experiments were performed on TA Q500 TGA under air at a 20^0C/min temperature ramp. Samples were mixed using Silverson LR4 shear mixer, Thinky ARE-250 planetary mixer, and Exakt 80E 3-roll mill. All rheology experiments were performed on TA AR-G2 rheometer. All optical microscopy was performed using a Leica AF6500 microscope. SEM images were obtained on a Hitachi S-4800 FE-SEM.

Experimental Procedures

(4) Allyl f-MWNTs (CLF-IV-1)

NH_3 was condensed into a 3L 4 neck round bottom flask equipped with a magnetic stir bar, using a Dewar condenser in a dry/ice acetone bath under N_2. After condensing ~1.5L of NH_3, Li metal (6.2g) was added to the flask, upon which the solution turned blue. The reaction was stirred for 5 min. VGF 22,24,27,33,34 MWNTs (10.4g) were added to the solution, upon which the solution turned black. The solution was stirred 30 min. Allyl bromide (100mL) was added slowly drop wise by syringe to the mixture. The reaction was stirred overnight until NH_3 had completely evaporated from the flask. H_2O (2L) and EtOH (500mL) were added to the flask and stirred for 30 min under open air. The suspension was filtered using a Buchner funnel and the filter cake was flushed with H_2O until pH of filtrate was neutral. The MWNTs were washed and filtered with EtOH

followed by CH_2Cl_2. The MWNTs were then collected and dried overnight under vacuum to produce 10.3g of material.

(5) Mono brominated f-MWNTs (CLF-IV-22)

Ally f-MWNTs (**4**) (0.1g) and HBr 48% (125mL) were placed into 250mL 3 neck round bottom flask equipped with magnetic stir bar. Solution was stirred overnight at $80^{O}C$ under reflux. The suspension was cooled to room temperature then filtered using a Buchner funnel and the filter cake was flushed with H_2O until pH of filtrate was neutral. The MWNTs were washed and filtered with EtOH. The MWNTs were then collected and dried overnight under vacuum to produce 0.1g of material.

(6) Mono brominated f-MWNTs (CLF-IV-13)

Allyl f-MWNTs (**4**) (0.1g) and $MeCl_2$ (250mL) were placed into 500mL 3 neck round bottom flask equipped with magnetic stir bar. 1 pipette of Br_2 was added drop wise to the solution. Solution was stirred overnight at $55^{O}C$ under reflux. The suspension was cooled to room temperature then filtered using a Buchner funnel and the filter cake was flushed with EtOH. The MWNTs were collected off the filter paper stirred in a 500mL 3 neck round bottom flask with 1.3 $NaHSO_3$ for 30 minutes. The suspension was then filtered using a Buchner funnel and the filter cake was flushed with H_2O. The MWNTs were washed and filtered with EtOH. The MWNTs were then collected and dried overnight under vacuum to produce 0.1g of material.

(7) Methyl f-MWNTs (CLF-III-60)

NH_3 was condensed into a 500mL 3 neck round bottom flask equipped with a magnetic stir bar, using a Dewar condenser in a dry/ice acetone bath under N_2. After condensing ~250mL of NH_3, Li metal (0.7g) was added to the flask, upon which the solution turned blue. The reaction was stirred for 5 min. VGE S-31 MWNTs (2.0g) were added to the solution, upon which the suspension turned black. The solution was stirred 30 min. Methyl Iodide (20mL) was added slowly dropwise by syringe to the mixture. The reaction was stirred overnight until NH_3 had completely evaporated from the flask. H_2O (250mL) was added to the flask and stirred for 30 min under open air. The suspension was filtered using a Buchner funnel and the filter cake was flushed with H_2O until pH of filtrate was neutral. The MWNTs were washed and filtered with EtOH followed by CH_2Cl_2. The MWNTs were then collected and dried overnight under vacuum to produce 2.1g of material.

(8) Butyl f-MWNTs (CLF-III-63)

NH_3 was condensed into a 500mL 3 neck round bottom flask equipped with a magnetic stir bar, using a Dewar condenser in a dry/ice acetone bath under N_2. After condensing ~250mL of NH_3, Li metal (0.8g) was added to the flask, upon which the solution turned blue. The reaction was stirred for 5 min. VGE S-31 MWNTs (2.0g) were added to the solution, upon which the solution turned black. The solution was stirred 30 min. 1-Bromobutane (10mL) was added slowly drop wise by syringe to solution. The reaction was stirred overnight until NH_3 had completely evaporated from the flask. H_2O (250mL) was added to the flask and stirred for 30 min under open air. The suspension was filtered

using a Buchner funnel and the filter cake was flushed with H_2O until pH of filtrate was neutral. The MWNTs were washed and filtered with EtOH followed by CH_2Cl_2. The MWNTs were then collected and dried overnight under vacuum. The MWNTs and CH_2Cl_2 (250mL) were placed in 500mL round bottom flask and sonicated for 30 min using a sonicating bath. The suspension was filtered using Buchner funnel. The MWNTs were then collected and dried overnight under vacuum to produce 1.9g of material.

(9) Nonodecyl f-MWNTs (CLF-III-52)

NH_3 was condensed into a 500mL 3 neck round bottom flask equipped with a magnetic stir bar, using a Dewar condenser in a dry/ice acetone bath under N_2. After condensing ~250mL of NH_3, Li metal (0.8g) was added to the flask, upon which the solution turned blue. The reaction was stirred for 5 min. VGE S-31 MWNTs (2.0g) were added to the solution, upon which the suspension turned black. The solution was stirred 30 min. 1-Bromononodecane (0.9g) was to added solution. The reaction was stirred overnight until NH_3 had completely evaporated from the flask. H_2O (250mL) was added to the flask and stirred for 30 min under open air. The suspension was filtered using a Buchner funnel and the filter cake was flushed with H_2O until pH of filtrate was neutral. The MWNTs were washed and filtered with EtOH followed by CH_2Cl_2. The MWNTs were then collected and dried overnight under vacuum. The MWNTs were soxhlet washed in THF for 24 hr. The MWNTs were collected and dried overnight under vacuum overnight to produce 1.9g of material.

(10) Ester f-MWNTs (CLF-III-45)

NH_3 was condensed into a 5L 4-neck round bottom flask equipped with a mechanical stirrer, using two Dewar condensers in a dry/ice acetone bath under N_2. After condensing ~2.5L of NH_3, Li metal (6.4g) was added to the flask, upon which the solution turned blue. The reaction was stirred for 5 min. VGE S-31 MWNTs (10.6g) were added to the solution, upon which the suspension turned black. The solution was stirred 30 min. Ethyl bromoacetate (125mL) was added slowly dropwise by syringe to the mixture. The reaction was stirred overnight until the NH_3 had completely evaporated from the flask. H_2O (2.5L) was added to the flask and stirred for 30 min under open air. The suspension was filtered using a Buchner funnel and the filter cake was flushed with H_2O until pH of filtrate was neutral. The MWNTs were washed and filtered with EtOH followed by CH_2Cl_2. The MWNTs were then collected and dried overnight under vacuum to produce 11.1g of material.

(11) Carboxylic Acid f-MWNTs (CLF-III-48)

Ester f-MWNTs (**10**) (11.0g) and KOH (600mL, 1M) were placed in 1L single neck round bottom flask equipped with magnetic stir bar. Solution was stirred overnight at 80^{o}C. The suspension was cooled to room temperature and filtered using a Buchner funnel. The suspension was filtered using a Buchner funnel and the filter cake was flushed with H_2O until pH of filtrate was neutral. MWNTs were washed off filter paper into 1L round bottom flask. 10% HCl (500mL) was added to the flask and stirred with magnetic stir bar for 30 min. The suspension was filtered using a Buchner funnel and the

filter cake was flushed with H_2O until pH of filtrate was neutral. MWNTs were washed and filtered with EtOH. The MWNTs were then collected and dried *in vacuo* to produce 9.9g of material.

(12) Acid Chloride f-MWNTs (CLF-III-53)

Carboxylic acid f-MWNTs (**11**) (2.0g) and $SOCl_2$ (150mL) were placed into 500mL 3 neck round bottom flask equipped with magnetic stir bar. Solution was stirred overnight at $100^{O}C$ under reflux. Solution was cooled to room temp and filtered with Buchner funnel and washed with toluene followed by hexane. MWNTs were collected and vacuumed overnight. Recovered weight 1.6g.

(13) Choline f-MWNTs (CLF-IV-19)

Carboxylic acid f-MWNTs (**11**) (0.9g) and EDC (0.3g) and H_2O (600mL) were placed into 1L 3 neck round bottom flask equipped with magnetic stir bar. Choline chloride (1.2g) was added to solution. Solution was stirred overnight at room temperature. Solution was filtered with Buchner funnel and washed with H_2O. MWNTs were collected and vacuumed overnight. Recovered weight 1.0g.

(14) Conjugate base f-MWNTs (CLF-IV-20)

Carboxylic acid f-MWNTs (**11**) (1.1g) and $NaHCO_3$ sat. solution (800mL) were placed into 1L 3 neck round bottom flask equipped with magnetic stir bar. Solution was stirred overnight at room temperature. Solution was filtered with Buchner funnel and washed with H_2O. MWNTs were collected and vacuumed overnight. Recovered weight 1.0g.

Mixing Methods

All MWNT/epoxy composites were mixed with pre-mixing followed by 3-roll milling and finally cured. These three stages are explained below.

Pre-mixing Method

MWNT/epoxy mixtures were hand mixed and then place into the THINKY mixer and mixed for 2 minutes at 2000rpm followed by defoaming for 3 minutes at 2200rpm. Mixtures were then mixed with 3-roll mill accordingly.

Long Method (CLF-III-64)

MWNT/epoxy mixture was poured into the feed roller using the following settings for the various passes. Speeds are measured by the rpm of the apron roller.

Pass	1^{st} Gap size(μm)	2^{nd} Gap size(μm)	Speed (rpm)
1	50	45	200
2	50	45	200
3	25	20	200
4	25	20	200
5	10	5	200
6	10	5	200
7	5	5	250
8	5	5	250
9	5	5	250
10	5	5	250
11	5	5	250

Short Method (CLF-III-65)

MWNT/epoxy mixture was pour into the feed roller using the following settings for the various passes. Speeds are measured by the rpm of the apron roller.

Pass	1st Gap size(μm)	2nd Gap size(μm)	Speed (rpm)
1	50	40	200
2	25	20	200
3	10	5	200
4	5	5	250
5	5	5	250

Method A (CLF-IV-11)

MWNT/epoxy mixture was pour into the feed roller using the following settings for the various passes. Speeds are measured by the rpm of the apron roller.

Pass	1st Gap size(μm)	2nd Gap size(μm)	Speed (rpm)
1	50	40	100
2	25	20	100
3	10	5	100
4	5	5	100
5	5	5	100

Method B (CLF-IV-11)

MWNT/epoxy mixture was pour into the feed roller using the following settings for the various passes. Speeds are measured by the rpm of the apron roller.

Pass	1st Gap size(μm)	2nd Gap size(μm)	Speed (rpm)
1	100	100	100
2	100	100	100
3	50	50	100
4	40	40	100
5	25	25	100

Method C (CLF-IV-11)

MWNT/epoxy mixture was pour into the feed roller using the following settings for the various passes. Speeds are measured by the rpm of the apron roller.

Pass	1st Gap size(μm)	2nd Gap size(μm)	Speed (rpm)
1	50	40	100
2	25	25	100
3	25	25	100

Curing Technique

After using one of the previous 3 roll mixing methods a catalytic amount of EMI-2,4 was added and then the sample was mixed in the Thinky mixer for 2 minutes at 2000rpm followed by defoaming for 3 minutes at 2200rpm. Sample was then poured into an

aluminum pan and place in a vacuum oven at 60^0C under vacuum for 30 minutes. The sample was then placed in oven at 130^0C and cured overnight

References

1. Iijima, S., Helical microtubules of graphitic carbon. *Nature* **1991,** *354* (6348), 56-58.
2. Oberlin, A.; Endo, M.; Koyama, T., Filamentous growth of carbon through benzene decomposition. *Journal of Crystal Growth* **1976,** *32* (3), 335-349.
3. Monthioux, M.; Kuznetsov, V. L., Who should be given the credit for the discovery of carbon nanotubes? *Carbon* **2006,** *44* (9), 1621-1623.
4. Bethune, D. S.; Klang, C. H.; de Vries, M. S.; Gorman, G.; Savoy, R.; Vazquez, J.; Beyers, R., Cobalt-catalysed growth of carbon nanotubes with single-atomic-layer walls. *Nature* **1993,** *363* (6430), 605-607.
5. Iijima, S.; Ichihashi, T., Single-shell carbon nanotubes of 1-nm diameter. *Nature* **1993,** *363* (6430), 603-605.
6. Baughman, R. H.; Zakhidov, A. A.; de Heer, W. A., Carbon Nanotubes--the Route Toward Applications. *Science* **2002,** *297* (5582), 787-792.
7. Niyogi, S.; Hamon, M. A.; Hu, H.; Zhao, B.; Bhowmik, P.; Sen, R.; Itkis, M. E.; Haddon, R. C., Chemistry of Single-Walled Carbon Nanotubes. *Accounts of Chemical Research* **2002,** *35* (12), 1105-1113.
8. Bayer builds world's largest production plant for carbon nanotubes in Chempark Leverkusen. http://www.research.bayer.com/en/News_Detail.aspx?id=8636 (accessed October 26, 2009).
9. Reibold, M.; Paufler, P.; Levin, A. A.; Kochmann, W.; Patzke, N.; Meyer, D. C., Materials: Carbon nanotubes in an ancient Damascus sabre. *Nature* **2006,** *444* (7117), 286-286.
10. Thostenson, E. T.; Ren, Z.; Chou, T.-W., Advances in the science and technology of carbon nanotubes and their composites: a review. *Composites Science and Technology* **2001,** *61* (13), 1899-1912.
11. Andrews, R.; Jacques, D.; Qian, D.; Rantell, T., Multiwall Carbon Nanotubes: Synthesis and Application. *Accounts of Chemical Research* **2002,** *35* (12), 1008-1017.
12. Jin, S. H.; Yoon, K. H.; Park, Y.-B.; Bang, D. S., Properties of surface-modified multiwalled carbon nanotube filled poly(ethylene terephthalate) composite films. *Journal of Applied Polymer Science* **2008,** *107* (2), 1163-1168.
13. Hexion Speciality Chemicals Epon 826 Technical Data Sheet. http://www.hexion.com/Products/TechnicalDataSheet.aspx?id=3937 (accessed Dec. 21, 2009).
14. Thinky Mixing and Degassing Machine. http://www.intertronics.co.uk/products/thiare25001.htm (accessed Dec. 21, 2009).
15. Silverson Products Technical Information. http://www.silverson.com/USA/Products/Lab-TechInfo.cfm (accessed Dec. 21, 2009).
16. Exakt Products Three Roll Mills. http://www.exaktusa.com/products/exakt_E.html (accessed Dec. 21, 2009).
17. THINKY Oil-based Clay Experiment. http://www.thinky.co.jp/en/mix_samples/oilbased_clay_experiment.html (accessed Dec. 21, 2009).
18. How it works, Silverson high shear mixer. http://www.silverson.com/USA/Products/Lab-HowItWorks.cfm (accessed 1/10/2010).
19. Wu, T.-L.; Lo, T.-S.; Kuo, W.-S., Effect of dispersion on graphite nanosheet composites. *Polymer Composites* **2009,** *9999* (9999), NA.
20. Jim W. Goodwin, R. W. H., *Rheology for Chemists*. 2nd ed. ed.; RSC Publishing: 2008.
21. Shenoy, A. V., *Rheology of filled polymer systems*. 1st. ed.; Kluwer Academic Publishers: Dordrecht, 1999; p 492.

22. Zheng, L. X.; O'Connell, M. J.; Doorn, S. K.; Liao, X. Z.; Zhao, Y. H.; Akhadov, E. A.; Hoffbauer, M. A.; Roop, B. J.; Jia, Q. X.; Dye, R. C.; Peterson, D. E.; Huang, S. M.; Liu, J.; Zhu, Y. T., Ultralong single-wall carbon nanotubes. *Nat Mater* **2004,** *3* (10), 673-676.
23. Nardelli, M. B.; Yakobson, B. I.; Bernholc, J., Brittle and Ductile Behavior in Carbon Nanotubes. *Physical Review Letters* **1998,** *81* (21), 4656.
24. Thostenson, E. T.; Ziaee, S.; Chou, T.-W., Processing and electrical properties of carbon nanotube/vinyl ester nanocomposites. *Composites Science and Technology In Press, Corrected Proof*.
25. Dresselhaus, M. S.; Dresselhaus, G.; Saito, R., Physics of carbon nanotubes. *Carbon* **1995,** *33* (7), 883-891.
26. Dresselhaus, M. S., NANOTUBES: Burn and Interrogate. *Science* **2001,** *292* (5517), 650-651.
27. Li, H. J.; Lu, W. G.; Li, J. J.; Bai, X. D.; Gu, C. Z., Multichannel Ballistic Transport in Multiwall Carbon Nanotubes. *Physical Review Letters* **2005,** *95* (8), 086601.
28. Stetter, A.; Vancea, J.; Back, C. H., Determination of the intershell conductance in a multiwall carbon nanotube. *Applied Physics Letters* **2008,** *93* (17), 172103-3.
29. Li, C.; Thostenson, E. T.; Chou, T.-W., Effect of nanotube waviness on the electrical conductivity of carbon nanotube-based composites. *Composites Science and Technology* **2008,** *68* (6), 1445-1452.
30. Sandler, J.; Shaffer, M. S. P.; Prasse, T.; Bauhofer, W.; Schulte, K.; Windle, A. H., Development of a dispersion process for carbon nanotubes in an epoxy matrix and the resulting electrical properties. *Polymer* **1999,** *40* (21), 5967-5971.
31. Sandler, J. K. W.; Kirk, J. E.; Kinloch, I. A.; Shaffer, M. S. P.; Windle, A. H., Ultra-low electrical percolation threshold in carbon-nanotube-epoxy composites. *Polymer* **2003,** *44* (19), 5893-5899.
32. Rosca, I. D.; Hoa, S. V., Highly conductive multiwall carbon nanotube and epoxy composites produced by three-roll milling. *Carbon In Press, Corrected Proof*.
33. Thostenson, E. T.; Chou, T.-W., Processing-structure-multi-functional property relationship in carbon nanotube/epoxy composites. *Carbon* **2006,** *44* (14), 3022-3029.
34. Kater, C. E.; Vilar, L.; Newell-Price, J., Harvey Cushing and Philip Hench: pituitary basophilism meets cortisone excess. *Arquivos Brasileiros de Endocrinologia & Metabologia* **2007,** *51*, 1182-1184.
35. Li, J. J., *Laughing Gas, Viagra, and Lipitor: The Human Stories behind the Drugs We Use*. 1st ed. ed.; Oxford Univsersity Press: U.S.A., 2006; p 336.
36. Birch, A. J., Reduction by Dissolving Metals I. *Journal of the Chemical Society* **1944**, 430-436.
37. Li, J. J., *Name Reactions: A collection of Detailed Reaction Mechanisms*. 3rd ed. ed.; Springer: New York, 2006; p 650.
38. Petrow, V., Contraceptive progestagens. *Chemical Reviews* **1970,** *70* (6), 713-726.
39. Birch, A. J., Reduction by dissolving metals. Part VII. The reactivity of mesomeric anions in relation to the reduction of benzene rings. *Journal of the Chemical Society* **1950**, 1551-1556.
40. Bachi, M. D.; Epstein, J. W.; Herzberg-Minzly, Y.; Loewenthal, H. J. E., Synthesis of compounds related to gibberellic acid. III. Analogs of ring A of the gibberellins. *The Journal of Organic Chemistry* **1969,** *34* (1), 126-135.
41. Pekker, S.; Salvetat, J.-P.; Jakab, E.; Bonard, J.-M.; Forro, L., Hydrogenation of Carbon Nanotubes and Graphite in Liquid Ammonia. *The Journal of Physical Chemistry B* **2001,** *105* (33), 7938-7943.

42. Liang, F.; Sadana, A. K.; Peera, A.; Chattopadhyay, J.; Gu, Z.; Hauge, R. H.; Billups, W. E., A Convenient Route to Functionalized Carbon Nanotubes. *Nano Letters* **2004,** *4* (7), 1257-1260.
43. Stephenson, J. J.; Sadana, A. K.; Higginbotham, A. L.; Tour, J. M., Highly Functionalized and Soluble Multiwalled Carbon Nanotubes by Reductive Alkylation and Arylation: The Billups Reaction. *Chemistry of Materials* **2006,** *18* (19), 4658-4661.
44. Cano-Maì□rquez, A. G.; RodrÃ-guez-Maciì□as, F. J.; Campos-Delgado, J.; Espinosa-Gonzaì□lez, C. G.; Tristaì□n-Loì□pez, F.; RamÃ-rez-Gonzaì□lez, D.; Cullen, D. A.; Smith, D. J.; Terrones, M.; Vega-Cantuì□, Y. I., Ex-MWNTs: Graphene Sheets and Ribbons Produced by Lithium Intercalation and Exfoliation of Carbon Nanotubes. *Nano Letters 0* (0).
45. Dresselhaus, M. S.; Dresselhaus, G., Intercalation compounds of graphite. *Advances in Physics* **2002,** *51* (1), 1 - 186.
46. Dresselhaus, M. S.; Dresselhaus, G.; Avouris, P., *Carbon Nanotubes Synthesis, Structure, Properties, and Application*. 1st ed.; 2001; Vol. 80.
47. Meier, M. S.; Andrews, R.; Jacques, D.; Cassity, K. B.; Qian, D., Tearing open nitrogen-doped multiwalled carbon nanotubes. *Journal of Materials Chemistry* **2008,** *18* (35), 4143-4145.
48. Maccoll, A.; Thomas, P. J., Studies in the pyrolysis of organic bromides. Part III. The pyrolysis of isopropyl bromide. *Journal of the Chemical Society* **1955**, 979 - 986.
49. Maccoll, A.; Angius, P. J., Studies in the pyrolysis of organic bromides. Part II. The pyrolysis of n-propyl bromide. *Journal of the Chemical Society* **1955**, 973 - 978.
50. Maccoll, A.; Good, P. T., Gas-phase eliminations. Part XIII. The pyrolysis of 1,1- and 1,2-dibromoethane. *Journal of the Chemical Society B: Physical Organic* **1971**, 268 - 272.
51. Joesten, B. L.; Johnston, N. W., Thermogravimetric Analysis of Vinyl Chloride/Acrylonitrile Copolymers. *Journal of Macromolecular Science, Part A: Pure and Applied Chemistry* **1974,** *8* (1), 83 - 94.
52. Orimo, S.; Majer, G.; Fukunaga, T.; Zuttel, A.; Schlapbach, L.; Fujii, H., Hydrogen in the mechanically prepared nanostructured graphite. *Applied Physics Letters* **1999,** *75* (20), 3093.
53. Bahr, J. L.; Yang, J.; Kosynkin, D. V.; Bronikowski, M. J.; Smalley, R. E.; Tour, J. M., Functionalization of Carbon Nanotubes by Electrochemical Reduction of Aryl Diazonium Salts: A Bucky Paper Electrode. *Journal of the American Chemical Society* **2001,** *123* (27), 6536-6542.
54. Dyke, C. A.; Tour, J. M., Overcoming the Insolubility of Carbon Nanotubes Through High Degrees of Sidewall Functionalization. *Chemistry - A European Journal* **2004,** *10* (4), 812-817.
55. Wang, Y.; Wu, J.; Wei, F., A treatment method to give separated multi-walled carbon nanotubes with high purity, high crystallization and a large aspect ratio. *Carbon* **2003,** *41* (15), 2939-2948.
56. Saito, T.; Matsushige, K.; Tanaka, K., Chemical treatment and modification of multi-walled carbon nanotubes. *Physica B: Condensed Matter* **2002,** *323* (1-4), 280-283.
57. Zhang, J.; Zou, H.; Qing, Q.; Yang, Y.; Li, Q.; Liu, Z.; Guo, X.; Du, Z., Effect of Chemical Oxidation on the Structure of Single-Walled Carbon Nanotubes. *The Journal of Physical Chemistry B* **2003,** *107* (16), 3712-3718.
58. Cano-Maìrquez, A. G.; Rodriguez-Maciìas, F. J.; Campos-Delgado, J.; Espinosa-Gonzaìlez, C. G.; Tristaìn-Loìpez, F.; Ramarez-Gonzaìlez, D.; Cullen, D. A.; Smith, D. J.; Terrones, M.; Vega-Cantuì, Y. I., Ex-MWNTs: Graphene Sheets and Ribbons Produced by Lithium Intercalation and Exfoliation of Carbon Nanotubes. *Nano Letters* **2009,** *9* (4), 1527-1533.
59. Kosynkin, D. V.; Higginbotham, A. L.; Sinitskii, A.; Lomeda, J. R.; Dimiev, A.; Price, B. K.; Tour, J. M., Longitudinal unzipping of carbon nanotubes to form graphene nanoribbons. *Nature* **2009,** *458* (7240), 872-876.

60. Spitalský, Z.; Krontiras, C. A.; Georga, S. N.; Galiotis, C., Effect of oxidation treatment of multiwalled carbon nanotubes on the mechanical and electrical properties of their epoxy composites. *Composites Part A: Applied Science and Manufacturing In Press, Corrected Proof*.
61. Kaiser, K. L., *Electromagnetic shielding.* CRC Press: Boca Raton, FL, 2006.
62. Schultz, R. B.; Plantz, V. C.; Brush, D. R., Shielding theory and practice. Electromagnetic compatibility. *IEEE Trans* **1988,** *30* (3), 187-201.
63. Tong, X. C., *Advanced Materials and Design for Electromagnetic Interference Shielding*. CRC: Boca Raton, FL, 2009.
64. Li, N.; Huang, Y.; Du, F.; He, X.; Lin, X.; Gao, H.; Ma, Y.; Li, F.; Chen, Y.; Eklund, P. C., Electromagnetic Interference (EMI) Shielding of Single-Walled Carbon Nanotube Epoxy Composites. *Nano Letters* **2006,** *6* (6), 1141-1145.
65. Huang, Y.; Li, N.; Ma, Y.; Du, F.; Li, F.; He, X.; Lin, X.; Gao, H.; Chen, Y., The influence of single-walled carbon nanotube structure on the electromagnetic interference shielding efficiency of its epoxy composites. *Carbon* **2007,** *45* (8), 1614-1621.
66. Jou, W.-S.; Cheng, H.-Z.; Hsu, C.-F., The electromagnetic shielding effectiveness of carbon nanotubes polymer composites. *Journal of Alloys and Compounds* **2007,** *434-435*, 641-645.
67. Al-Saleh, M. H.; Sundararaj, U., Electromagnetic interference shielding mechanisms of CNT/polymer composites. *Carbon* **2009,** *47* (7), 1738-1746.
68. Liu, Z.; Bai, G.; Huang, Y.; Ma, Y.; Du, F.; Li, F.; Guo, T.; Chen, Y., Reflection and absorption contributions to the electromagnetic interference shielding of single-walled carbon nanotube/polyurethane composites. *Carbon* **2007,** *45* (4), 821-827.
69. Das, N.; Maiti, S., Electromagnetic interference shielding of carbon nanotube/ethylene vinyl acetate composites. *Journal of Materials Science* **2008,** *43* (6), 1920-1925.
70. Yuen, S.-M.; Ma, C.-C. M.; Chuang, C.-Y.; Yu, K.-C.; Wu, S.-Y.; Yang, C.-C.; Wei, M.-H., Effect of processing method on the shielding effectiveness of electromagnetic interference of MWCNT/PMMA composites. *Composites Science and Technology* **2008,** *68* (3-4), 963-968.
71. Yang, Y.; Gupta, M. C.; Dudley, K. L.; Lawrence, R. W., Novel Carbon Nanotubeâˆ'Polystyrene Foam Composites for Electromagnetic Interference Shielding. *Nano Letters* **2005,** *5* (11), 2131-2134.
72. Li, Y.; Chen, C.; Zhang, S.; Ni, Y.; Huang, J., Electrical conductivity and electromagnetic interference shielding characteristics of multiwalled carbon nanotube filled polyacrylate composite films. *Applied Surface Science* **2008,** *254* (18), 5766-5771.
73. Chung, D. D. L., Electrical applications of carbon materials. *Journal of Materials Science* **2004,** *39* (8), 2645-2661.
74. Amarasekera, J., Conductive plastics for electrical and electronic applications. *Reinforced Plastics* **2005,** *49* (8), 38-41.
75. Yang, S.; Lozano, K.; Lomeli, A.; Foltz, H. D.; Jones, R., Electromagnetic interference shielding effectiveness of carbon nanofiber/LCP composites. *Composites Part A: Applied Science and Manufacturing* **2005,** *36* (5), 691-697.
76. Huang, J.-C., EMI shielding plastics: A review. *Advances in Polymer Technology* **1995,** *14* (2), 137-150.
77. Staros, J. V.; Wright, R. W.; Swingle, D. M., Enhancement by N-hydroxysulfosuccinimide of water-soluble carbodiimide-mediated coupling reactions. *Analytical Biochemistry* **1986,** *156* (1), 220-222.
78. Cutnell, J.; Johnson, K., *Physics*. 4th ed.; Wiley: New York, 1998.

79. Eitan, A.; Jiang, K.; Dukes, D.; Andrews, R.; Schadler, L. S., Surface Modification of Multiwalled Carbon Nanotubes: Toward the Tailoring of the Interface in Polymer Composites. *Chemistry of Materials* **2003,** *15* (16), 3198-3201.
80. Hatton, R. A.; Blanchard, N. P.; Stolojan, V.; Miller, A. J.; Silva, S. R. P., Nanostructured Copper Phthalocyanine-Sensitized Multiwall Carbon Nanotube Films. *Langmuir* **2007,** *23* (11), 6424-6430.
81. Wang, Y.; Chen, H.-Z.; Li, H.-Y.; Wang, M., Fabrication of carbon nanotubes/copper phthalocyanine composites with improved compatibility. *Materials Science and Engineering B* **2005,** *117* (3), 296-301.
82. Joseph Wang, Carbon-Nanotube Based Electrochemical Biosensors: A Review. *Electroanalysis* **2005,** *17* (1), 7-14.

Vita

Christopher Lee Fitzwater was born on August 28, 1979 in Sheridan, Montana. He holds a B.S. Chemistry from the University of Kentucky. He has been a research and teaching assistant for several years in addition to various duties he has performed in the Kentucky National Guard. He still currently resides in Lexington, Kentucky.